

8-2011

The effect of shoulder variation on IMRT and SmartArc for Head and Neck Cancer

Emily H. Neubauer

Follow this and additional works at: https://digitalcommons.library.tmc.edu/utgsbs_dissertations



Part of the [Other Analytical, Diagnostic and Therapeutic Techniques and Equipment Commons](#)

Recommended Citation

Neubauer, Emily H., "The effect of shoulder variation on IMRT and SmartArc for Head and Neck Cancer" (2011). *The University of Texas MD Anderson Cancer Center UTHealth Graduate School of Biomedical Sciences Dissertations and Theses (Open Access)*. 163.

https://digitalcommons.library.tmc.edu/utgsbs_dissertations/163

This Thesis (MS) is brought to you for free and open access by the The University of Texas MD Anderson Cancer Center UTHealth Graduate School of Biomedical Sciences at DigitalCommons@TMC. It has been accepted for inclusion in The University of Texas MD Anderson Cancer Center UTHealth Graduate School of Biomedical Sciences Dissertations and Theses (Open Access) by an authorized administrator of DigitalCommons@TMC. For more information, please contact digitalcommons@library.tmc.edu.

THE EFFECT OF SHOULDER VARIATION ON IMRT AND SMARTARC FOR HEAD
AND NECK CANCER

by

Emily Neubauer, B.S., C.M.D.

APPROVED:

Stephen Kry, Ph.D.
Supervisory Professor

David Followill, Ph.D.

Lei Dong, Ph.D.

Laurence Court, Ph.D.

R. Allen White, Ph.D.

Adam Garden, M.D.

APPROVED:

Dean, The University of Texas
Health Science Center at Houston
Graduate School of Biomedical Sciences

THE EFFECT OF SHOULDER VARIATION ON IMRT AND SMARTARC FOR HEAD
AND NECK CANCER

A
THESIS

Presented to the Faculty of
The University of Texas
Health Science Center at Houston
Graduate School of Biomedical Sciences
and
The University of Texas
M. D. Anderson Cancer Center

in Partial Fulfillment
of the Requirements
for the Degree of
MASTER OF SCIENCE

by

Emily Neubauer, B.S., C.M.D.
Houston, Texas

August 2011

Copyright © 2011 Emily Neubauer All Rights Reserved

Acknowledgements

I would like to thank Dr. Kry and the committee for their guidance during this process and to Dr. Garden in particular for procuring patients for me to study. Thanks also to Adam Yock, Joey Cheung, Ryan Williamson, and Patty Park for their assistance with CAT and Pinnacle. Thanks to Kelly Kissling for providing a fine model for a thesis. Last, but not least, thanks to Kiley Pulliam for sharing the giggles.

Abstract

Purpose: First, to determine an average and maximum displacement of the shoulder relative to isocenter over the course of treatment. Second, to establish the dosimetric effect of shoulder displacements relative to correct isocenter alignment on the dose delivered to the target and the surrounding structures for head and neck cancer patients.

Method and Materials: The frequency of shoulder shifts of various magnitudes relative to isocenter was assessed for 4 patients using image registration software. The location of the center of the right and left humeral head relative to isocenter (usually C2) was found daily from CT on rails scans, and was compared to the location of the humeral heads relative to isocenter on the initial simulation CT. Three Baseline head and neck IMRT and SmartArc plans were generated in Pinnacle based on simulation CTs. The CT datasets (external contour and boney structures) were then modified to represent shifts of the shoulder (relative to isocenter) between 3 mm and 15 mm in the SI, AP, and LR directions. The initial plans were recalculated on the image sets with shifted shoulders.

Results: On average, shoulder variation was 2-5 mm in each direction, although displacements of over 1 cm in the inferior and posterior directions occurred. Shoulder shifts induced perturbations in the dose distribution, although generally only for large shifts. Most substantially, large, superior shifts resulted in coverage loss by the 95% isodose line for targets in the lower neck. Inferior shifts elevated the dose to the brachial plexus by 0.6-4.1 Gy. SmartArc plans showed similar loss of target coverage as IMRT plans.

Conclusions: The position of the shoulder can have an impact on target coverage and critical structure dose. Shoulder position may need to be considered for setup of head and neck patients depending on target location.

Table of Contents

| | <i>Page</i> |
|---|-------------|
| CHAPTER 1 Introduction | |
| 1.1 Statement of Problem..... | 1 |
| 1.2 Head and Neck Cancer Treatment Overview..... | 3 |
| <i>1.2.1 Background: Radiation therapy for the head and neck.....</i> | <i>3</i> |
| <i>1.2.2 Current radiation therapy methods: IMRT.....</i> | <i>4</i> |
| <i>1.2.3 Current radiation therapy methods: VMAT.....</i> | <i>6</i> |
| <i>1.2.4 Pre-treatment: Immobilization, Simulation, and Setup.....</i> | <i>7</i> |
| 1.3 The Assessment of Shoulder Variation in Setup Uncertainty Studies..... | 10 |
| 1.4 Hypothesis and Specific Aims..... | 12 |
| CHAPTER 2 Methods and Materials | |
| 2.1 Daily CT on rails and CT Aided Targeting..... | 13 |
| <i>2.1.1 Daily CT on rails protocol.....</i> | <i>13</i> |
| <i>2.1.2 Registering the Images with CAT Software</i> | <i>14</i> |
| <i>2.1.3 Calculating the shoulder shift.....</i> | <i>15</i> |
| 2.2 Treatment Planning..... | 17 |
| <i>2.2.1 The Patients and Their Clinical Target Volumes.....</i> | <i>17</i> |
| <i>2.2.2: The Clinical IMRT plan.....</i> | <i>18</i> |
| <i>2.2.3 The Non-Clinical Arc Plan.....</i> | <i>22</i> |
| 2.3 Applying the Shifts and Evaluating the Impact on the Treatment Plans..... | 24 |
| <i>2.3.1 Choosing the shifts to evaluate.....</i> | <i>24</i> |
| <i>2.3.2 Modeling the shifts with “hand editing”.....</i> | <i>24</i> |

| | | |
|----------------------------------|---|----|
| 2.3.3 | <i>Drawing the superior and inferior shifts.....</i> | 25 |
| 2.3.4 | <i>Drawing the anterior and posterior shifts.....</i> | 28 |
| 2.3.5 | <i>Drawing the right or left shift.....</i> | 31 |
| 2.3.6 | <i>Evaluating the impact of each shift on dose distribution.....</i> | 32 |
| 2.4 | Verification of the dose findings using CT data..... | 34 |
| 2.4.1 | <i>Choosing a patient for verification.....</i> | 34 |
| 2.4.2 | <i>Comparing the daily CT shift to the hand edited shift.....</i> | 34 |
| CHAPTER 3 Results | | |
| 3.1 | Measured Shoulder Shift from CT on Rails Data..... | 36 |
| 3.2 | Dosimetric Impact of Shoulder Shifts..... | 45 |
| 3.2.1 | <i>Target Coverage.....</i> | 45 |
| 3.2.2 | <i>Critical Structure Dose.....</i> | 66 |
| 3.3 | Comparing the Daily CT Shift to the Hand Edited Shift: Confirmation with CAT...77 | |
| CHAPTER 4 Discussion | | |
| 4.1 | Interpretation of the Results..... | 81 |
| 4.1.1 | <i>Measured shoulder shifts.....</i> | 81 |
| 4.1.2 | <i>Dosimetric Impact.....</i> | 82 |
| 4.1.3 | <i>Confirmation with CAT.....</i> | 84 |
| 4.2 | Clinical Impact..... | 85 |
| 4.3 | Comparison to the Literature..... | 91 |
| 4.4 | Future Work..... | 92 |
| CHAPTER 5 Conclusions | | |
| 5.1 | Summary..... | 94 |

| | |
|---|-----|
| 5.2 Conclusions..... | 95 |
| APPENDIX A: CT on rails patient data extracted from Pinnacle..... | 97 |
| APPENDIX B: Dosimetric data extracted from Pinnacle..... | 102 |
| BIBLIOGRAPHY..... | 111 |
| VITA..... | 113 |

List of Illustrations

| | <i>Page</i> |
|--|-------------|
| <i>Figure 2-1: CAT registering images.....</i> | 15 |
| <i>Figure 2-2: Center points of humeral heads and C2.....</i> | 16 |
| <i>Figure 2-3a: Patient 1: Red CTV 60 Gy, Blue CTV 57 Gy, Yellow CTV 54 Gy.....</i> | 17 |
| <i>Figure 2-3b: Patient 2: Red CTV 70 Gy, Blue CTV 65 Gy, Yellow (outline) CTV 63 Gy..</i> | 18 |
| <i>Figure 2-3c: Patient 3: Red CTV 60 Gy, Orange (outline) CTV 54 Gy.....</i> | 18 |
| <i>Figure 2-4a: 9 field IMRT beam arrangement.....</i> | 19 |
| <i>Figure 2-4b: 7 field IMRT beam arrangement.....</i> | 19 |
| <i>Figure 2-5: Example of Acceptable CTV coverage and Spinal Cord Dose.....</i> | 21 |
| <i>Figure 2-6: Two arcs used for SmartArc plan.....</i> | 22 |
| <i>Figure 2-7: Comparable IMRT and SmartArc Plans for Patient 1.....</i> | 23 |
| <i>Figure 2-8: 15 mm Superior Shift.....</i> | 28 |
| <i>Figure 2-9: 15 mm Inferior Shift.....</i> | 28 |
| <i>Figure 2-10: 15 mm Anterior Shift.....</i> | 30 |
| <i>Figure 2-11: 15 mm posterior shift.....</i> | 31 |
| <i>Figure 2-12: 15 mm left shift.....</i> | 32 |
| <i>Figure 3.1: Patient 1 shoulder shifts broken down by 3 orthogonal directions.....</i> | 36 |
| <i>Figure 3.2: Patient 1 shoulder shifts broken down by all 6 directions.....</i> | 36 |
| <i>Figure 3.3: Patient 2 shoulder shifts broken down by 3 orthogonal directions.....</i> | 37 |
| <i>Figure 3.4: Patient 2 shoulder shifts broken down by all 6 directions.....</i> | 37 |
| <i>Figure 3.5: Patient 3 shoulder shifts broken down by 3 orthogonal directions.....</i> | 38 |
| <i>Figure 3.6: Patient 3 shoulder shifts broken down by all 6 directions.....</i> | 38 |

| | |
|--|-----------|
| <i>Figure 3.7: Patient 4 shoulder shifts broken down by 3 orthogonal directions.....</i> | <i>39</i> |
| <i>Figure 3.8: Patient 4 shoulder shifts broken down by all 6 directions.....</i> | <i>39</i> |
| <i>Figure 3.9: Shoulder Shift vs. Fraction for Patient 1.....</i> | <i>42</i> |
| <i>Figure 3.10: Shoulder Shift vs. Fraction for Patient 2.....</i> | <i>42</i> |
| <i>Figure 3.11: Shoulder Shift vs. Fraction for Patient 3</i> | <i>43</i> |
| <i>Figure 3.12: Shoulder Shift vs. CT for Patient 4's first plan.....</i> | <i>44</i> |
| <i>Figure 3.13: Shoulder Shift vs. Fraction for Patient 4's replan.....</i> | <i>44</i> |
| <i>Figure 3.14: DVH for Patient 1 IMRT plans.....</i> | <i>49</i> |
| <i>Figure 3.15: DVH for Patient 1 SmartArc plans.....</i> | <i>49</i> |
| <i>Figure 3.16a: Patient 1 IMRT no shift.....</i> | <i>50</i> |
| <i>Figure 3.16b: Patient 1 IMRT 5 mm superior shift.....</i> | <i>50</i> |
| <i>Figure 3.16c: Patient 1 SmartArc no shift.....</i> | <i>51</i> |
| <i>Figure 3.16d: Patient 1 SmartArc 5 mm superior shift.....</i> | <i>51</i> |
| <i>Figure 3.17a: Patient 1 IMRT no shift.....</i> | <i>52</i> |
| <i>Figure 3.17b: Patient 1 IMRT 15 mm superior shift.....</i> | <i>52</i> |
| <i>Figure 3.17c: Patient 1 SmartArc no shift.....</i> | <i>53</i> |
| <i>Figure 3.17d: Patient 1 SmarArc 15 mm superior shift.....</i> | <i>53</i> |
| <i>Figure 3.18a: Patient 1 IMRT no shift.....</i> | <i>54</i> |
| <i>Figure 3.18b: Patient 1 IMRT 15 mm posterior shift.....</i> | <i>54</i> |
| <i>Figure 3.19a: Patient 2 IMRT no shift.....</i> | <i>55</i> |
| <i>Figure 3.19b: Patient 2 IMRT 5 mm superior shift.....</i> | <i>55</i> |
| <i>Figure 3.19c: Patient 2 SmartArc no shift.....</i> | <i>56</i> |
| <i>Figure 3.19d: Patient 2 SmartArc 5 mm superior shift.....</i> | <i>56</i> |

| | |
|--|-----------|
| <i>Figure 3.20a: Patient 2 IMRT no shift.....</i> | <i>57</i> |
| <i>Figure 3.20b: Patient 2 IMRT 15 mm superior shift.....</i> | <i>57</i> |
| <i>Figure 3.20c: Patient 2 SmartArc no shift.....</i> | <i>58</i> |
| <i>Figure 3.20d: Patient 2 IMRT 15 mm superior shift.....</i> | <i>58</i> |
| <i>Figure 3.21a: Patient 2 IMRT no shift.....</i> | <i>59</i> |
| <i>Figure 3.21b: Patient 2 IMRT 15 mm posterior shift.....</i> | <i>59</i> |
| <i>Figure 3.22a: Patient 3 IMRT no shift.....</i> | <i>60</i> |
| <i>Figure 3.22b: Patient 3 IMRT 15 mm superior shift.....</i> | <i>60</i> |
| <i>Figure 3.22c: Patient 3 SmartArc no shift.....</i> | <i>61</i> |
| <i>Figure 3.22d: Patient 3 SmartArc 15 mm superior shift.....</i> | <i>61</i> |
| <i>Figure 3.23a: Patient 3 IMRT no shift.....</i> | <i>62</i> |
| <i>Figure 3.23b: Patient 3 IMRT 15 mm posterior shift.....</i> | <i>62</i> |
| <i>Figure 3.24a: Volume loss Patient 1 IMRT plan.....</i> | <i>63</i> |
| <i>Figure 3.24b: Volume loss Patient 1 SmartArc plan.....</i> | <i>63</i> |
| <i>Figure 3.25a: Volume loss Patient 2 IMRT plan.....</i> | <i>64</i> |
| <i>Figure 3.25b: Volume loss Patient 2 SmartArc plan.....</i> | <i>64</i> |
| <i>Figure 3.26a: Volume loss Patient 3 IMRT Plan.....</i> | <i>65</i> |
| <i>Figure 3.26b: Volume loss Patient 3 SmartArc plan.....</i> | <i>65</i> |
| <i>Figure 3.27a: Change in dose to 0.1 cc of the spinal cord plotted vs. shoulder displacement in the superior/inferior and anterior/posterior directions for Patient 3's IMRT plan.....</i> | <i>68</i> |

| | |
|--|----|
| <i>Figure 3.27b:</i> Change in dose to 0.1 cc of the spinal cord plotted vs. shoulder displacement in the superior/inferior and anterior/posterior directions for Patient 3's SmartArc plan..... | 68 |
| <i>Figure 3.28a:</i> Change in dose to 0.1 cc of the spinal cord plotted vs. shoulder displacement in the superior/inferior and anterior/posterior directions for Patient 1's IMRT plan..... | 69 |
| <i>Figure 3.28b:</i> Change in dose to 0.1 cc of the spinal cord plotted vs. shoulder displacement in the superior/inferior and anterior/posterior directions for Patient 1's SmartArc plan..... | 69 |
| <i>Figure 3.29a:</i> Change in dose to 0.1 cc of the spinal cord plotted vs. shoulder displacement in the superior/inferior and anterior/posterior directions for Patient 2's IMRT plan..... | 70 |
| <i>Figure 3.29b:</i> Change in dose to 0.1 cc of the spinal cord plotted vs. shoulder displacement in the superior/inferior and anterior/posterior directions for Patient 2's SmartArc plan..... | 70 |
| <i>Figure 3.30a:</i> Change in dose to 0.1 cc of the brachial plexus plotted vs. shoulder displacement in the superior/inferior and anterior/posterior directions for Patient 2's IMRT plan..... | 74 |
| <i>Figure 3.30b:</i> Change in dose to 0.1 cc of the brachial plexus plotted vs. shoulder displacement in the superior/inferior and anterior/posterior directions for Patient 2's SmartArc plan..... | 74 |

| | |
|--|----|
| <i>Figure 3.31a:</i> Change in dose to 0.1 cc of the brachial plexus plotted vs. shoulder displacement in the superior/inferior and anterior/posterior directions for Patient 3's IMRT plan..... | 75 |
| <i>Figure 3.31b:</i> Change in dose to 0.1 cc of the brachial plexus plotted vs. shoulder displacement in the superior/inferior and anterior/posterior directions for Patient 3's SmartArc plan..... | 75 |
| <i>Figure 3.32a:</i> Change in dose to 0.1 cc of the brachial plexus plotted vs. shoulder displacement in the superior/inferior and anterior/posterior directions for Patient 1's IMRT plan..... | 76 |
| <i>Figure 3.32b:</i> Change in dose to 0.1 cc of the brachial plexus plotted vs. shoulder displacement in the superior/inferior and anterior/posterior directions for Patient 1's SmartArc plan..... | 76 |
| <i>Figure 3.33:</i> Case 1 hand edited shoulder shifts..... | 78 |
| <i>Figure 3.34:</i> Case 1 daily CT with shoulder shifts..... | 78 |
| <i>Figure 3.35:</i> Case 2 hand edited shoulder shifts..... | 79 |
| <i>Figure 3.36:</i> Case 2 daily CT with shoulder shifts..... | 79 |

List of Tables

| | <i>Page</i> |
|--|-------------|
| <i>Table 2-1: Dose Constrains for Head and Neck IMRT Planning.....</i> | 20 |
| <i>Table 3-1: Average Observed Shoulder Shift for Each Patient (cm).....</i> | 40 |
| <i>Table 3-2: Maximum Observed Shoulder Shift (cm).....</i> | 41 |
| <i>Table 3-3: Average shoulder shifts (cm).....</i> | 45 |
| <i>Table 3-4: Target Coverage Change (cc): IMRT.....</i> | 46 |
| <i>Table 3-5: Target Coverage Change (cc): SmartArc.....</i> | 47 |
| <i>Table 3-6: Spinal Cord Dose Change.....</i> | 67 |
| <i>Table 3-7: Brachial Plexus Dose Change.....</i> | 72 |
| <i>Table 3-8: Comparison of Target Coverage lost for hand edited shifts and daily CT (cc)...</i> | 80 |
| <i>Table 4-1: Dose per fraction and total dose lost to a point in the lower neck CTV, to 99% of the CTV, and the total dose lost during treatment for superior and posterior shifts.....</i> | 87 |
| <i>Table 4-2: Dose change per fraction, and total dose change to 0.1 cc of the brachial plexus and total change over treatment for inferior, posterior and superior shifts.....</i> | 89 |
| <i>Table A-1: CT on rails Patient 1 Boney Alignment structure coordinates, humeral head coordinates, and displacement between the two (Left shift, Right shift).....</i> | 97 |
| <i>Table A-2: CT on rails Patient 2 C2 coordinates, humeral head coordinates, and displacement between the two.....</i> | 98 |
| <i>Table A-3: CT on rails Patient 3 C2 coordinates, humeral head coordinates, and displacement between the two.....</i> | 99 |

| | |
|---|-----|
| <i>Table A-4a:</i> CT on rails Patient 4, First plan, boney alignment structure coordinates, humeral head coordinates, and displacement between the two..... | 100 |
| <i>Table A-4b:</i> CT on rails Patient 4, Replan, boney alignment structure coordinates, humeral head coordinates, and displacement between the two..... | 101 |
| <i>Table B-1:</i> Dosimetric Patient 1 target volumes and structure doses..... | 102 |
| <i>Table B-2:</i> Dosimetric Patient 2 target volumes and structure doses..... | 105 |
| <i>Table B-3:</i> Dosimetric Patient 3 target volumes and structure doses..... | 108 |

CHAPTER 1: Introduction

1.1 Statement of the Problem

One area of improvement in radiation therapy technique over the last decade is the ability to deliver doses to the tumor site with better precision while avoiding healthy tissues at the same time. Many factors contribute to achieving this goal including delivery mode, patient setup methods, and use of patient immobilization devices. For head and neck cancers, tumor targeting is especially complex because of the existence of normal tissues near the target, including the spinal cord, brainstem, and brachial plexus, that are critical to normal function, and damage to these would be detrimental. In addition, areas of potential tumor spread are often treated prophylactically, and these often extend the treatment volume into the lower neck. If the radiation is to be delivered as planned, hitting the target and missing the critical organs, then each day the patient must be positioned and immobilized so that everything is in the same place as planned.

Patient immobilization has become more essential since the advent of Intensity Modulated Radiation Therapy (IMRT). This technique uses an inverse planning computer algorithm to create a treatment plan that allows for precise targeting of the tumor volume with rapid dose fall off so that tissues nearby do not get a high dose. As a result, the target can receive a higher dose. This is especially beneficial for head and neck cancer where local recurrence has been seen at doses used in conventional 3D planning, and so IMRT has become nearly ubiquitous for head and neck treatments (Lee, Puri et al. 2007).

A disadvantage of high target doses with rapid fall off is that small amounts of motion disrupt the dose distribution. If the patient were to move during treatment, the dose

would not go where it is supposed to. To prevent movement, a variety of thermoplastic masks and head and shoulder boards are used to immobilize the patient. The use of more frequent imaging techniques has also been used to setup the patient each day to make sure positioning is accurate. While these techniques take precaution to confirm the patient position, they focus on the location of or near the radiation isocenter, such as the second cervical vertebra (C2) (Court, Wolfsberger et al. 2008).

While setting up to the correct isocenter location is important so the dose is delivered correctly, the position of the body far from isocenter can also have an impact on the delivered dose distribution. For head and neck therapy, the position of the shoulders is of particular concern. The position of the shoulders is generally not looked at when setting up the patient each day. Without any apparent shift in isocenter, the shoulders can still be in a position different from the one in the treatment plan. If the patient's shoulders moved superior relative to the planning setup, the shoulders could intercept the radiation beams and cause an underdosing of the tumor. Conversely, if the shoulders moved inferior relative to the planning setup, the shoulders could not provide anticipated attenuation, and thereby increase the dose to critical structures. For these reasons, shoulder variation needs to be assessed independently of isocenter setup variability. This impact is of particular concern in treatments that have segments near or through the shoulders, as is the case with symmetrically placed IMRT fields. The issue is also important with a newer treatment technique, Volumetric Modulated Arc Therapy, which delivers an IMRT plan while the gantry travels in an arc around the patient, and passes through the shoulders if the planning system does not allow skipping any angles. However, the dosimetric impact of shoulder motion has not been previously evaluated. In order to understand the dosimetric importance

of shoulder motion, knowing how much the shoulder moves is essential. Therefore, this study sought to answer two questions. First, the magnitude of shoulder motion relative to treatment isocenter associated with radiotherapy of the head and neck. And second, the effect of shoulder variability on the dose distribution for IMRT and VMAT plans.

1.2 Head and Neck Cancer Treatment Overview

1.2.1 Background: Radiation therapy for the head and neck

In order to appreciate the importance of shoulder motion on treatment delivery, understanding the patient population affected by this problem is necessary. Head and neck cancer comprises of cancers of the nasal cavity, nasal sinuses, oral cavity, nasopharynx, larynx, hypopharynx, and thyroid. According to the American Cancer Society, about 90,000 new cases of head and neck cancer were diagnosed in the United States in 2010 (ACS 2010). Seventy eight percent of head and neck cancer patients receive head and neck radiotherapy (Joiner 2009) so approximately 70,200 patients in the United States were treated with radiation to the head and neck last year. Almost all of these patients get treatment in the lower neck region, and as a result, may have their treatments impacted by their shoulder variability.

Historically, these treatments were delivered with a 6 MV 3-field technique comprised of right and left lateral beams and an anterior-posterior beam that covered the supraclavicular nodes. The lateral beams were matched with the anterior beam along the inferior border by use of a half-beam-block where one of the linear accelerator jaws was closed to create a non-divergent edge. These fields could only be treated to the tolerance dose of the spinal cord. In order to achieve higher doses, a cord block was added to the

anterior field, and the posterior jaws of the lateral fields were closed to block the cord superiorly creating “off-cord” fields. The cervical nodes in the posterior neck were treated with electron fields, usually 9 MeV, matched to the off-cord photon fields. In addition, the primary tumor received smaller boost fields to escalate its dose further. The most common doses delivered were 60-66 Gy (Bentel 1996). With this beam arrangement, movement of the shoulders had minimal impact because they were outside of the treatment fields. However, other dosimetric problems did occur. As a result of the conventional treatment, damage to the parotid glands was frequent, and xerostomia was a problem. Dry mouth is an often cited quality of life issue associated with head and neck radiotherapy treatment, as it is a very uncomfortable side effect for patients (Joiner 2009).

1.2.2 Current radiation therapy methods: IMRT

The problem of sparing the parotids and other normal tissues, such as the spinal cord, that limited the dose of 3D plans, was, for the most part, solved with IMRT. Studies at UCSF showed that IMRT provided better tumor coverage than 3D plans while sparing the surrounding tissues (Lee, Puri et al. 2007) and a study at the Mallinckrodt Institute of Radiology in St. Louis showed a reduction in xerostomia with no change in local control or survival (Ozyigit, Yang et al. 2004). Despite this success, some tissues, specifically the brachial plexus, are often not considered when generating the treatment plan, and as a result, get higher doses with IMRT plans. A study at UC Davis Medical center showed that the maximum dose to 1% of the brachial plexus was 3.1 Gy higher for IMRT plans than conventional plans. In addition, the volume of the brachial plexus receiving the tolerance dose for a 5% complication rate in 5 years (60 Gy) was increased by 3 cm³ for IMRT plans over conventional plans. The patients in this study had IMRT fields that extended into the

lower neck where the impact of shoulder motion on dose could be significant (Chen, Hall et al.). Still, the overall ability to escalate dose to the target and spare critical structures has resulted in IMRT being used for almost all head and neck cancer patients.

For patients receiving head and neck IMRT, the treatment area is divided into areas of primary tumor and obvious or potential metastatic spread into the lymph nodes. The primary tumor, or gross tumor volume (GTV), is what is visible on a CT or MRI. The areas of likely spread, or clinical target volumes (CTVs), are drawn based on visibly involved lymph nodes and most probable drainage chains. The CTVs are ranked based on level of risk of nodal disease: CTV1 denotes a high risk region and CTV2 denotes a low risk region. CTV3 delineates uninvolved cervical or supraclavicular lymph nodes that are being treated prophylactically (Ozyigit, Yang et al. 2004).

An IMRT treatment simultaneously delivers different doses to all of the CTVs delineated by the physician. The primary tumor site that was once treated with opposed lateral beams, is now treated with 7-9 evenly spaced coplanar beams. IMRT beams are not parallel opposed in order to avoid the inverse planning optimizer pushing too much dose through certain ideally placed beams. Evenly spaced beams allow for more uniform weighting. These beams may extend into the lower neck to cover the supraclavicular nodes, or they may be matched via half-beam-block to an anterior field in the same fashion used in the conventional treatment.

The creation of the treatment plan is done with inverse planning on a treatment planning computer. The computer is given certain dose constraints for the targets and the normal tissue. The computer algorithm divides the beam into small beamlets and adjusts their weights and intensities to produce the ideal fluence map which would yield a perfect

dose distribution. To optimize the beamlet weights and intensity, the computer uses an iterative method to reduce the value of a cost function that represents the difference from desired dose and the true dose. In the Pinnacle treatment planning system (Phillips, Fitchburg, WI) however, the machine parameters are used to compute a truly feasible dose distribution for each iteration. This is called the Direct Machine Parameter Optimization algorithm. Once the ideal fluence map is found, the dose per MU is calculated based on achievable positions of the MLC with a dose calculation algorithm. The algorithm used depends on the treatment planning system. Pinnacle, for example, uses the convolution algorithm which calculates primary radiation interactions in a medium separately from secondary interactions. The MU is found by calculating the dose per energy fluence at the point of interest relative to its value at a calibration point. Treatment plans may be delivered via a static “step and shoot” method or a dynamic “sliding window” method. In the static method the MLC move to create a segment shape, stop, and the beam turns on. The beam shuts off while the MLC move to the next position. In the dynamic method the MLC move across the field to each segment position while the beam is turned on (Kahn 2003).

1.2.3 Current radiation therapy methods: VMAT

While IMRT plans have better target coverage and normal tissue sparing than their conventional 3D counterparts, they do deliver more MU and have longer treatment times. In an effort to reduce the time the patients must lie still on the table, a faster delivery technique that delivers fewer MU, Volumetric Modulated Arc Therapy, has been developed (Clemente, Wu et al.). A VMAT treatment is essentially an IMRT treatment that is delivered while the gantry moves in an arc around the patient. The plan is developed with inverse planning, just as it is for IMRT. In Pinnacle SmartArc planning, the user defines the arc

length (gantry start and stop angles) and the target and normal tissue parameters. The optimizer divides the arc into segments 24° apart and a fluence map is created using the same iterative method as in IMRT. Once the fluence map is created, it is converted into MLC segments which are distributed around the arc. The computer optimizes these segments based on machine parameters to create the ideal dose distribution. Interpolation and continued optimization of control points within the segments allows for a finer spacing of 4° between segments. The final dose calculation is performed with the convolution algorithm (Bzdusek, Friberger et al. 2009).

The large number of segments used in a SmartArc plan result in a long planning time, but the delivery has been shown to be shorter with fewer MU. A study at John's Hopkins University showed that the SmartArc plans showed comparable target coverage and critical structure sparing compared to 9-field IMRT plans for 8 patients with oropharyngeal cancer. The SmartArc plans had fewer MU per fraction, and the delivery time was shorter than for IMRT. This study also found SmartArc plans were also more conformal. All of the patients had 3 CTVs treated to 3 different dose levels (Clemente, Wu et al.).

1.2.4 Pre-treatment: Immobilization, Simulation, and Setup

Because IMRT and VMAT plans are highly conformal, target the tumor with high doses, and have steep dose gradients, patient positioning for these treatments requires a great deal of accuracy. At initial simulation, patients are immobilized with a custom made thermo-plastic mask that covers the head, or both the head and shoulders, and attaches to the immobilization board on the treatment table. The mask is heated in water so it becomes flexible, and is placed over the patient's face and molded around the nose, eyes and chin. As the mask dries it hardens, and keeps the patient's shape. A head cup is placed against the

back of the head to extend the neck. If the mask does not cover the shoulders, shoulder restraints push the shoulders inferiorly, or a vacuum bean bag is created to hold the patient's upper body in position. If the mask does cover the shoulders, wrist straps may be used to pull the shoulders down while the mask is being shaped. Extending the neck and pushing or pulling the shoulders inferiorly all serve to open up the treatment area around the neck for beam clearance. Once the patient is properly immobilized, the mask is marked at isocenter for reference, and the patient receives a CT scan on which the treatment plan will be designed.

The treatment plan also aims to set the beams for optimal clearance of the shoulders. Wherever possible, beams that enter the patient directly through the shoulders are avoided, and if an angle that goes through the shoulder is necessary to treat a target on the lateral neck, the inferior jaw will be closed above the shoulder so there is no beam divergence into it.

In order for the plan that is delivered to match the plan that was created, the patient's anatomy must be in the exact same location as it was on the day of the simulation. While this is generally unlikely, careful setup methods are used to be sure it matches as closely as possible. The most common method of daily setup is the portal image. Here, the lasers in the treatment room are set up to the marks on the patient's mask. Shifts are made to the treatment isocenter if it is a different point, and MV x-rays are used to take Anterior-Posterior and Lateral images. The images are compared to a digitally reconstructed radiograph (DRR) that was created by the planning system. The treatment couch is shifted so the bony anatomy, often C2, in the port film and the DRR are aligned. The margin of error in portal film alignment is typically 3 mm, so often the patient is shifted only if the

difference between the images is greater than 3 mm. The study concluded that for IMRT, set up images port films are best taken daily to ensure accurate setup (Court, Wolfsberger et al. 2008).

As an alternative to MV images, KV images can be taken if the treatment machine has an on-board imager. The KV images are of better quality and also have 3 mm action level. As with MV images, these images are also aligned to boney anatomy. In addition, software that overlays the DRR with the x-ray image can be used to compute a couch shift and move it automatically so the therapist does not have to re-enter the room.

For an even more sophisticated setup, a system of Cone Beam CT (CBCT), which uses the on-board KV imager to take a CT image, CT on rails can be used for daily setup imaging. This CBCT allows for soft tissue alignment with 3D matching software. Some institutions also have a CT on rails, and this method is often reserved for patients who are expected to have large changes in their anatomy over the course of treatment and may require a new treatment plan (adaptive planning). In this case the patient is setup on the treatment couch which is then rotated 180° towards the CT scanner. The CT moves over the patient, acquiring a CT scan, and then the couch returns to treatment position under the linear accelerator. The daily CT is compared to bony and soft tissue anatomy of the planning CT, and software computes and applies a couch shift. A study at MD Anderson looking at setup shifts based on 3 regions of interest: C2, C6, and the palatine process of the maxilla, showed that the CT could detect translational differences of less than 1 mm and rotational differences of less than 1° (Zhang, Garden et al. 2006). As demonstrated by this study, the areas of interest used to determine setup error are generally in the neck and do not include any evaluation of the shoulders.

1.3 The Assessment of Shoulder Variation in Setup Uncertainty Studies

While the shoulders are usually not a part of setup uncertainty studies, a few researchers have taken note of how the shoulders move day to day. Shoulder motion itself has been included in a study on setup variability and immobilization devices used for 3D-CRT brain and head and neck treatments that was done by Laurent Gilbeau et al. at St. Luc University Hospital in Belgium (2001). This group looked at 3 types of thermoplastic masks for 915 patients: a head only mask with 3 fixation points (2 laterals and one on the apex of the head), a head and shoulder mask with 4 fixation points (2 on each lateral side one at shoulder and one at the head), and a head and shoulder mask with 5 fixation points (the same 4 points as previously, plus another at the apex of the head). Weekly port films were used to determine the 3D shifts of the head and neck, and the 2D shift of the shoulders by auto-registering portal images to a template with the field borders, mandible, clavicle, and maxillary sinus outlined. Because there was just an anterior supraclavicular field used for treatment of this area, only AP port films at 100 SSD were needed, so the shoulder shifts were measured in the SI and RL direction only, which only allowed for 2D information. Ninety percent of the shoulder displacements were less than 5.5 mm for the head and neck patients. The largest observed displacements were 10-12 mm in the RL direction. The authors concluded that shoulder motion was less with the 4 and 5 point head and shoulder masks (Gilbeau, Octave-Prignot et al. 2001). This paper did not discuss how the shoulder variability affected the dose delivery, and there was likely error in their shoulder position measurements due to the poor image quality of port films.

Another study by Court et al. from Brigham and Women's in Boston, MA (2008) discussed using daily port films to check for setup variability for 15 patients undergoing head and neck IMRT. For these patients, the 5-point head and shoulder mask was used. After checking the location of isocenter (C2), the therapists would shift the couch and patient before each treatment if isocenter was displaced more than 3 mm from its planned location. They found that isocenter shifts were usually less than 3 mm. As the therapists did the repositioning each day, they made note of the shoulder shifts based on how much they needed to move them. Of all the daily shoulder shifts, 59% were less than 5mm, 11% were 6-9 mm and 30% were 1 cm or greater. The large, 1 cm shifts were in the RL direction. (Court, Wolfsberger et al. 2008). The authors evaluated the dose effect in the shoulder region of a 1 cm lateral shift of isocenter by visual assessment of the isodose lines on treatment plans, but they did not look at the effect of shoulder motion.

No computational analysis of the impact of shoulder shifts has been performed. In addition, the use of portal images, which have poor image quality, does not give the most accurate assessment of how large shoulder shifts are. In order to address this problem, more accurate methods must be applied.

1.4 Hypothesis and Specific Aims

Hypothesis: The average shoulder shift over the course of treatment will not have a clinical impact on target coverage or normal tissue doses, however, the dose degradation in absolute volume of target coverage lost will be worse for SmartArc than for IMRT.

Specific Aims:

- 1) Using daily setup CTs, establish an average and maximum displacement of the shoulder over the course of treatment for patients at MD Anderson.
- 2) Establish the effect of average, intermediate, and large shoulder displacements on the dose delivered to the target and the surrounding structures by modeling the shoulder shifts and recalculating the treatment plan for IMRT and VMAT therapies.

CHAPTER 2: Methods and Materials

2.1 Daily CT on rails and CT Aided Targeting

2.1.1 Daily CT on rails protocol

The first objective of this project was to quantify the extent of shoulder variation experienced by patients undergoing radiation therapy. Shoulder variation was tracked for four patients with cancer of the Head and Neck that were assigned to an adaptive planning protocol used daily to setup to isocenter and monitor tumor response. This protocol used an in-room CT scanner that moves on rails. The CT on rails allowed for a large field of view (50 cm) which captured the shoulders. The CT on rails works better than other imaging techniques, such as cone beam CT (field of view 45 cm), because of its large bore.

For the patients in this study, three were immobilized using a 5 point head and shoulder thermoplastic mask. The fourth patient had an initial plan with an upper body vacuum bag immobilization, and a second, replan with a head only mask and an upper body vacuum bag. On each treatment day, the patients were set up on the couch in treatment position based on marks on the mask and radio-opaque fiducial markers. The couch was rotated 180° toward the CT scanner and an image was acquired by moving over the couch along the rails. After image acquisition the couch was rotated back into treatment position. The isocenter was aligned using the second cervical vertebra (C2) on the 3D image from the daily scan and comparing it to the treatment planning CT. The CT Aided Targeting (CAT) software (MD Anderson, Houston, TX) allowed the physician to move the daily image to the correct isocenter location. The offset of the isocenter was calculated by the software, and any couch shifts greater than 3mm were made. The patients were scanned from ear to axilla

with a 50 cm field of view to capture their humeral heads, and these were used to assess the shoulder shifts.

2.1.2 Registering the Images with CAT Software

The CAT software was used to locate C2 and each humeral head on all of the daily CT scans acquired for each patient. C2 usually represented the isocenter alignment (if it did not, the appropriate vertebral body was used instead), and the humeral heads represented the location of each shoulder. C2 and the right and left humeral head were contoured on the original treatment plan. CAT used the original planning CT scan to find the same structures on each of the daily scans. An alignment set consisting of C2, the right humeral head, and the left humeral head was created for each patient in the CAT system. C2 was selected as the target for the automatic alignment of the structures, and the alignment was based on bony anatomy. To get the contours on every scan, each daily scan was selected and a reference isocenter was placed by the user based on the location of fiducials on the treatment mask. Next, the software positioned the structures by finding the target, C2, and aligning the humeral heads in reference to it. Deformable registration was used so the structures were overlaid with the correct shape as well as in the correct location. Deformable image registration used pixel values to determine the shape of the anatomy in the new scan rather than copy the contour shape from the original scan and place it on the new scan. This process can be seen in Fig. 2-1 below.

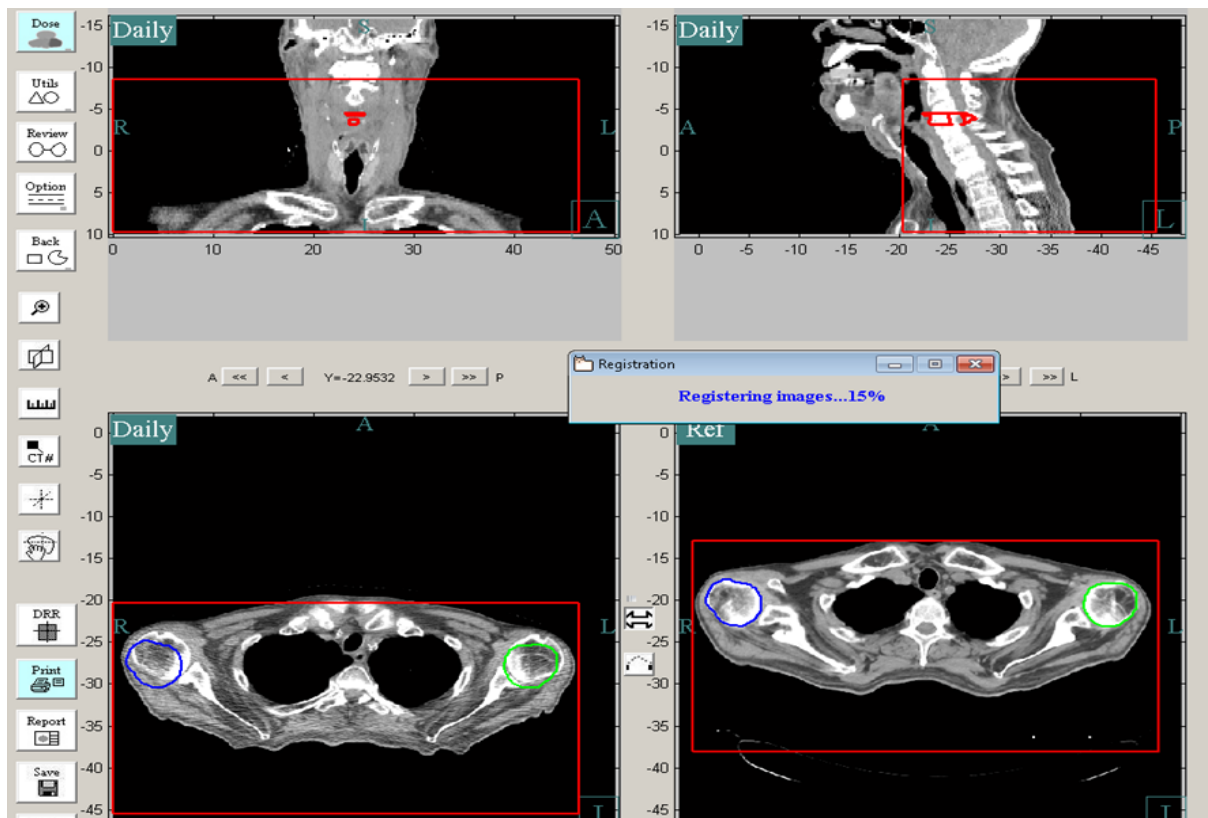


Figure 2-1: CAT registering images: The structures drawn on the Reference scan on the bottom right are being aligned on the daily CT, bottom left.

2.1.3 Calculating the shoulder shift

After C2, was identified, contoured and the reference isocenter set, the right humeral head, and the left humeral head were put on each of the daily scans in CAT, the scans were exported from CAT to the Pinnacle treatment planning system. For each scan, a new patient was created in Pinnacle and the images and contours were imported into that patient. On all of the daily CTs, and on the original treatment CT, points of interest were created in Pinnacle as centroid points marking the centers of C2, the right humeral head, and the left humeral head (Fig. 2-2).

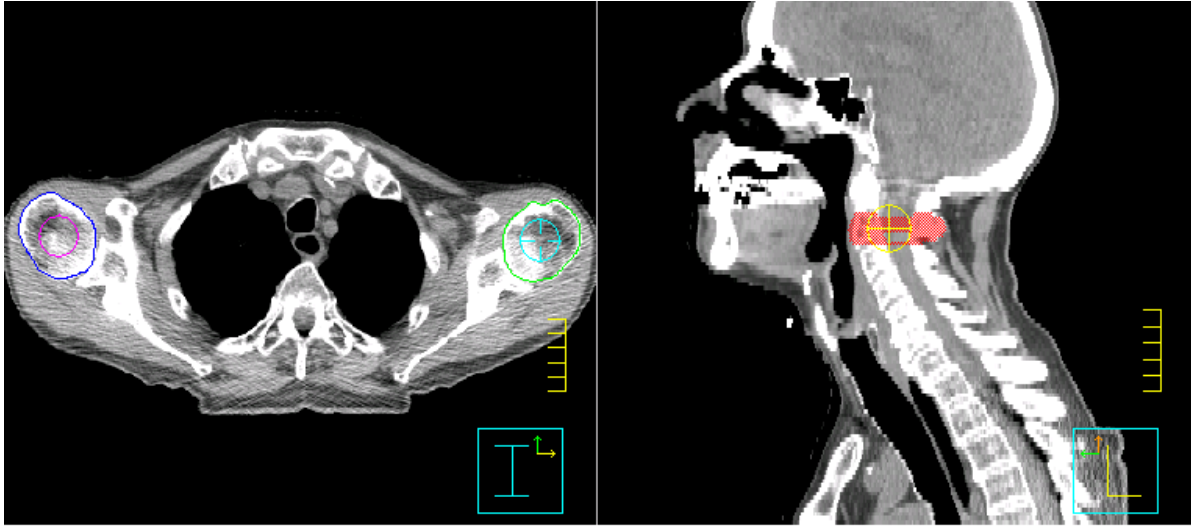


Figure 2-2: Center points of humeral heads and C2

The position of the shoulder on the treatment planning CT was determined by finding the displacement of each humeral head in the superior/inferior, anterior/posterior, and left/right directions with respect to C2 relative to the original structure location and plan. Because the coordinate system of the original plan and the daily CTs had different origin, the displacement was found by subtracting the C2 coordinates from humeral head coordinates. The displacement found on the treatment planning CT was considered to be the initial shoulder position. The displacements on the planning CT were subtracted from the displacements found on subsequent daily CTs to establish the daily difference in shoulder position in each direction. Positive values represented either an inferior, anterior, or left shift, and negative values represented a superior, posterior, or right shift. The average magnitude of the shift in each direction was calculated for each shoulder. An average value that took direction into account so as to have an average displacement over the course of treatment was also calculated.

2.2 Treatment Planning

2.2.1 The Patients and Their Clinical Target Volumes

Three patients were chosen to assess the impact of shoulder shifts on their clinical treatment plans. These patients were a separate population from those whose shoulder shifts were evaluated. The patients selected had lower neck nodes treated by a full set of treatment fields so that the beams extended inferiorly into the shoulder region. Patients that had critical structures near a high dose target were also of interest. The treatment volumes and critical structures were delineated by the physician for their clinical treatment plan. Up to 3 CTVs were drawn. The primary tumor site, CTV1, received the highest dose of 66-72 Gy. Areas with intermediate to high risk of metastasis, CTV2, received 60-63 Gy. Areas with low risk of metastasis, CTV3, received 50-54 Gy. The exact dose to these volumes varied based on the physician's assessment. Patient 1 had a primary tumor treated to 60 Gy (CTV1), and lower neck nodes treated to 57 Gy (CTV2) and 54 Gy (CTV3). Patient 2 had a primary tumor treated to 70 Gy (CTV1), and lower nodes treated to 63 Gy (CTV3) as well as a 65 Gy (CTV2) target surrounding parts of the brachial plexus. Patient 3 had a Primary tumor treated to 60 Gy (CTV1) and nodal volumes treated to 54 Gy (CTV2).

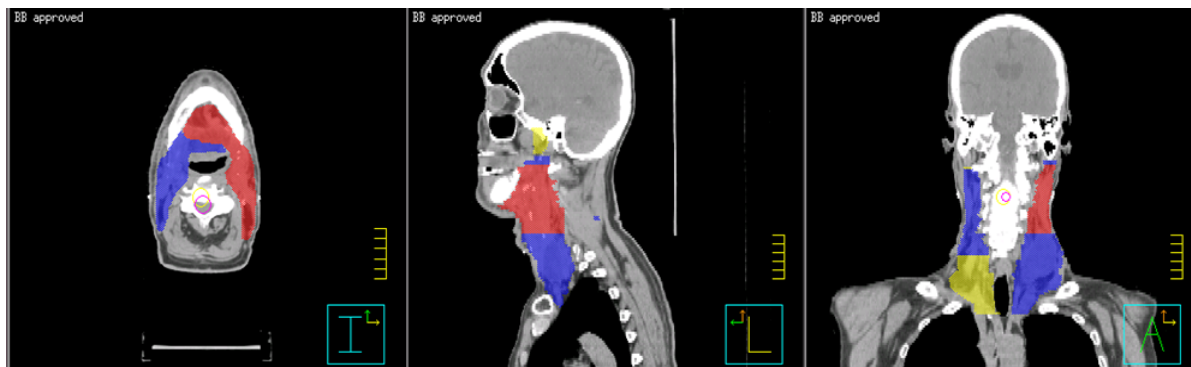


Figure 2-3a: Patient 1 Red CTV 60 Gy, Blue CTV 57 Gy, Yellow CTV 54 Gy

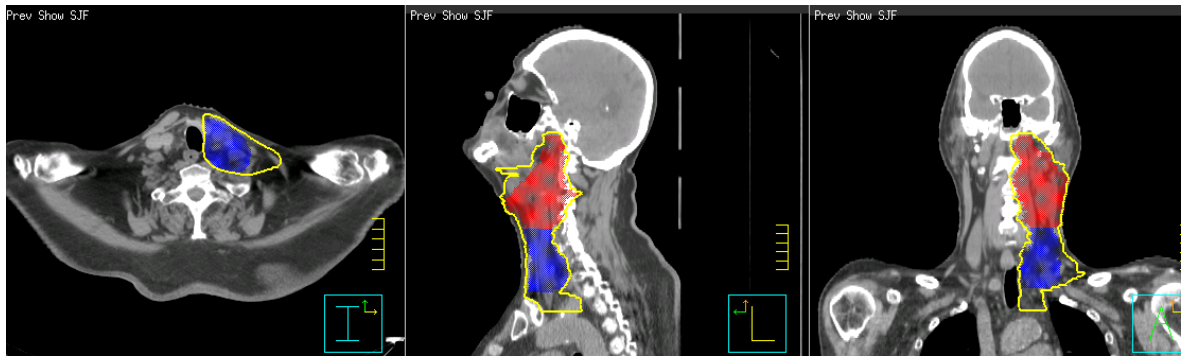


Figure 2-3b: Patient 2: Red CTV 70 Gy, Blue CTV 65 Gy, Yellow (outline) CTV 63 Gy

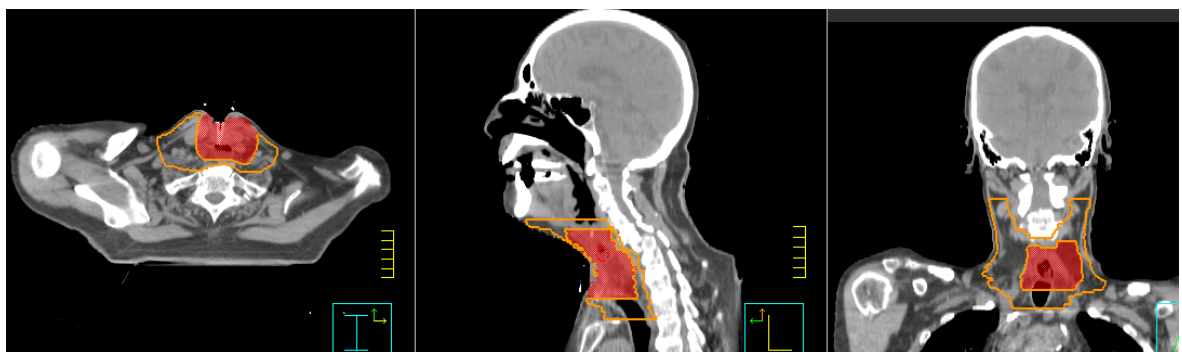


Figure 2-3c: Patient 3: Red CTV 60 Gy, Orange (outline) CTV 54 Gy

2.2.2: The Clinical IMRT plan

The patients were treated clinically with IMRT Plans. The plans were created by dosimetrists at The UT MD Anderson using the Pinnacle treatment planning system version 8.0, and they were planned based on the clinical protocol used at The UT MD Anderson Cancer Center. The planning volumes (PTVs) were made by a 3 mm expansion around the CTVs. The volume of the PTV1 surrounding the primary site (CTV1) was subtracted out of the PTV2 and PTV3 (surrounding CTV2 and CTV3, respectively) to avoid overlapping structures. Additionally PTV2 was subtracted out of PTV3. Planning Risk Volumes (PRV) were created for the spinal cord and brainstem by expanding those structures by 5 mm. A normal tissue avoidance volume was created by subtracting a 1.5 cm expansion around the

PTVs from the patients' entire body contour. An isocenter was marked on the treatment mask during simulation, and either this point, or another point determined more suitable for planning by the dosimetrist, was used as a planning isocenter. A standard plan of nine 6 MV, coplanar, evenly spaced fields (each 40° apart—200°, 240°, 280°, 320°, 0°, 40°, 80°, and 160°) was used for bilateral disease on Patient 3 (Fig. 2-4a) and a 180° beam was also added for Patient 1. For the unilateral disease on Patient 2, a plan with seven fields on one side was used (350°, 20°, 55°, 85°, 120°, 150°, and 175° for left-sided disease, Fig. 2-4b). The 85° beam had the lower jaw closed over the shoulder. For both types the couch was set to 0°, and the collimator was set to optimize coverage, leaf motion, and blocking of critical structures.

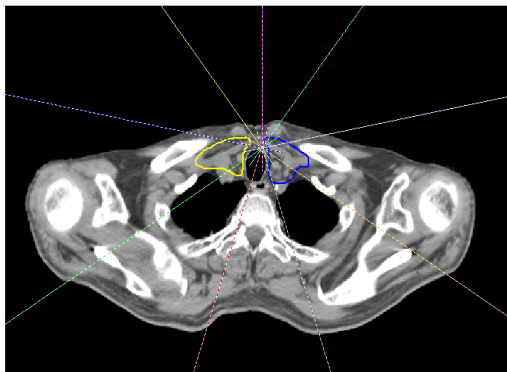


Figure 2-4a: 9 field IMRT beam arrangement: Colored lines represent the central axes of the beams. Two bilateral CTVs (blue and yellow) are contoured.

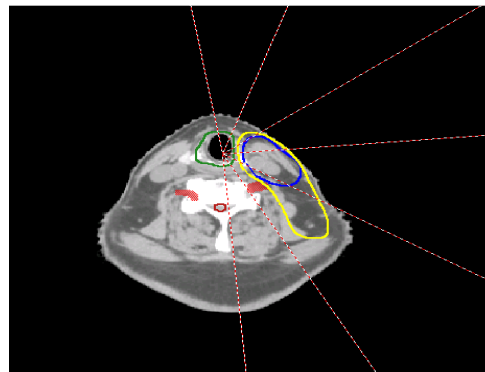


Figure 2-4b: 7 field IMRT beam arrangement: Red lines are central axes of the beams. Two unilateral CTVs (blue and yellow) are contoured.

The fields were optimized to deliver a simultaneous integrated boost to the primary tumor (CTV1) while treating nodal areas (CTV2 and CTV3) to lower doses. The plan prescription was set to the volume PTV1 and given the dose the physician chose for CTV1. The prescription was renormalized to the 98% line for Patients 1 and 2 to improve coverage of the CTVs. For Patient 3, the plan was normalized to the 96% line. The optimization

algorithm used was Direct Machine Parameter Optimization (DPMO), which uses the actual MLC parameters of the machine to calculate the dose for each optimization run. The optimization parameters were set to 15 segments per beam (or a total of 135 segments), for Patients 1 and 3, and 14 segments per beam (or a total of 98 segments) for Patient 2. The minimum MU per segment was set to 2 MU for Patient 1, 3 MU for Patient 2, and 1 MU for Patient 3. The minimum segment size was 2 cm². The maximum number of iterations was set to 20, and the optimization stopped after these 20 iterations or if the convergence between the optimized and the objective value for the plan was 10⁻⁵. The final dose was calculated with the Collapsed-Cone Convolution algorithm. A dose grid of 3 mm was used for Patient 1, and 4 mm was used for Patients 2 and 3. Each of the PTVs was given a Uniform Dose Constraint of the appropriate prescription dose. The PRVs and other organs at risk were given maximum dose constraints or maximum volume constraints. The constraints for critical structures can be found in Table 2-1.

Table 2-1: Dose Constrains for Head and Neck IMRT Planning

| STRUCTURE | DOSE TOLERANCE |
|-------------------------------|---|
| Parotid | Mean dose of 26 Gy |
| Brainstem | Maximum Dose of 54 Gy |
| Spinal Cord | Maximum Dose of 45 Gy |
| Oral Cavity | Mean Dose of 30-33 Gy |
| Brain | Maximum Dose of 50Gy Minimize volume of 30 Gy |
| Optic Nerves and Optic Chiasm | Maximum Dose of 54 Gy |
| Lens | Maximum of 10 Gy |
| Mandible | Maximum of 70 Gy |
| Brachial Plexus | Maximum of 66 Gy to < 1% |
| Cochlea | Maximum of 45 Gy |
| Larynx | Mean Dose of 45 Gy |
| Normal Tissue Avoidance | Max Dose of 40 Gy |

The dose constraints were also varied per the judgment of the physician. For example, Patient 2 had a constraint of 60 Gy to the Brachial Plexus, and Patients 1 and 2 had a mean dose over 26 Gy to at least one parotid due to proximity of CTV1. An acceptable plan was achieved when 99% of each CTV was covered by its prescription dose, and constraints were met for the critical structures. Acceptability of the plan was evaluated by looking at a Dose Volume Histogram (DVH) as seen in Fig. 2-5.

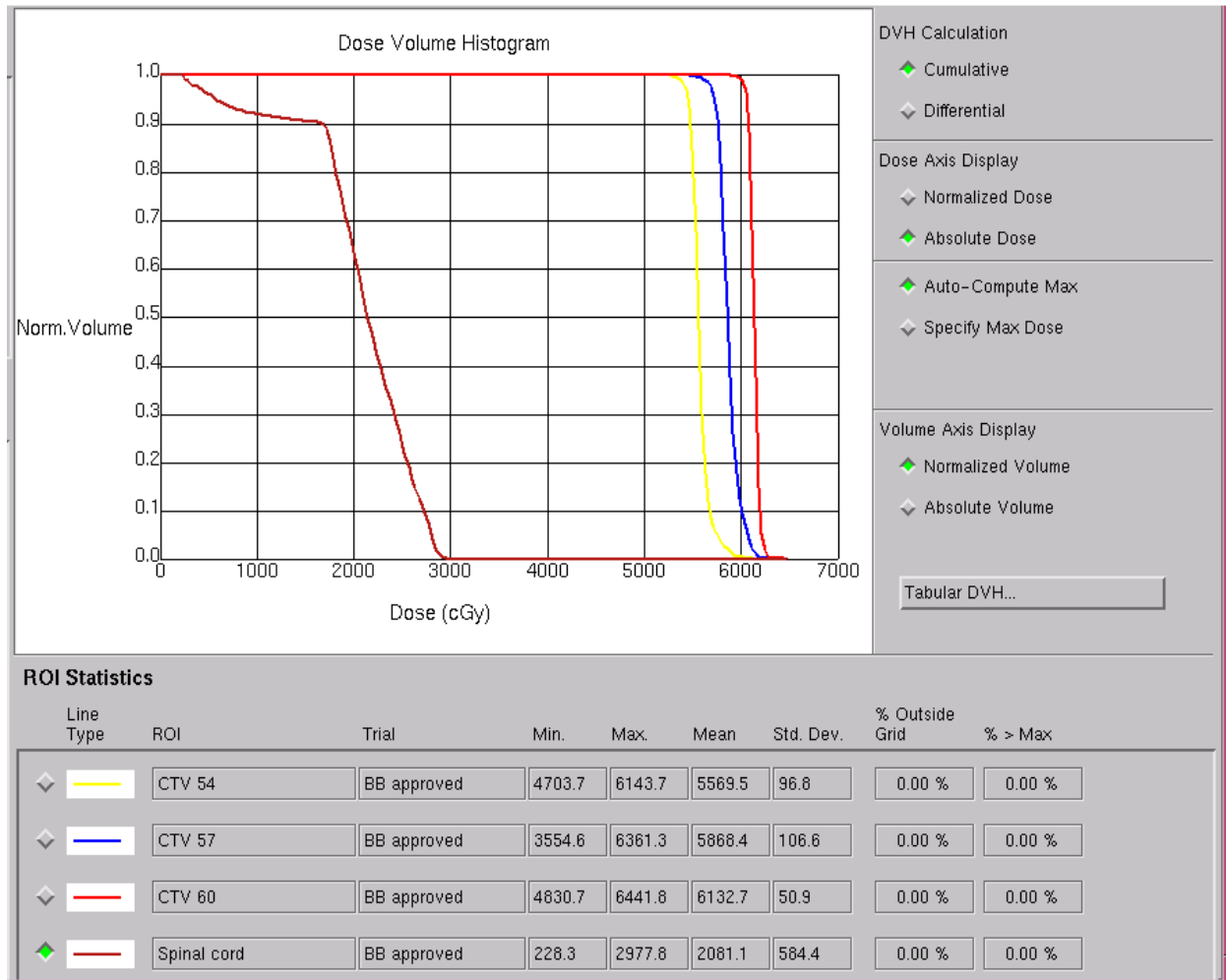


Figure 2-5: Example of Acceptable CTV coverage and Spinal Cord Dose. Ninety-nine percent of the CTVs were covered by the prescription dose, and the cord received less than 45 Gy.

2.2.3 The Non-Clinical Arc Plan

A VMAT treatment was planned by this author on the same CT as the 3 patients' IMRT plans. The VMAT plan was done using SmartArc in Pinnacle version 9.0, which included the SmartArc capability. The same PTVs, PRVs, and isocenter used in the IMRT plan were used in the SmartArc plan. Two arcs were created: one with the gantry moving clockwise from 181° to 180° , and the other with the gantry moving counter-clockwise from 180° to 181° (Fig. 2-6). The collimator was offset by 5° on the plans for Patients 1 and 3 on each arc so the two arcs would not act like parallel opposed beams. At MD Anderson, collimator offsets are used to prevent this effect. The collimator was set to 35° for Patient 2's plan so it matched the RapidArc plan the patient was treated with.

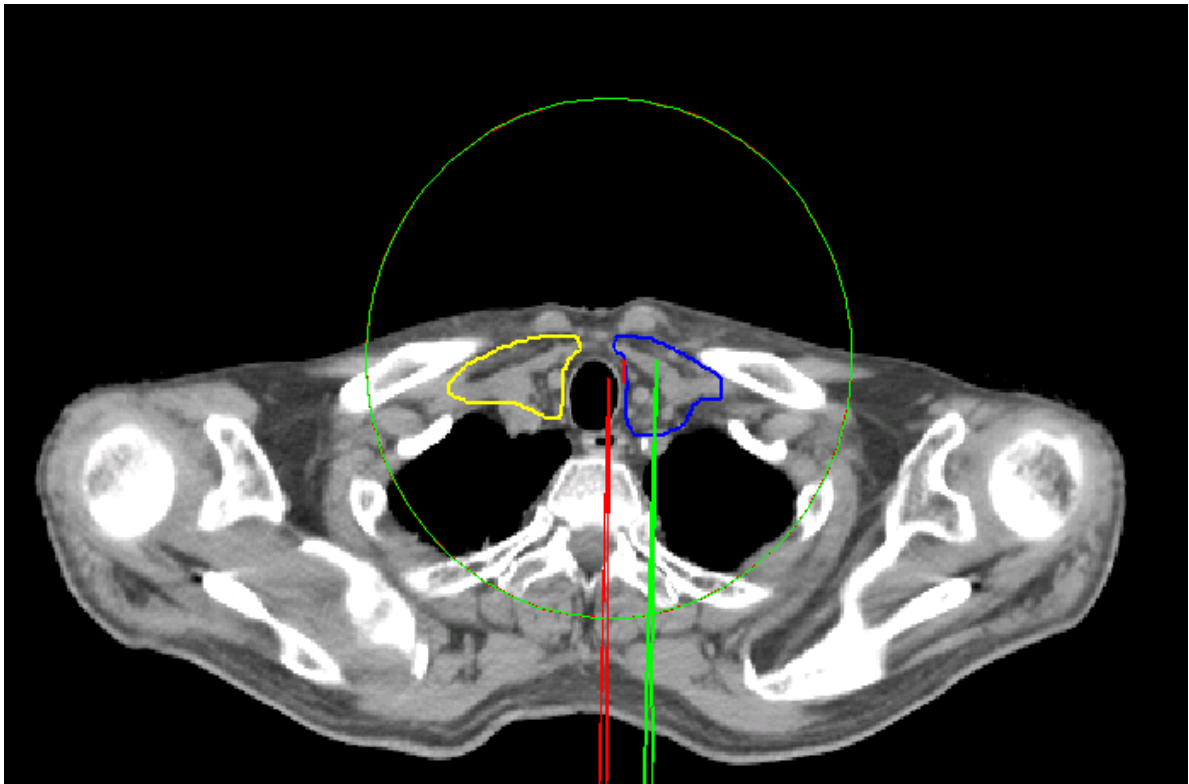


Figure 2-6: Two arcs used for SmartArc plan. Arc 1 (red) rotates counter clockwise around the patient and Arc 2 (green) rotates clockwise around the patient. The paths of the arc overlap.

The initial planning constraints were the same as for the IMRT plan, and then they were edited after further optimization to better suit the SmartArc plan. The beams were optimized with the SmartArc algorithm which created a fluence map every 4° for a total of 91 control points. The minimum segment MU was 2 MU and minimum segment size was 4 cm². The optimizer was stopped after 40 iterations or a convergence between the optimized and the objective value for the plan of 10⁻⁵. After each optimization, a final dose was calculated using the Adaptive Convolve algorithm. Once a clinically acceptable plan was achieved, the dose was recalculated with Collapsed-Cone Convolution. The dose grid was 4 mm x 4 mm x 4 mm. The goal was to create SmartArc plans that were comparable to the patients' IMRT plans (Fig. 2-7) using similar dose prescriptions and constraints.

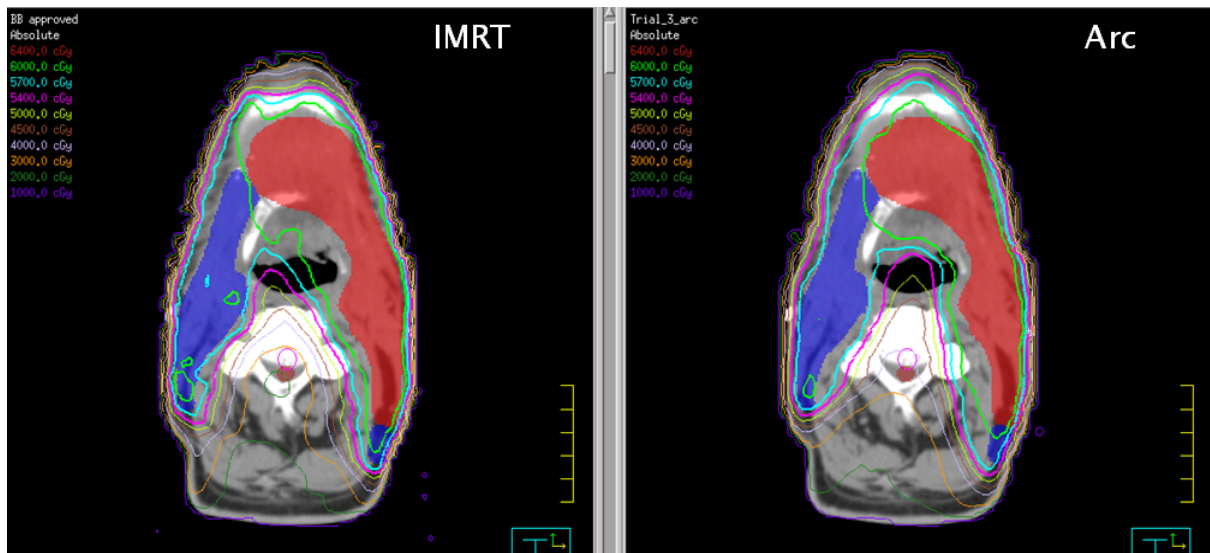


Figure 2-7: Comparable IMRT and SmartArc Plans for Patient 1

2.3 Applying the Shifts and Evaluating the Impact on the Treatment Plans

2.3.1 Choosing the shifts to evaluate

In order to assess the impact of shoulder displacement on dose distribution for each of the three patients in this study, a set of shifts were chosen to model the impact of an average shift and a worst case scenario. The shifts chosen as a model were 3 mm, 5 mm, and 15 mm in the superior and inferior directions, 3 mm and 15 mm in the anterior and posterior directions, and 15 mm in either the right or left direction. Each of the shoulders was moved in the same direction and by the same amount for each evaluation.

The magnitude and direction of the shifts were chosen based on the data found using CAT to analyze the position of the right and left humeral heads on daily CTs. The choice of shifts was also influenced by the results of the study done at Brigham and Women's in 2008 as discussed in section 1.3, where most of the shifts greater than 10 mm were in the right or left direction. More shifts were analyzed in the superior and inferior direction based on the expectation that movement into or out of the treatment fields in these directions would have a greater impact than movement within the treatment fields in an anterior, posterior, or lateral direction.

2.3.2 Modeling the shifts with “hand editing”

The shifts described above were modeled on the original treatment plan by adjusting the body contours and redrawing bony anatomy in the Pinnacle treatment plan. The method of drawing each shift by hand was chosen so that the motion of the shoulder could be isolated. Recalculating the original treatment plan on the daily CTs that were available would have included the impact of internal motion, tumor shrinkage, and other anatomical

changes. Editing the contours by hand to represent the position of the shoulder allowed for isolated analysis of the impact of shoulder motion only.

2.3.3 Drawing the superior and inferior shifts

The superior and inferior shifts were created by copying the contours for the body, the right and left humeral heads, and the bones in the shoulder (the acromion, and the lateral parts of the clavicle and scapula) superiorly or inferiorly the appropriate amount. The slices copied extended 9-10 cm from the base of the neck to the axilla. Only bones that were considered to have translational motion with the motion of the shoulder were adjusted. Rotational motion was not feasible to draw. For the 3 mm and 5 mm superior and inferior shifts, the acromion, clavicle, and scapula were not expected to have as much influence as the humeral heads and were not contoured. The anatomy located centrally in the thorax was not expected to move. Each CT slice was spaced 2.5 mm.

The 3 mm superior shift was created by copying the body surface contour on each slice to one slice superior. The medial anterior and posterior aspects of the contour along the chest and the back, where no motion would occur if the shoulders were the only thing displaced, were edited to be flush with the CT image on each slice. This newly created contour extended outside of the CT image around the shoulders, so the volume within this contour (and outside the original body surface) had its density set to that of tissue, 1 g/cc. The contours for the right and left humeral heads were also shifted superiorly by one slice. The density of new, 3 mm shifted humeral heads was set to the average density of the original humeral heads as calculated by Pinnacle.

Similarly, the 3 mm inferior shift was drawn by copying each slice of the body surface contour inferior one slice. Again, the medial anterior and posterior aspects of the

contour along the chest and the back were edited to be flush with the CT image on each slice. At the shoulders, the new 3 mm shifted contour was inside the CT image, so a structure that was the subtraction of the original body surface contour and the shifted contour was created and the density was set to that of air, 0 g/cc. The contours for the right and left humeral heads were copied inferiorly by one slice, and the density of the shifted contour was set to the average density of the original as calculated by Pinnacle. Because the new humeral heads were inferior to the originals, a structure was created by subtracting the shifted from the originals and the density was set to 1 g/cc to represent soft tissue at the superior aspect of the non-shifted humeral heads.

Additionally, the 5 mm superior and 5 mm inferior shifts were drawn in the exact same manner, except each contour was copied 2 slices superior or inferior.

The 15 mm superior shift (Fig 2-8) was created by copying the body contour superior 6 slices. Again, the medial parts of the contour were edited to be flush with the chest and back. The most superior slices of the contour were edited to gradually conform to the CT image so there would not be a large change in patient thickness from the last slice of the new (shifted) contour and the original patient surface. The density of the area of the new contour that extended outside the CT image was set to 1 g/cc. The humeral heads were each copied superior 6 slices, and their densities were set to the average of the originals. Inferior to each new, shifted humeral head, the contour of the humerus was copied superiorly to meet the inferior slice of the shifted humeral heads. The bone outside the extended humerus that was part of the original humeral head was set to a density of 1 g/cc so it would represent soft tissue. The contour for the acromion, and lateral aspects of the clavicle and scapula were also shifted superiorly 6 slices and set to a density that was an average of the original

contour as calculated by Pinnacle. The new bony contours were subtracted from the old contours, and this structure had its density set to 1 g/cc. Any overlap between bone structures and soft tissue structures was avoided by contour subtraction. Areas that needed to have a density of bone were subtracted out of areas that needed to be soft tissue.

Similarly, for the 15 mm inferior shift (Fig 2-9), the body surface contour was copied inferiorly 6 slices. Again, the medial aspects of the contour were edited to conform to the chest and back, and the most superior slices of the new contour were edited to gradually conform to the CT image. The areas of the patient that extended beyond the new, shifted contour were set to a density of 0 g/cc. The humeral heads were copied 6 slices inferior, and their densities were set to the original average density. The superior aspects of the original humeral heads that did not overlap with the new, shifted humeral heads were set to a density of 1 g/cc. The acromion and lateral parts of the clavicle and scapula were also copied 6 slices inferior and set to the average density of the originals. The original contours were set to a density of 1 g/cc while avoiding any overlap between areas that needed to have the density of tissue and areas that were now outside of the patient and needed to have the density of air.

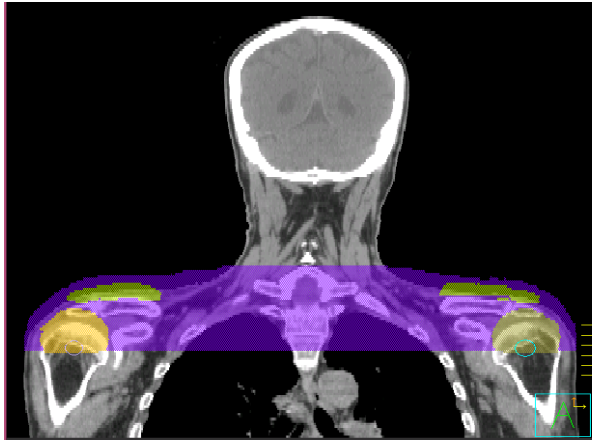


Figure 2-8: 15 mm Superior Shift. The body contour is in purple, the humeral heads in orange and the shoulder bones in yellow. All are shifted 6 slices superiorly.

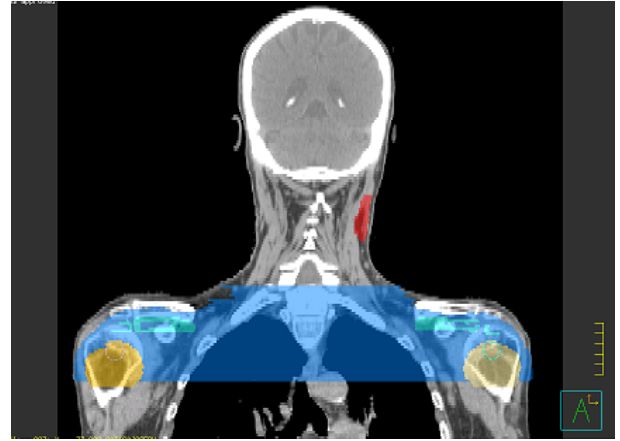


Figure 2-9: 15 mm Inferior Shift. The body contour is in light blue, the humeral heads in orange, and the shoulder bones in turquoise. All are shifted 6 slices inferiorly.

2.3.4 Drawing the anterior and posterior shifts

The 3 mm anterior shift was drawn with the aid of the measuring and labeling tool in Pinnacle. On each slice, a line of 3 mm in length was drawn perpendicular to the body surface contour in the anterior direction. The whole contour was then moved 3 mm anterior along this line. This was repeated on every slice of the body contour. The medial parts of the new, shifted contour were edited to conform to the CT image just as they were for the superior and inferior shifts. At the shoulders, an anterior portion of the new body surface contour was outside the CT image and a posterior portion was inside the contour. Subtracting the original contour from the new contour allowed the density of the anterior portion to be set to 1 g/cc to represent soft tissue. Subtracting the new contour from the original contour allowed the density of the posterior portion to be set to 0 g/cc to represent air. The humeral heads were not shifted, as a 3 mm shift would not significantly alter the density correction in this direction.

The 3 mm posterior shift was drawn in the same way. A 3 mm line was drawn perpendicular to the posterior surface on each slice of the original body contour, and the contour on each slice was moved along it. The new contour was edited to conform to the chest and back. At the shoulders, an anterior portion of the new, shifted contour was inside the CT image and a posterior portion was outside the image. The anterior portion had the density set to 0 g/cc by creating a contour that was the subtraction of the new from the original. The posterior portion had the density set to 1 g/cc by creating a contour that was the subtraction of the original from the new. Again the humeral heads were not moved in this direction.

The body surface contour for the 15 mm anterior shift (Fig. 2-10) was designed in the same fashion as the 3 mm shifts, by using a 15 mm line perpendicular to the anterior surface of the original body contour. The densities of the anterior and posterior portions of the new shifted contour that were outside and inside the CT image were also set to 1 g/cc and 0 g/cc, respectively. The measure and label tool was also used to move the humeral heads, the acromion, and the lateral aspects of the clavicle and scapula in the same fashion as the body contour. The humeral heads and the shoulder bones were set to the average density of each as calculated by Pinnacle for the original contour. For all of the bones, the parts of the original contours that were outside the new contours were outlined by subtracting the new from the original contours and the densities were set to 1 g/cc to represent soft tissue. Again overlap between structures that needed have different densities was avoided.



Figure 2-10: 15 mm Anterior Shift: The new body contour is in aqua. The areas of the shift where the shoulder comes off the CT image has a density forced to 1. The humeral heads (peach and red) are shifted anteriorly and have density set to bone. The areas on the CT image where the body is no longer present have density set to 0.

The 15 mm posterior shift (Fig. 2-11) was drawn the same way as the 3 mm posterior shift. Using subtracted contours, the density of the anterior portion of the CT image that was outside the new, shifted contour was set to 0 g/cc for air and the posterior portion of the contour that was outside the CT image was set to a density of 1 g/cc for soft tissue. The humeral heads, acromion, and lateral aspects of the scapula and clavicle were also shifted 15 mm posterior using the measure and label tool as a guide. Each of the new bone contours had the density set to the average of its corresponding original, and the portions of the original shoulder bone contours that were not part of the new contours were subtracted out and set to a density of 1 g/cc.

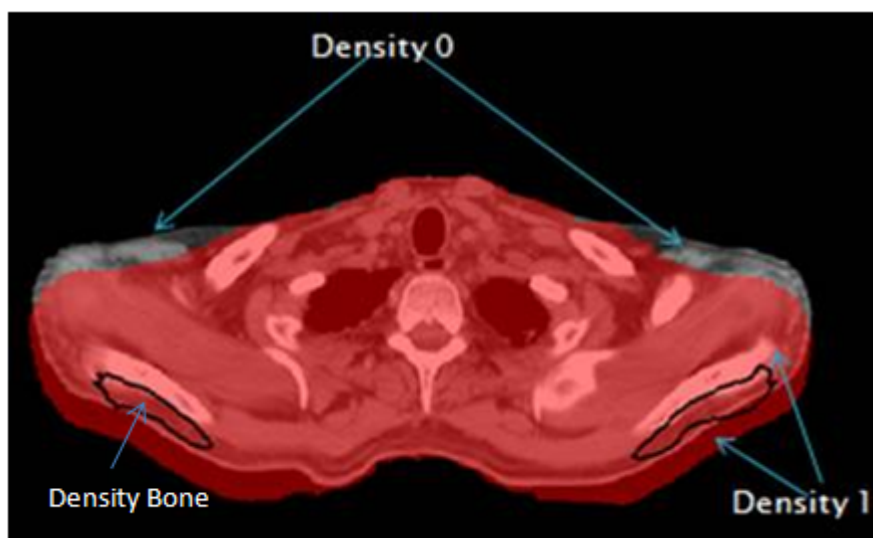


Figure 2-11: 15 mm posterior shift: The new body contour is in read. Areas where the tissue in the image is no longer part of the contour have a density forced to 0. Areas where new tissue has moved have density forced to 1. The area of the new position of the bones has density forced to bone.

2.3.5 Drawing the right or left shift

Each of the patients was given either a 15 mm right or 15 mm left shift (Fig 2-12). The shift was made using the measure and label tool to draw a 15 mm line on every slice of the body surface contour perpendicular to the right or left side of the patient, and then moving the contour 15 mm along this line. The new, shifted contour was edited to conform to the chest and back. The new contour extended beyond the CT image in the direction of the shift and cut inside the CT image on the opposite side. By subtracting the old contour from the new one a structure was made on the side where the new contour extended outside the CT image, and its density was set to 1 g/cc to represent soft tissue. By subtracting the new contour from the old contour, a structure was made on the side where the new contour cut into the CT image, and this was given a density of 0 g/cc to represent air. The right and left humeral heads, the acromion, and the lateral aspects of the clavicles and scapulae were also shifted 15 mm right or left using the measure and label tool as a guide. The new, boney

contours were given the average density from the original contours. The new, shifted contours were subtracted from the original contours, and this structure was given a density of 1 g/cc. Overlap of areas where tissues needed to be set to bone, air, or tissue density was avoided using structure subtraction.



Figure 2-12: 15 mm left shift. The new body contour is in magenta. The bones of the shoulder have also been shifted and the areas are forced to density of bone. The areas where tissue is absent is forced to density 0 and the areas where tissue is now present is forced to density 1.

2.3.6 Evaluating the impact of each shift on dose distribution

To assess the impact of the shifts on the dose distribution, two parameters were evaluated: target coverage and dose to critical structures. For each of the patients' CTVs, the volume of the CTV receiving 100%, 98% and 95% of the prescription dose in their original IMRT and SmartArc plans was recorded. Additionally the volume of the spinal cord receiving a tolerance dose of 45 Gy and a typical, planned mean dose of 25 Gy was recorded, as well as the maximum point dose and the maximum dose to 0.1 cc of the spinal cord. The volume of the brachial plexus receiving 75 Gy (the tolerance dose for 50%

complications in 5 years) and 60 Gy (the TD 5/5) was recorded along with the maximum point dose and the maximum dose to 0.1 cc of the brachial plexus. This information was found using the DVH tables in Pinnacle.

For each of the shifts drawn, the patients' IMRT and SmartArc plans were recalculated without changing any treatment parameters. By setting the densities to 1 g/cc inside the body contour or 0 g/cc outside the body contour, and by setting the density of the new, shifted bony contours to their original average density, the calculation algorithm treated those areas as if they were tissue, air or bone and produced a dose distribution that showed how the plan would look if the patient had his or her shoulders in the shifted position. The same CTV, spinal cord and brachial plexus dose parameters that were recorded for the original plans were recorded for each of the shifted plans. The values for the original plans were subtracted from the values for the shifted plans. For the volume of CTVs receiving 100%, 98%, and 95% of the prescription dose, a negative result of the subtraction indicated that the CTV lost coverage and a positive result would indicate that it gained coverage. For the volume of the spinal cord and brachial plexus receiving a certain dose, a negative result of the subtraction indicated that less of the structure volume received that dose and a positive result meant that more of the structure received that dose. For the maximum doses to the spinal cord and brachial plexus the results of the subtraction indicated whether the maximum dose to the structure increased or decreased. Clinically significant loss of CTV coverage and increase in dose to critical structures were the main points of interest. Clinical significance was determined by whether the change in dose distribution rendered the treatment plan unacceptable for patient treatment based on the standards described in section 2.2.2.

2.4 Verification of the dose findings using CT data

2.4.1 Choosing a patient for verification

In order to confirm the results found by editing the patient contours by hand, two treatment plans were recalculated on a daily CT that showed large, superior humeral head shifts from one day to the next day. Using two scans taken one day apart was intended to remove the effects of tumor response and other anatomical changes. Two patients were chosen. The first patient, Case 1, had left shoulder shifts of 1.12 cm left, 0.42 cm anterior, and 1.32 cm superior; and right shoulder shifts of 1.04 cm right, 0.46 cm posterior, and 2.77 cm superior between CT 12 and CT 13. The other patient, Case 2, had left shoulder shifts of 0.05 cm right, 0.09 cm anterior, and 1.04 cm superior; and right shoulder shifts of 0.06 cm left, 0.36 cm anterior, and 1.01 cm superior between CT 8 and CT 9. The first scan (CT 12 for Case 1 and CT 8 for Case 2) was used as a baseline, and the second scan (CT 13 and CT 9) was compared to the baseline to see the effect of the shift.

2.4.2 Comparing the daily CT shift to the hand edited shift

Neither of the patients that demonstrated these large daily shifts had a standard 9-field IMRT plan for their treatment, therefore, a 9-field plan was created for the original planning CT. The CAT software was used to apply the plan and the target volumes from the planning CT to the two daily scans. An alignment set consisting of the CTV, PTV and the vertebral bodies used for each patient's isocenter setup was created. Deformable image registration was used to put the structures on the scan. A Pinnacle coding script was used to send the treatment plan to CAT so that both the treatment plan and the daily CT could be exported back to Pinnacle together. The original treatment plan was calculated on the

baseline CT, and the V100%, V98% and V95% for the CTV and PTV were recorded. Case 1 had a single CTV prescribed to 40 Gy and Case 2 had a single CTV prescribed to 36 Gy.

After the plan was calculated on the baseline CT, the shoulder shifts stated above were drawn onto the baseline CT using the methods described in sections 2.3.3-2.3.5. The plan was recalculated with the drawn shifts and the volumes (cc) covered by 100%, 98% and 95% were recorded again. The difference between the volumes covered with the shoulder shift and the baseline was found. Next, the plan was recalculated on the next day's scan that represented the shoulder shift, and the same parameters were recorded. The values for the shifted plan were subtracted from the values for the baseline plan, and the difference was compared to the results of the shift that was drawn by hand.

CHAPTER 3: Results

3.1 Measured Shoulder Shift from CT on Rails Data

To determine the daily shoulder displacement for 4 patients, the center coordinates of the right and left humeral head were compared to the center coordinates of vertebral body nearest to isocenter (usually C2) in Pinnacle. The Pinnacle x, y and z coordinates represent the RL, AP and SI directions, respectively. The magnitude and direction of the shoulder shifts were evaluated for each patient and are displayed in Figures 3.1-3.8.

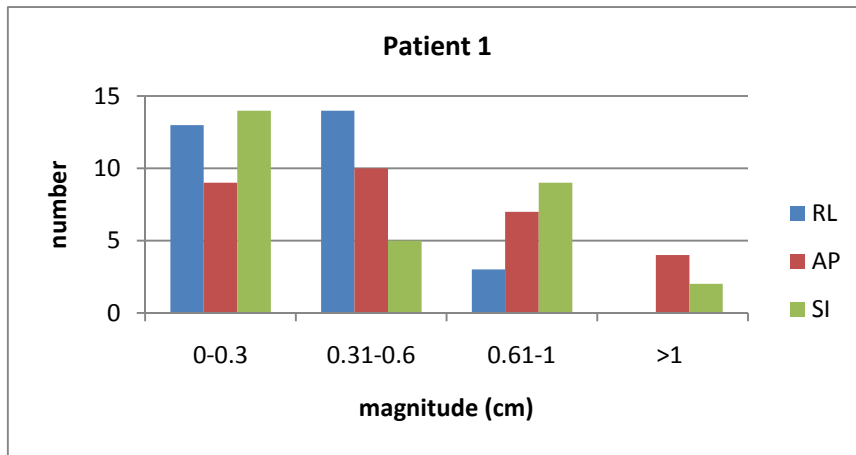


Figure 3.1: Patient 1 shoulder shifts broken down by 3 orthogonal directions. The magnitude of the shifts is on the x-axis and the frequency of shifts is on the y-axis.

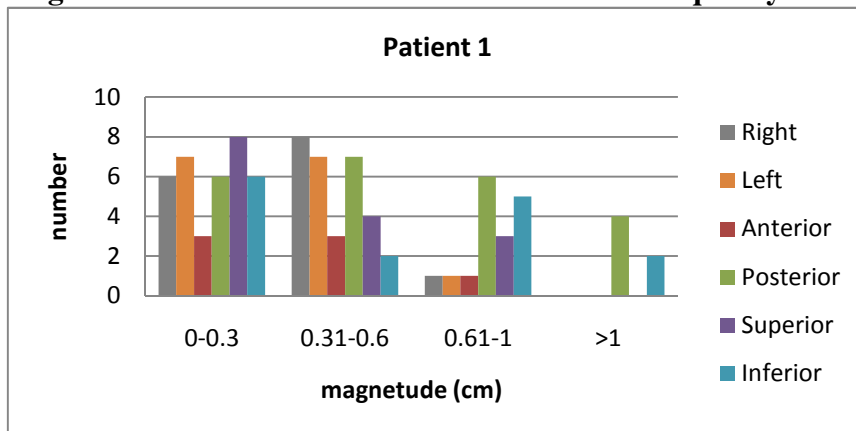


Figure 3.2: Patient 1 shoulder shifts broken down by all 6 directions. The magnitude of the shift is on the x-axis and the frequency of the shift is on the y-axis.

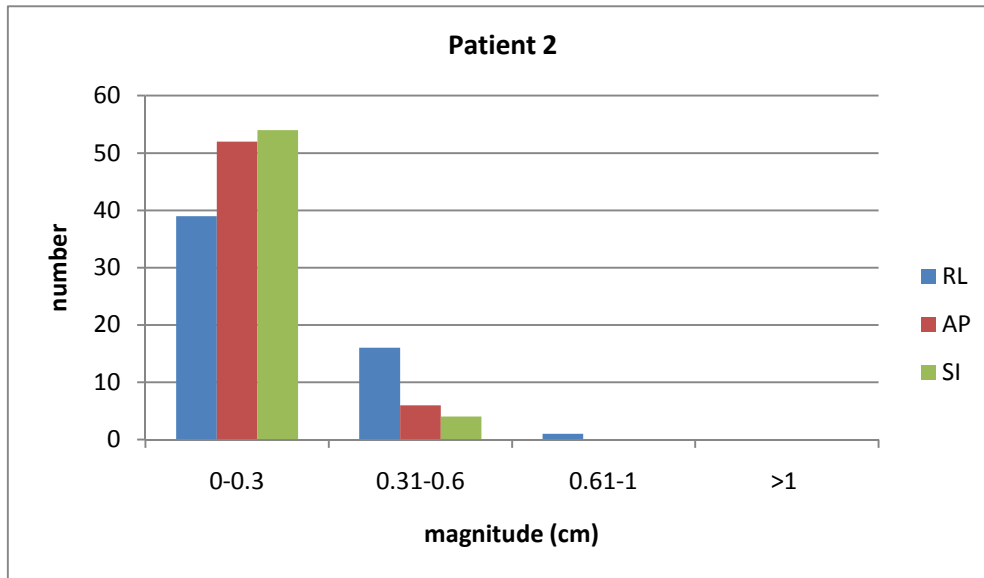


Figure 3.3: Patient 2 shoulder shifts broken down by 3 orthogonal directions: The magnitude of the shift is on the x-axis and the frequency of the shift is on the y-axis.

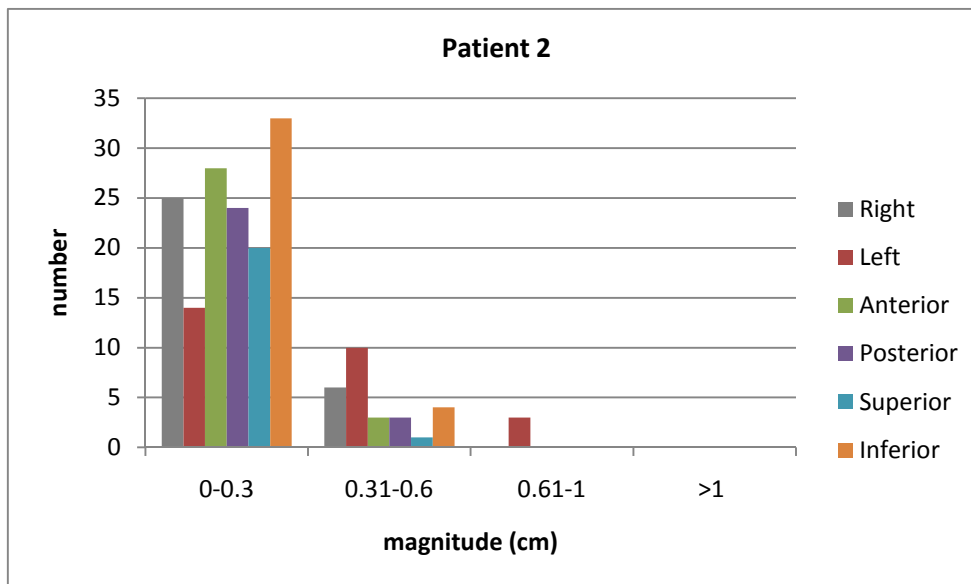


Figure 3.4: Patient 2 shoulder shifts broken down by all 6 directions: The magnitude of the shift is on the x-axis and the frequency of the shift is on the y-axis.

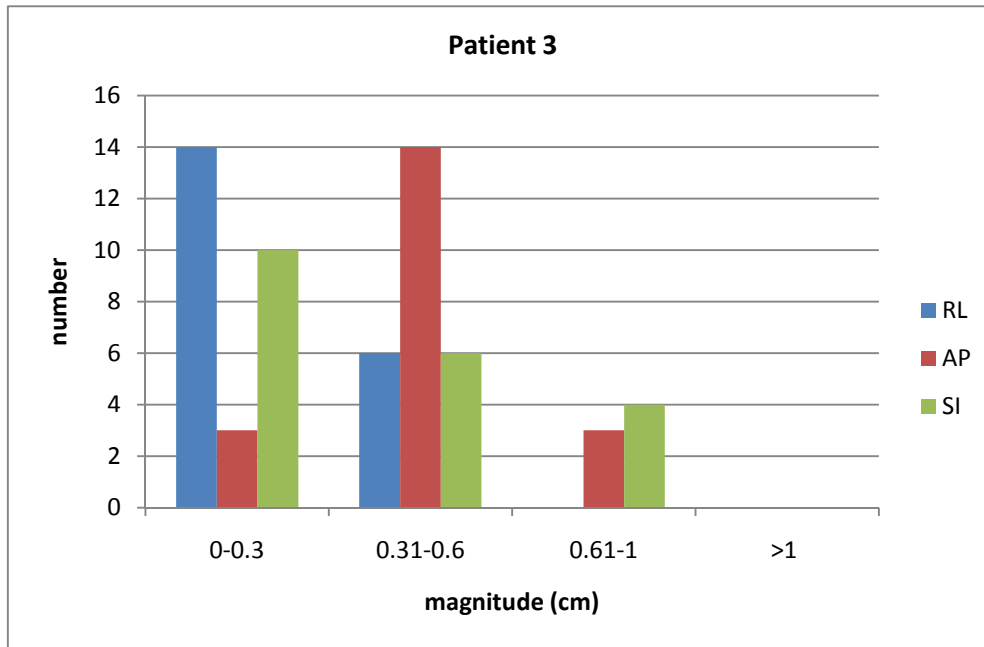


Figure 3.5: Patient 3 shoulder shifts broken down by 3 orthogonal directions: The magnitude of the shift is on the x-axis and the frequency of the shift is on the y-axis.

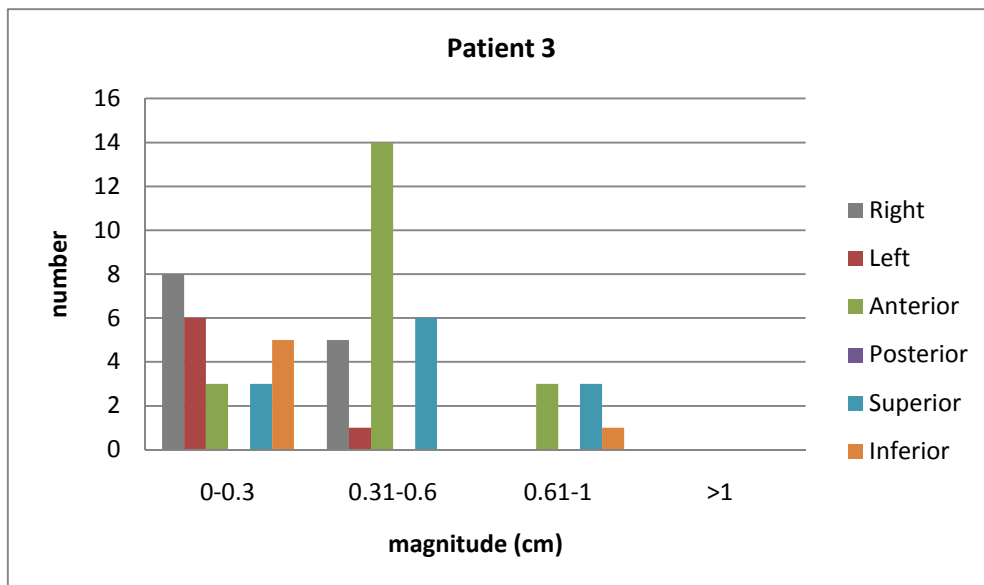


Figure 3.6: Patient 3 shoulder shifts broken down by all 6 directions: The magnitude of the shift is on the x-axis and the frequency of the shift is on the y-axis.

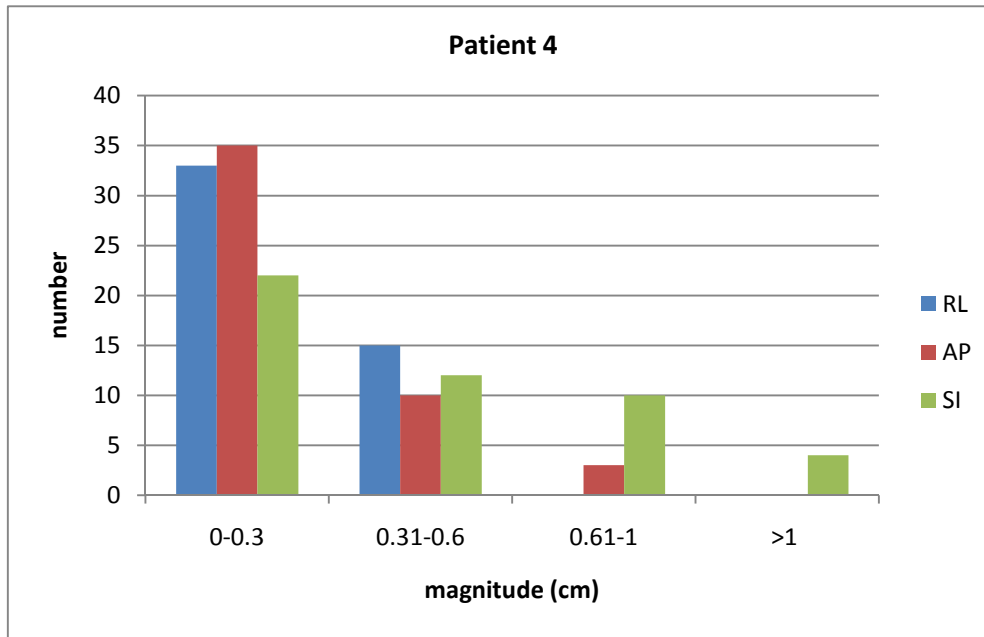


Figure 3.7: Patient 4 shoulder shifts broken down by 3 orthogonal directions: The magnitude of the shift is on the x-axis and the frequency of the shift is on the y-axis.

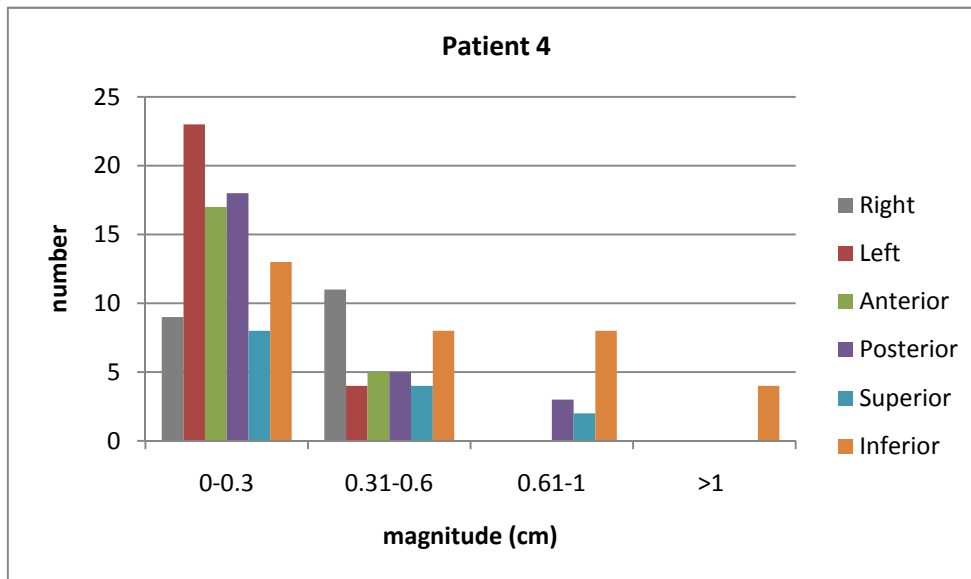


Figure 3.8: Patient 4 shoulder shifts broken down by all 6 directions: The magnitude of the shift is on the x-axis and the frequency of the shift is on the y-axis.

As shown in Figs.3.1-3.8, the majority of the shifts are less than 6 mm, however, large shifts of greater than one centimeter do occur as seen for patients 1 and 4. Patient 1 appeared to have the largest shifts while patients 2 and 3 had the smallest shifts. In the RL direction,

97% of the shifts were less than 6 mm, and 0% were greater than 1 cm. In the AP direction, 89% of the shifts were less than 6 mm and 3% of the shifts were greater than 1 cm. In the SI direction, 82% of the shifts were less than 6 mm and 4% of the shifts were greater than 1 cm. The average magnitude of the shifts as well as an average that took the direction into account were computed. Positive values indicated left, anterior and inferior shift directions. Negative values indicated right, posterior, and superior shift directions. These averages are displayed in Table 3-1.

| Table 3-1: Average Observed Shoulder Shift for Each Patient (cm) | | | | | |
|--|---------------------|-------------------|---------------------|-------------------|---------------------|
| | | Right Shoulder | | Left Shoulder | |
| | | Average Magnitude | Average w/direction | Average Magnitude | Average w/direction |
| RL | <i>Pt. 1</i> | 0.36 | -0.25 | 0.36 | 0.23 |
| | <i>Pt. 2</i> | 0.29 | -0.25 | 0.18 | -0.18 |
| | <i>Pt. 3</i> | 0.16 | -0.03 | 0.30 | -0.26 |
| | <i>Pt. 4 Plan 1</i> | 0.12 | 0.10 | 0.11 | 0.06 |
| | <i>Pt. 4 Replan</i> | 0.18 | 0.18 | 0.38 | -0.38 |
| AP | <i>Pt. 1</i> | 0.87 | -0.81 | 0.35 | -0.09 |
| | <i>Pt. 2</i> | 0.19 | 0.06 | 0.14 | -0.03 |
| | <i>Pt. 3</i> | 0.42 | 0.42 | 0.50 | 0.50 |
| | <i>Pt. 4 Plan 1</i> | 0.20 | 0.07 | 0.15 | 0.06 |
| | <i>Pt. 4 Replan</i> | 0.35 | -0.33 | 0.29 | 0.16 |
| SI | <i>Pt. 1</i> | 0.45 | 0.09 | 0.44 | 0.16 |
| | <i>Pt. 2</i> | 0.17 | 0.08 | 0.16 | 0.10 |
| | <i>Pt. 3</i> | 0.46 | -0.46 | 0.13 | 0.08 |
| | <i>Pt. 4 Plan 1</i> | 0.53 | 0.43 | 0.61 | 0.60 |
| | <i>Pt. 4 Replan</i> | 0.29 | -0.19 | 0.55 | 0.48 |

Table 3-1: The average observed shoulder shift for each patient (cm): The average wshift on the right and left shoulders was 2-5 mm, with the exception of patient 1 who had an average shift of 8.1 mm in the AP direction.

Except for Patient 1, who had an average shifts over 0.8 cm in the AP direction, both the average magnitude of shoulder shift and average including direction were 2-5 mm in the RL, AP and SI directions. In addition to the average shoulder displacement, the maximum shoulder shift in each direction was tabulated in Table 3-2.

| Table 3-2: Maximum Observed Shoulder Shift (cm) | | | |
|---|---------------------|----------------|---------------|
| | | Right Shoulder | Left Shoulder |
| RL | <i>Pt. 1</i> | 0.73 | -0.58 |
| | <i>Pt. 2</i> | 0.76 | -0.44 |
| | <i>Pt. 3</i> | -0.34 | -0.49 |
| | <i>Pt. 4 Plan 1</i> | 0.17 | 0.15 |
| | <i>Pt. 4 Replan</i> | 0.36 | -0.58 |
| AP | <i>Pt. 1</i> | -1.83 | 0.92 |
| | <i>Pt. 2</i> | -0.45 | -0.43 |
| | <i>Pt. 3</i> | 0.74 | 0.92 |
| | <i>Pt. 4 Plan 1</i> | 0.43 | 0.29 |
| | <i>Pt. 4 Replan</i> | -0.99 | 0.72 |
| SI | <i>Pt. 1</i> | 1.15 | 1.96 |
| | <i>Pt. 2</i> | 0.55 | 0.44 |
| | <i>Pt. 3</i> | -0.83 | 0.61 |
| | <i>Pt. 4 Plan 1</i> | 1.33 | 1.77 |
| | <i>Pt. 4 Replan</i> | -0.91 | 0.96 |

Table 3-2: The Maximum observed shoulder shifts for all patients. The largest shifts, greater than 1 cm were seen in the posterior and inferior directions for Patients 1 and 4.

The largest shifts were seen in the posterior and inferior directions. The magnitude of the shifts were plotted versus fraction to determine any trends in the size of shift, and to better understand when during the course of treatment larger shifts might be likely. This was done for patients 1, 2 and 3 as seen in the scatterplots in figures 3.9-11, respectively. Patient 4 had several CTs for the first plan, so the shifts were plotted for each scan taken as seen in Figure 3.12. The second, replan shoulder shifts were plotted versus fraction (Fig. 3.13). In the plots below, the displacement of the shoulder in each direction is plotted vs. fraction.

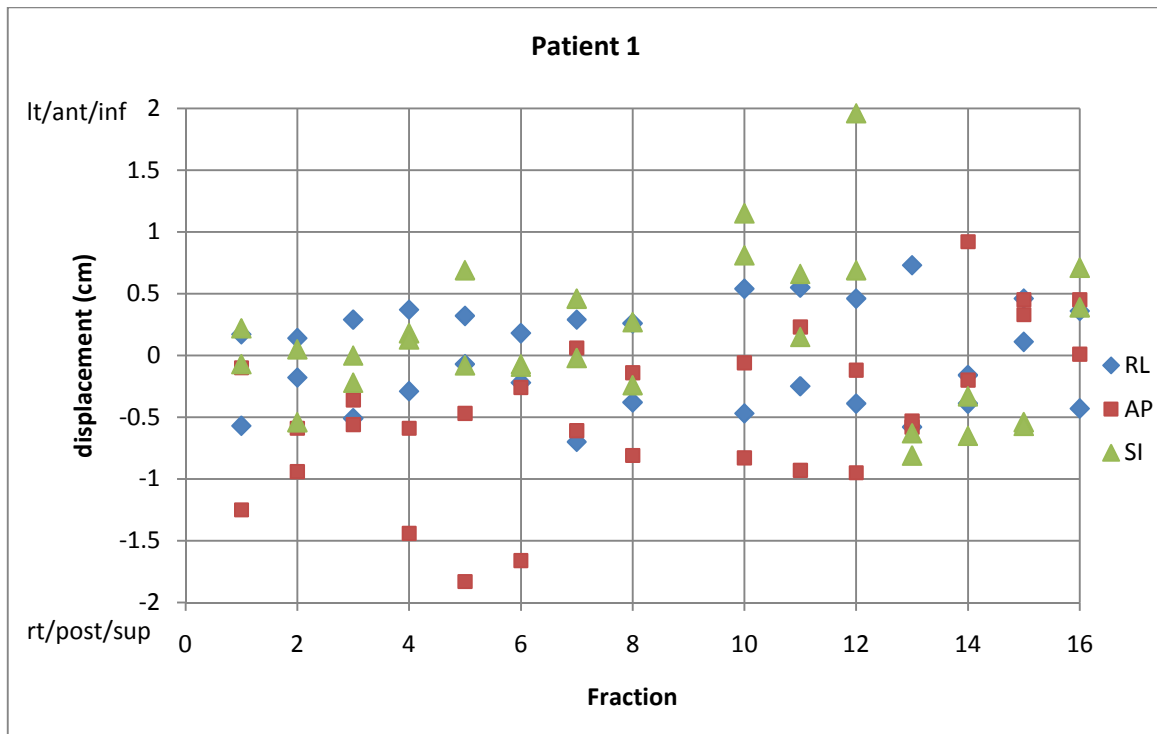


Figure 3.9: Shoulder Shift vs. Fraction for Patient 1: RL shifts are in blue, AP in red and SI in green. Positive displacement is in the left, anterior or inferior direction. Negative displacement is in the right, posterior or superior direction.

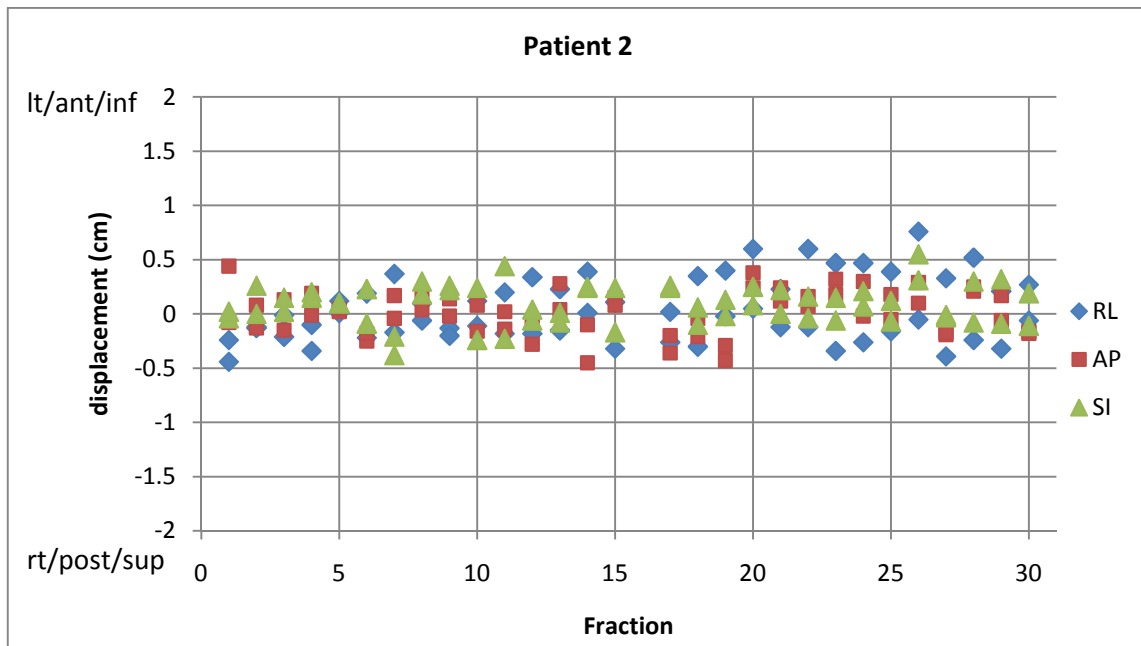


Figure 3.10: Shoulder Shift vs. Fraction for Patient 2: RL shifts are in blue, AP in red and SI in green. Positive displacement is in the left, anterior or inferior direction. Negative displacement is in the right, posterior or superior direction.

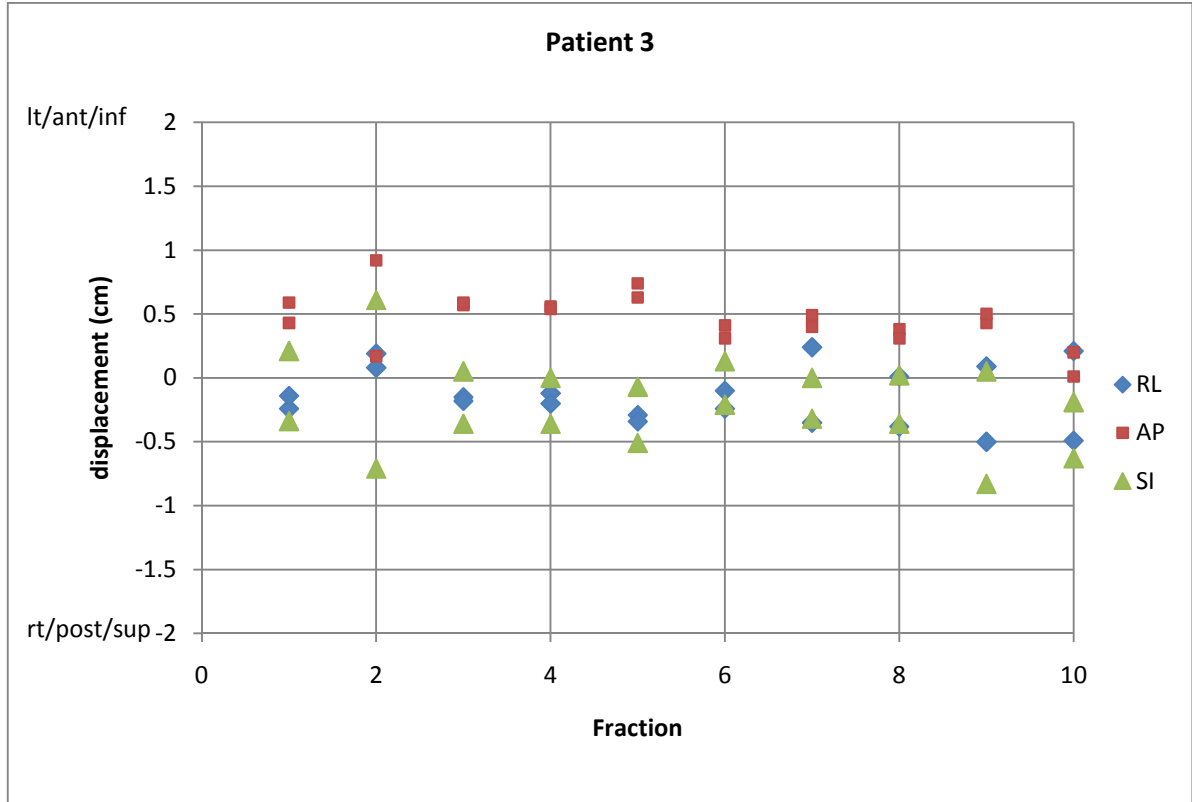


Figure 3.11: Shoulder Shift vs. Fraction for Patient 3: RL shifts are in blue, AP in red and SI in green. Positive displacement is in the left, anterior or inferior direction. Negative displacement is in the right, posterior or superior direction.

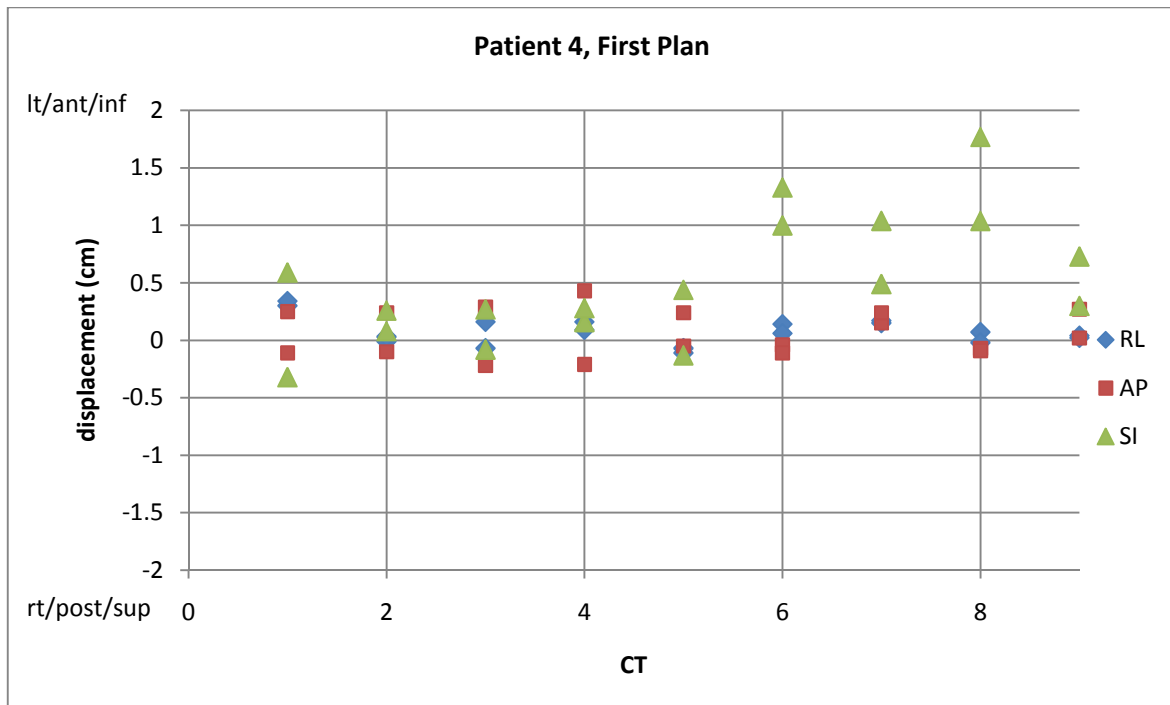


Figure 3.12: Shoulder Shift vs. CT for Patient 4’s first plan: RL shifts are in blue, AP in red and SI in green. Positive displacement is in the left, anterior or inferior direction. Negative displacement is in the right, posterior or superior direction.

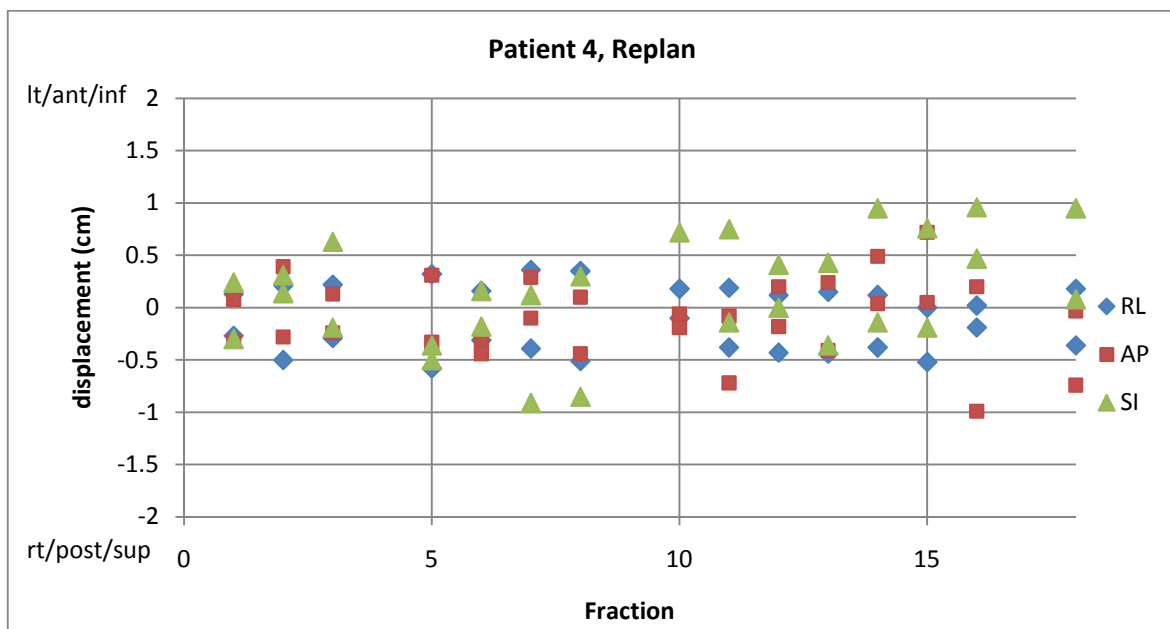


Figure 3.13: Shoulder Shift vs. Fraction for Patient 4’s replan: RL shifts are in blue, AP in red and SI in green. Positive displacement is in the left, anterior or inferior direction. Negative displacement is in the right, posterior or superior direction.

As demonstrated by these scatterplots in figures 3.9-3.12, large shifts occur early and late in treatment. There were AP shifts of greater than 1 cm seen early in treatment, and the large, inferior shifts greater than 1 cm occurred in the second half of treatment for these patients.

While large shifts were observed, the average magnitude of the shifts in each direction for each shoulder were less than 4 mm as seen in Table 3-3 below. The net displacement of the average shifts on each shoudler, calculated as a vector magnitude, was less than 6 mm, and the average net displacement of the two shoulders was 5.5 mm.

| Table 3-3: Average shoulder shifts (cm) | | | | |
|--|-----------|-----------|-----------|-------------|
| | RL | AP | SI | Net |
| <i>Right Shoulder</i> | 0.22 | 0.34 | 0.38 | 0.55 |
| <i>Left Shoulder</i> | 0.26 | 0.29 | 0.38 | 0.54 |
| Average Net | | | | 0.55 |

Table 3-3: Average shoulder shifts. The average magnitude of shift in each direction, and a net, 3D displacement for each shoulder. An average 3D displacement for both shoudlers is also shown.

3.2 Dosimetric Impact of Shoulder Shifts

3.2.1 Target Coverage

The impact of shoulder shifts on target coverage was evaluated by determining absolute volume loss for the 100%, 98%, and 95% isodose lines. The change in target coverage due to the shoulder shifts discussed in section 2.3.1 is displayed in Table 3-4 for IMRT plans and Table 3-5 for SmartArc Plans. Highlighted in red are changes in coverage greater than 4 cc. Positive numberes indicate an increase in coverage and negative numbers indicate a loss of coverage.

| Table 3-4: Target Coverage Change (cc): IMRT | | | | | | | | | | |
|--|------|-----------|--------|-------|-----------|--------|-------|-----------|--------|-------|
| Shift | | Patient 1 | | | Patient 2 | | | Patient 3 | | |
| | | V100% | V98% | V95% | V100% | V98% | V95% | V100% | V98% | V95% |
| 3 mm superior | CTV1 | 0.02 | 0 | 0 | 0.11 | 0.03 | 0 | -0.24 | 0.2 | 0.22 |
| | CTV2 | -4.35 | -0.15 | -0.02 | -4.46 | -0.01 | 0.01 | -0.86 | 0.03 | 0.01 |
| | CTV3 | -0.01 | -0.13 | -0.01 | -1.15 | 0.15 | 0.07 | n/a | n/a | n/a |
| 5 mm superior | CTV1 | 0.05 | 0.02 | 0 | 0.17 | 0.1 | 0.02 | -2.24 | 0.14 | 0.25 |
| | CTV2 | -19.12 | -0.89 | -0.04 | -13.85 | -1.7 | 0 | -7.25 | -0.43 | -0.01 |
| | CTV3 | -3.24 | -0.44 | -0.06 | -9.28 | -0.93 | 0.17 | n/a | n/a | n/a |
| 15 mm superior | CTV1 | 0.09 | 0.07 | 0.01 | 0.51 | 0.21 | 0.07 | -58.02 | -20.37 | -1.56 |
| | CTV2 | -131.79 | -73.16 | -9.35 | -52.96 | -31.01 | -3.8 | -76.84 | -24.96 | -6.8 |
| | CTV3 | -29.41 | -4.8 | -0.5 | -63.93 | -34.71 | -12.4 | n/a | n/a | n/a |
| 3 mm inferior | CTV1 | -0.04 | -0.01 | -0.01 | -0.09 | -0.03 | -0.01 | 0.02 | -0.19 | -0.18 |
| | CTV2 | 0.73 | -0.04 | -0.03 | 0.46 | -0.11 | -0.03 | -1.62 | -1.34 | -0.83 |
| | CTV3 | -0.02 | -0.04 | -0.02 | -3.66 | -2.46 | -1.34 | n/a | n/a | n/a |
| 5 mm inferior | CTV1 | 0.16 | 0.03 | 0 | -0.07 | -0.04 | -0.02 | 0.23 | -0.1 | -0.14 |
| | CTV2 | 1.76 | 0.15 | -0.01 | 0.72 | -0.04 | -0.02 | -0.47 | -0.64 | -0.36 |
| | CTV3 | -0.02 | -0.09 | -0.04 | -0.66 | -0.6 | -0.39 | n/a | n/a | n/a |
| 15 mm inferior | CTV1 | 0.05 | 0.02 | 0 | -0.2 | -0.08 | -0.03 | 0.53 | 0.19 | 0.05 |
| | CTV2 | 1.72 | 0.05 | -0.05 | 0.99 | 0.11 | 0 | 0.48 | -0.3 | -0.32 |
| | CTV3 | -1.39 | -0.7 | -0.57 | 0.55 | 0.16 | 0.02 | n/a | n/a | n/a |
| 3 mm anterior | CTV1 | 0 | 0 | 0 | 0.05 | 0 | 0 | 0.79 | 0.54 | 0.37 |
| | CTV2 | -0.13 | -0.13 | -0.07 | 0.71 | 0.12 | 0.01 | 0.27 | -0.1 | -0.08 |
| | CTV3 | -0.17 | 0.02 | -0.01 | 0.7 | 0.41 | 0.17 | n/a | n/a | n/a |
| 15 mm anterior | CTV1 | 0.01 | -0.01 | 0 | 0.05 | 0 | 0 | -0.28 | 0.46 | 0.39 |
| | CTV2 | -0.9 | -0.18 | 0.01 | 1.38 | 0.19 | 0.02 | 0.98 | 0.11 | -0.03 |
| | CTV3 | -4.33 | -0.65 | -0.01 | 1.35 | 0.71 | 0.28 | n/a | n/a | n/a |
| 3 mm posterior | CTV1 | -0.03 | 0 | -0.01 | -0.01 | -0.01 | 0 | -0.67 | -0.19 | -0.03 |
| | CTV2 | -1.91 | -0.87 | -0.34 | -0.82 | -0.01 | -0.01 | -3.34 | -1.51 | -0.57 |
| | CTV3 | -1.8 | -0.67 | -0.25 | -0.5 | -0.09 | 0.01 | n/a | n/a | n/a |
| 15 mm posterior | CTV1 | -0.02 | 0.01 | 0 | 0.01 | 0.02 | 0 | -3.69 | -1.03 | -0.41 |
| | CTV2 | -11.53 | -0.29 | -0.05 | -7.57 | -0.42 | -0.12 | -24.82 | -4.06 | -0.72 |
| | CTV3 | -5.43 | -0.99 | -0.19 | -7.45 | -1.8 | -0.74 | n/a | n/a | n/a |
| 15 mm Right or Left* | CTV1 | 0.01 | 0.01 | 0 | 0 | -0.01 | 0 | -2.23 | -0.26 | 0.13 |
| | CTV2 | -1.11 | 0.06 | -0.01 | 1.05 | 0.11 | 0.01 | -1.78 | -0.63 | -0.16 |
| | CTV3 | -0.08 | 0.06 | 0.01 | 0.31 | 0.12 | 0.03 | n/a | n/a | n/a |

Table 3-4: Target Coverage change (cc) for IMRT. The amount of volume lost by the 100%, 98% and 95% isodose lines for each of the Dosimetric Patient's CTVs as a result of specified shoulder shifts.

| Table 3-5: Target Coverage Change (cc): SmartArc | | | | | | | | | | |
|--|------|-----------|---------|--------|-----------|--------|-------|-----------|--------|-------|
| Shift | | Patient 1 | | | Patient 2 | | | Patient 3 | | |
| | | V100% | V98% | V95% | V100% | V98% | V95% | V100% | V98% | V95% |
| 3 mm superior | CTV1 | 0.06 | 0.02 | -0.43 | 0.07 | 0.06 | 0.03 | -0.23 | 0.01 | 0.08 |
| | CTV2 | -4.22 | -0.26 | -0.04 | -1.61 | -2.01 | 0.02 | -1.48 | 0.04 | 0.08 |
| | CTV3 | -1.5 | -0.3 | -0.08 | 0.03 | 0.24 | 0.14 | n/a | n/a | n/a |
| 5 mm superior | CTV1 | 0.18 | 0.07 | 0.02 | 0.11 | 0.09 | 0.05 | -0.46 | 0.03 | 0.11 |
| | CTV2 | -24.3 | -3.06 | -0.23 | -6.51 | -4.17 | 0.02 | -5.6 | -1.02 | -0.06 |
| | CTV3 | -9.79 | -1.4 | -0.22 | -4.74 | 0.33 | 0.27 | n/a | n/a | n/a |
| 15 mm superior | CTV1 | 0.81 | 0.27 | 0.08 | 0.34 | 0.26 | 0.17 | -49.07 | -7.46 | -0.33 |
| | CTV2 | -151.77 | -102.29 | -41.02 | -36.13 | -13.2 | -0.8 | -64.79 | -29.28 | -6.58 |
| | CTV3 | -42.74 | -22.28 | -9.55 | -36.45 | -11.15 | 0.24 | n/a | n/a | n/a |
| 3 mm inferior | CTV1 | -0.1 | -0.03 | -0.01 | -0.06 | -0.05 | -0.04 | 0.07 | -0.08 | -0.14 |
| | CTV2 | 0.47 | -0.16 | -0.11 | 2.73 | -0.03 | -0.01 | -1.29 | -1.61 | -0.96 |
| | CTV3 | 0.54 | 0.16 | 0 | -2.79 | -1.88 | -0.97 | n/a | n/a | n/a |
| 5 mm inferior | CTV1 | -0.22 | -0.07 | -0.03 | -0.09 | -0.05 | -0.04 | 0.28 | 0.01 | -0.12 |
| | CTV2 | 0.49 | -0.33 | -0.22 | 3.75 | -0.01 | 0 | 0.03 | -0.69 | -0.4 |
| | CTV3 | 0.81 | 0.24 | -0.01 | -0.5 | -0.45 | -0.31 | n/a | n/a | n/a |
| 15 mm inferior | CTV1 | 0.2 | -0.01 | -0.02 | 1.11 | 0.64 | 0.3 | 0.81 | 0.4 | 0.15 |
| | CTV2 | 1.93 | 0.33 | -0.04 | 4.24 | 0.1 | 0.04 | 1.59 | -0.18 | -0.3 |
| | CTV3 | 0.99 | 0.19 | -0.16 | 1.03 | 0.5 | 0.26 | n/a | n/a | n/a |
| 3 mm anterior | CTV1 | -0.01 | 0 | 0 | 0.01 | 0.01 | 0 | 0.96 | 0.65 | 0.34 |
| | CTV2 | -0.39 | -0.12 | -0.18 | 0.31 | 0.01 | 0.01 | -0.11 | -0.07 | -0.07 |
| | CTV3 | -0.64 | -0.17 | -0.04 | 0.41 | 0.25 | 0.12 | n/a | n/a | n/a |
| 15 mm anterior | CTV1 | 0.04 | 0.02 | 0.01 | 0.06 | 0.05 | 0.03 | 0.37 | 0.45 | 0.27 |
| | CTV2 | -2.31 | -0.03 | 0.09 | 1.52 | 0.01 | 0.01 | 2.37 | 0.15 | 0.27 |
| | CTV3 | -0.51 | -0.06 | -0.02 | 0.73 | 0.4 | 0.2 | n/a | n/a | n/a |
| 3 mm posterior | CTV1 | -0.06 | -0.02 | 0 | -0.01 | -0.02 | -0.01 | -0.43 | -0.21 | -0.03 |
| | CTV2 | -1.36 | -0.88 | -0.45 | -0.1 | -0.01 | 0 | -2.47 | -1.63 | -0.65 |
| | CTV3 | -0.9 | -0.63 | -0.39 | -0.21 | -0.07 | 0.01 | n/a | n/a | n/a |
| 15 mm posterior | CTV1 | -0.07 | -0.02 | -0.01 | -0.05 | -0.05 | -0.03 | -0.41 | -0.28 | -0.1 |
| | CTV2 | -1.19 | -0.39 | -0.14 | -1.29 | -1.43 | -0.04 | -3.15 | -2.09 | -0.85 |
| | CTV3 | 0.21 | 0.03 | -0.02 | -1.35 | -0.93 | -0.54 | n/a | n/a | n/a |
| 15 mm Right or Left* | CTV1 | 0.08 | 0.03 | 0.01 | -0.02 | -0.02 | -0.02 | -0.21 | 0 | 0.14 |
| | CTV2 | -2.78 | 0.04 | 0.02 | 1.04 | 0.01 | 0 | -2.35 | -0.38 | -0.05 |
| | CTV3 | 0 | 0.02 | -0.03 | 0.06 | -0.02 | -0.02 | n/a | n/a | n/a |

Table 3-5: Target Coverage change (cc) for SmartArc. The amount of volume lost by the 100%, 98% and 95% isodose lines for each of the Dosimetric Patient's CTVs as a result of specified shoulder shifts.

Targets in the upper neck (CTV1 for Patients 1 and 2) were far enough from the shoulder region that the shoulder variation did not show a large loss in coverage. However, changes greater than 4 cc can be seen in the volume of lower neck targets covered by the 100% isodose line for superior shifts on both IMRT and SmartArc Plans, as well for the 15 mm posterior shift for IMRT plans only. Shifts in the inferior, anterior, and right or left direction showed little change in target coverage for all CTVs. With large superior shifts, the loss of coverage is the most substantial. For both IMRT and SmartArc, a 3 mm or 5 mm superior shift can cause loss of coverage in the 100% isodose line. For these patients, the 100% isodose line no longer covers 99% of the CTV2 and CTV3 in the lower neck. With a 15 mm superior shift coverage loss on the lower neck targets was consistently lost in the 100% and 98% isodose lines, and frequently in the 95% isodose line, for both IMRT and SmartArc plans. For these patients, the 95% isodose line no longer covers 100% of the lower neck CTVs. These dose changes due to superior shifts are considered clinically unacceptable.

In Fig. 3.14 and 3.15 below for Patient 1, a comparison of the original plan DVH to the DVH after the 15 mm superior shift shows a loss of coverage on the lower neck targets. The slope on the original DVH is steeper, and the lower neck CTVs (CTV 57 and 54) show a shift towards lower dose after the shift. Ninety nine percent of CTV 57 shifts down to 54 Gy for the IMRT and SmartArc plans, and 99% of CTV 54 shifts down to 53 Gy for the IMRT plan and lower (52 Gy) for SmartArc plan. CTV 60 was in the upper neck, and was not affected by the shoulder shift.

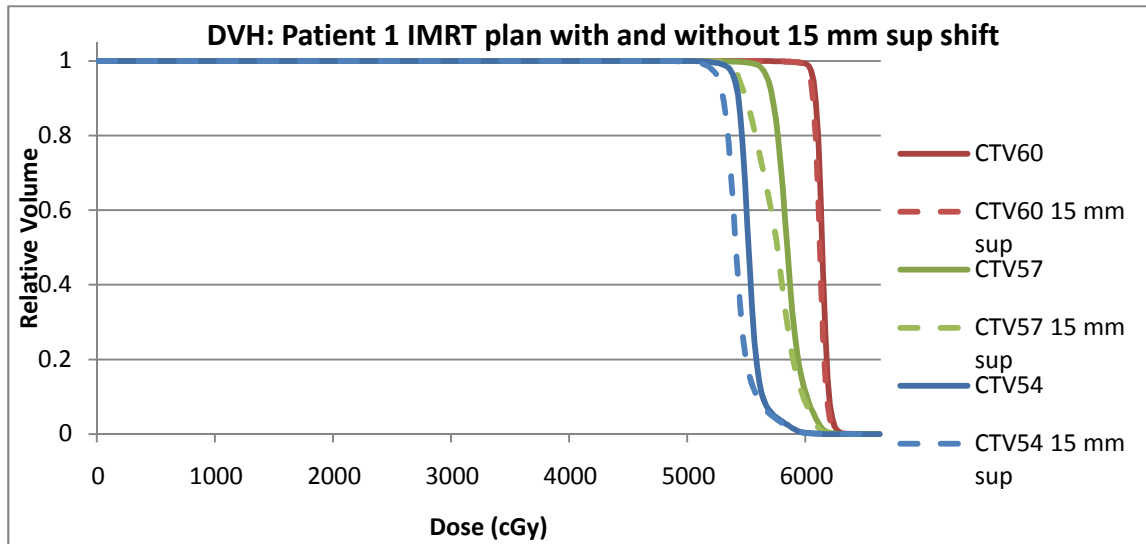


Figure 3.14: DVH for Patient 1 IMRT plans. Solid line is original. Dashed line shows 15 mm sup shift

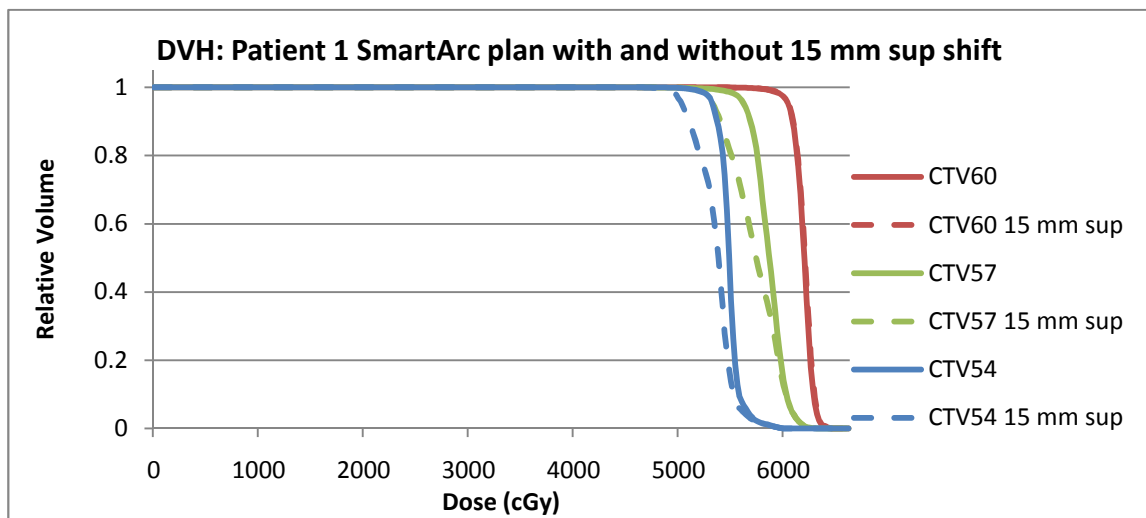


Figure 3.15: DVH for Patient 1 SmartArc plans. Solid line is original. Dashed line shows 15 mm sup shift.

The dosimetric impact of superior shifts is also evident when comparing axial slices of the isodose distribution of the original plans to isodose distribution of the plans recalculated after the shift. The targets are well covered by the prescription line before the shift, but coverage is degraded after the shift.

In the figures 3.16- 3.23 that follow, comparisons of axial slices in the original treatment plan to the same slices with a shoulder shift are shown.

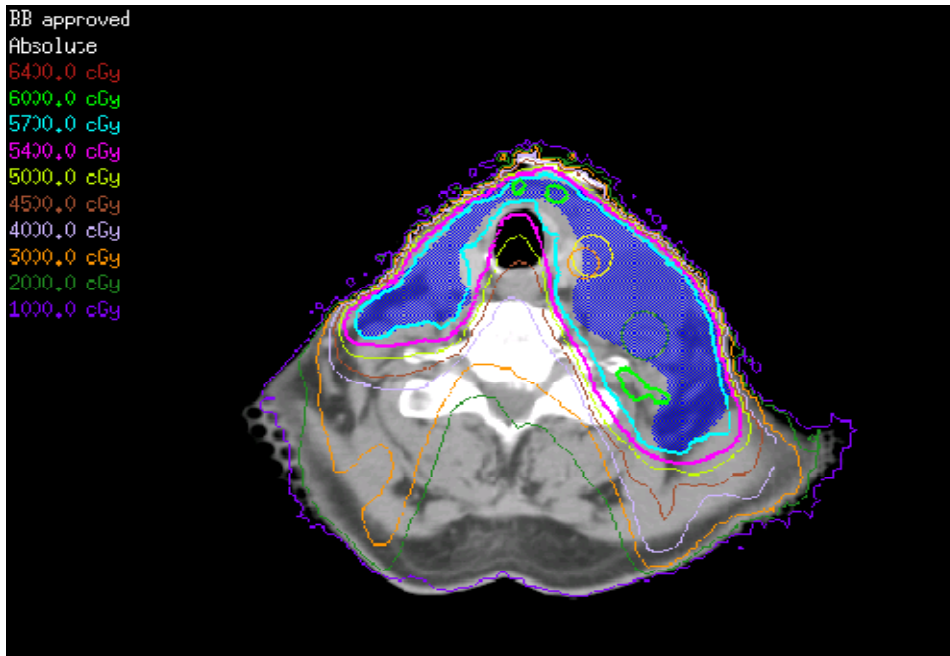


Figure 3.16a: Patient 1 IMRT no shift. CTV 57 (blue) is covered by the 57 Gy line (aqua).

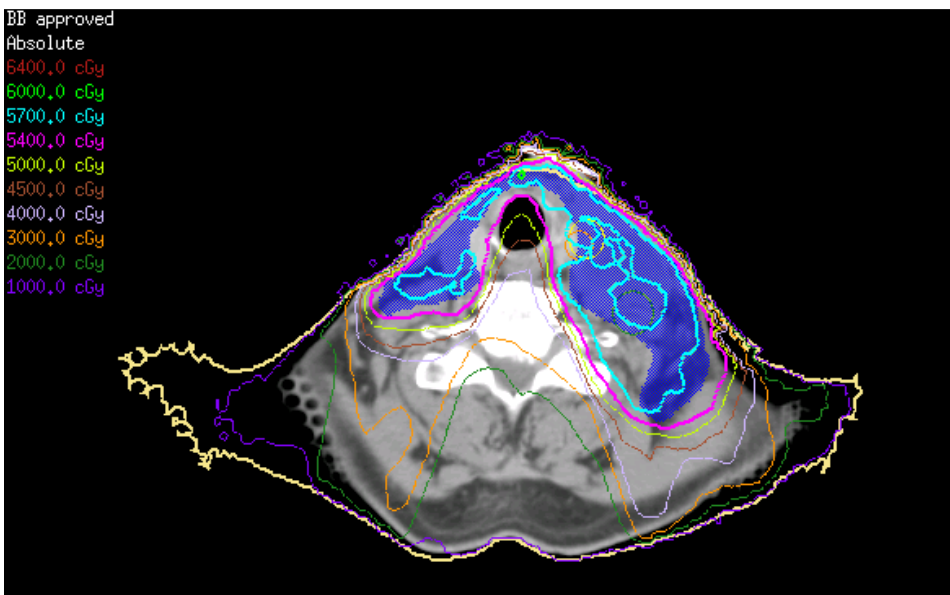


Figure 3.16b: Patient 1 IMRT 5 mm superior shift. 57 Gy line no longer covers CTV.



Figure 3.16c: Patient 1 SmartArc no shift. CTV 57 is covered by 57 Gy, and CTV 54 (yellow) is covered by 54 Gy (pink).

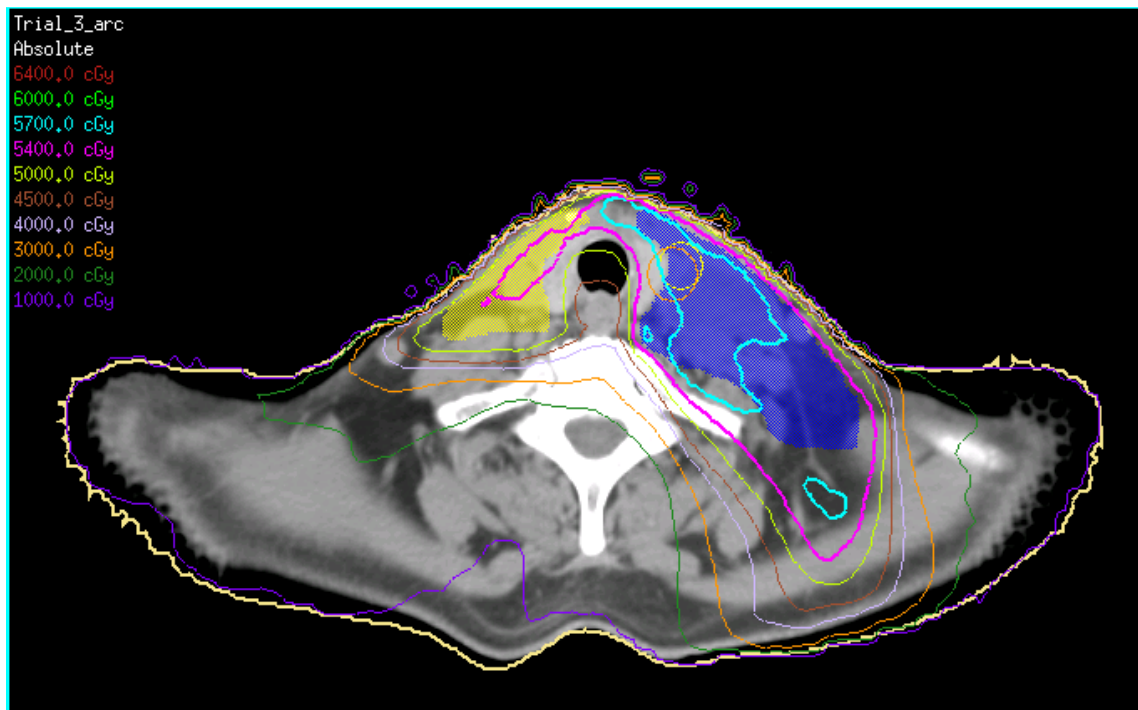


Figure 3.16d: Patient 1 SmartArc 5 mm superior shift. 57 Gy and 54 Gy lines no longer cover CTVs.

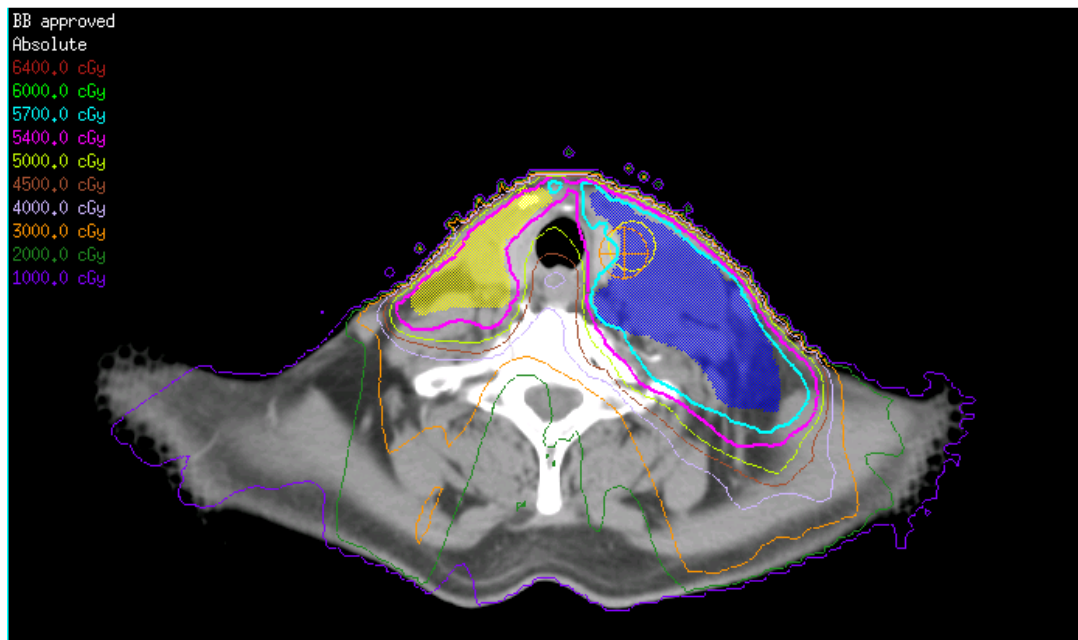


Figure 3.17a: Patient 1 IMRT no shift. CTV 57 (blue) is covered by the 57 Gy line (aqua) and CTV 54 (yellow) is covered by 54 Gy (pink).

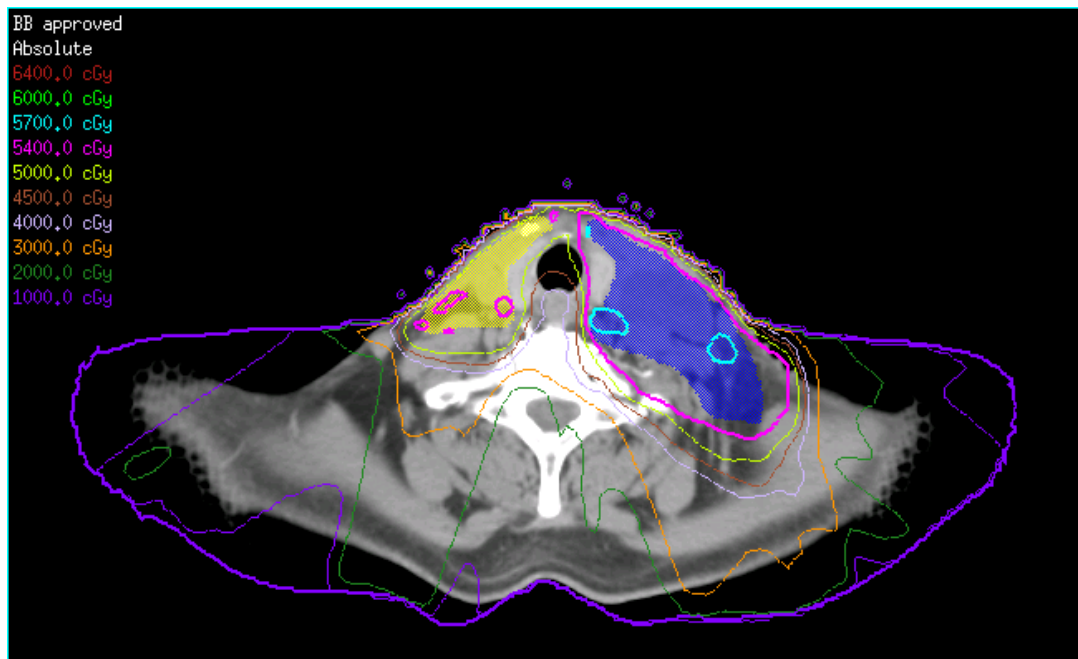


Figure 3.17b: Patient 1 IMRT 15 mm superior shift. 57 Gy and 54 Gy lines no longer covers CTVs.

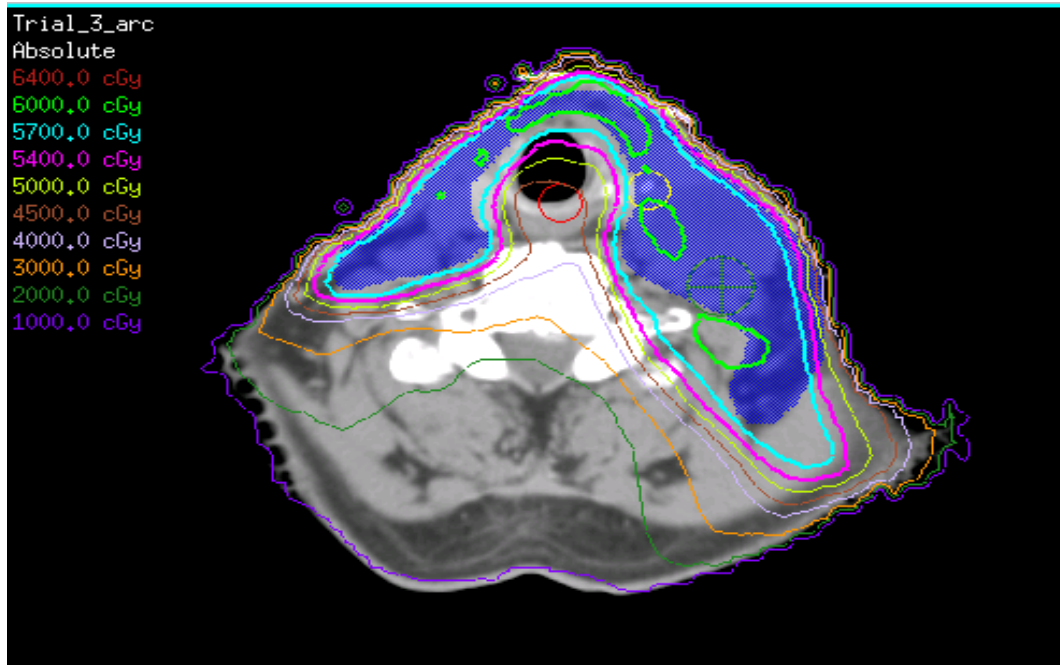


Figure 3.17c: Patient 1 SmartArc no shift. CTV 57 is covered by 57 Gy, and CTV 54 is covered by 54 Gy.

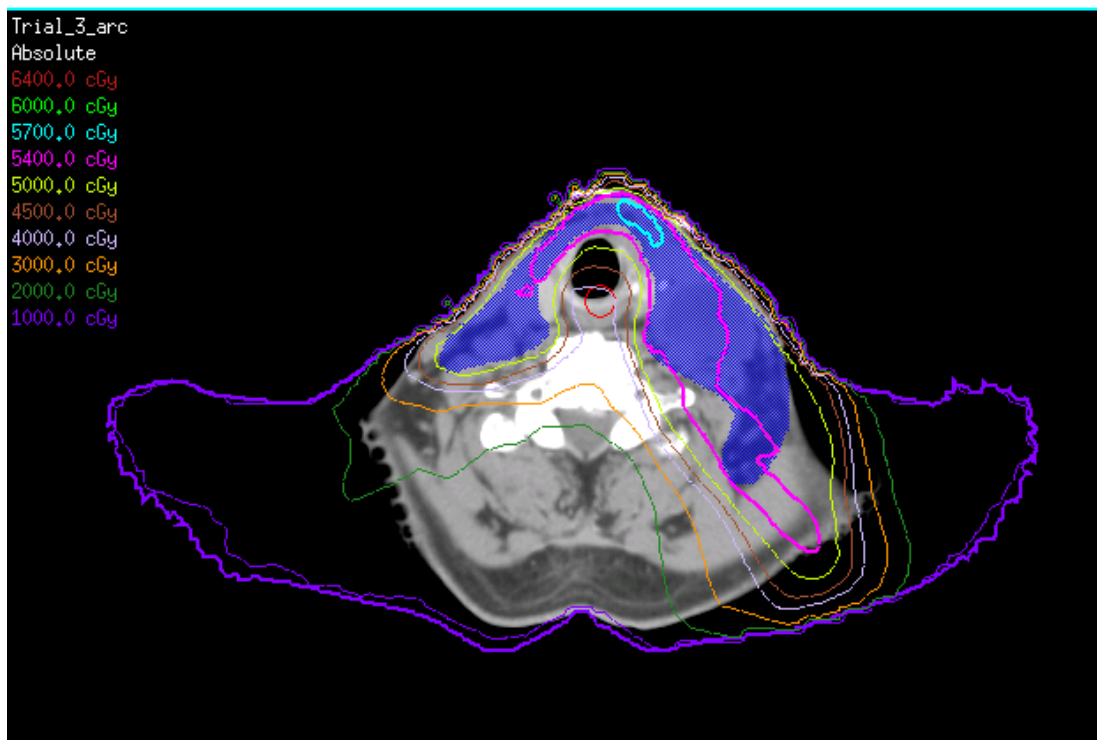


Figure 3.17d: Patient 1 SmartArc 15 mm superior shift. 57 Gy and 54 Gy lines no longer covers CTVs.

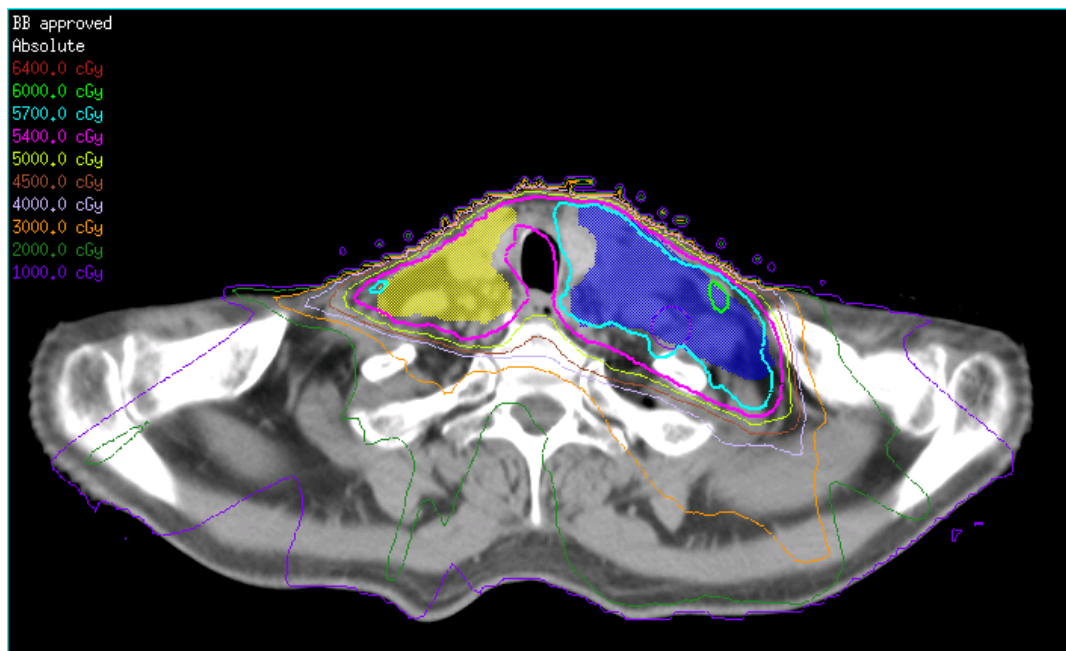


Figure 3.18a: Patient 1 IMRT no shift. CTV 57 (blue) is covered by the 57 Gy line (aqua) and CTV 54 (yellow) is covered by 54 Gy (pink).

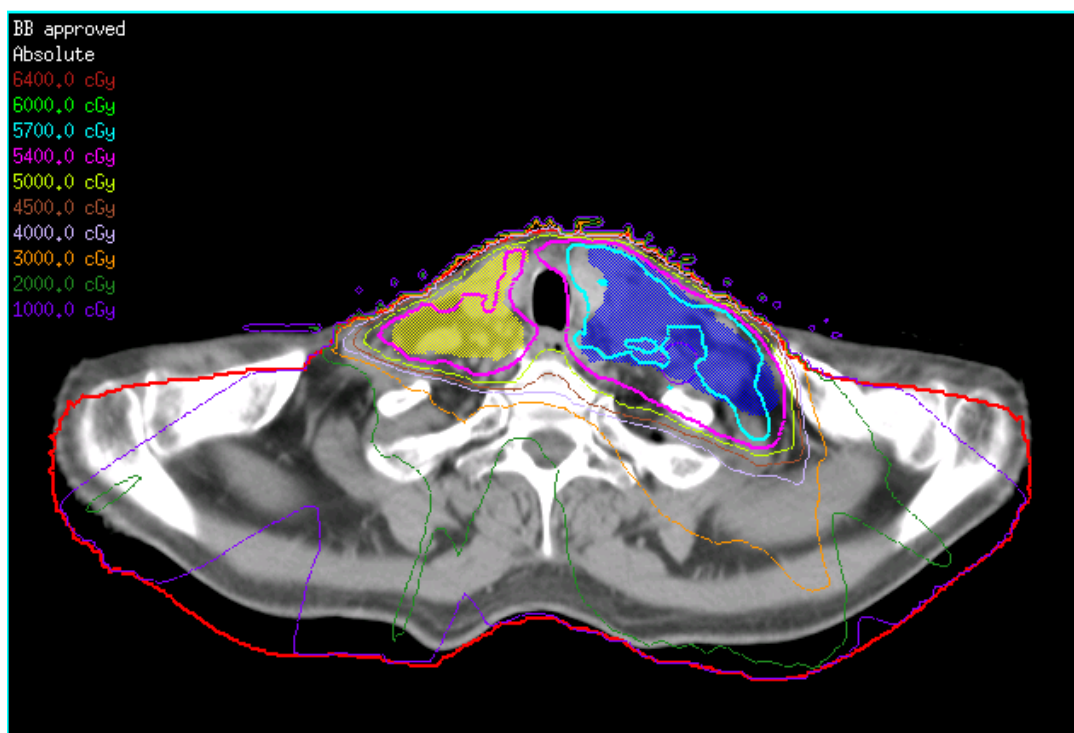


Figure 3.18b: Patient 1 IMRT 15 mm posterior shift. 57 Gy and 54 Gy lines no longer covers CTVs.

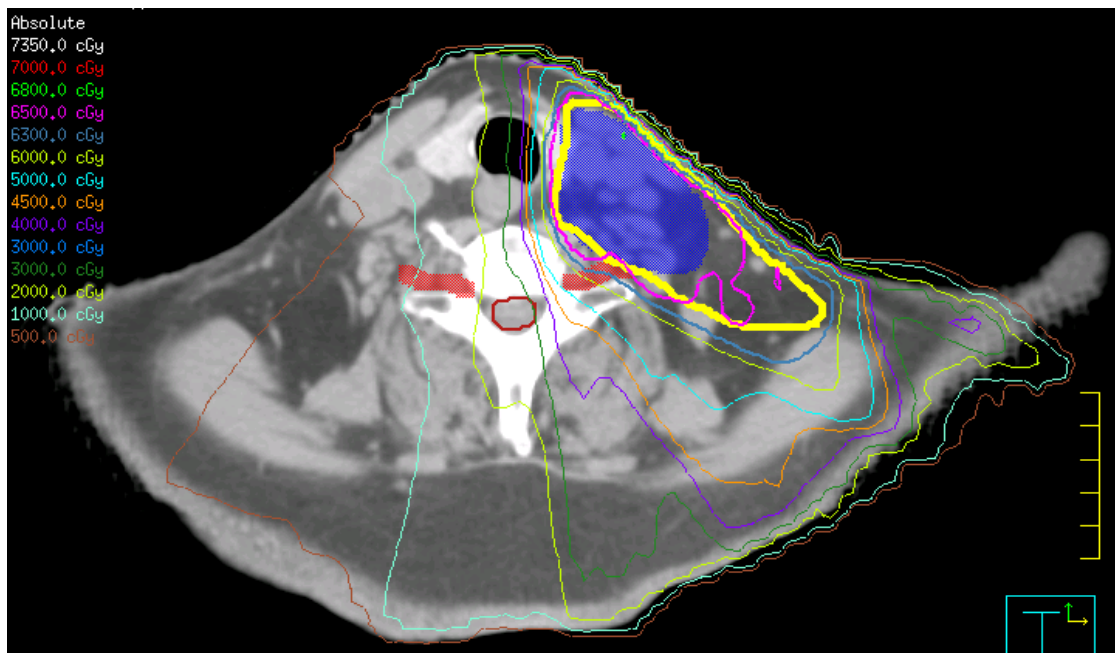


Figure 3.19a: Patient 2 IMRT no shift. CTV 65 (blue) is covered by 65 Gy (pink) and CTV 63 (thick yellow) is covered by 63 Gy (steel blue).

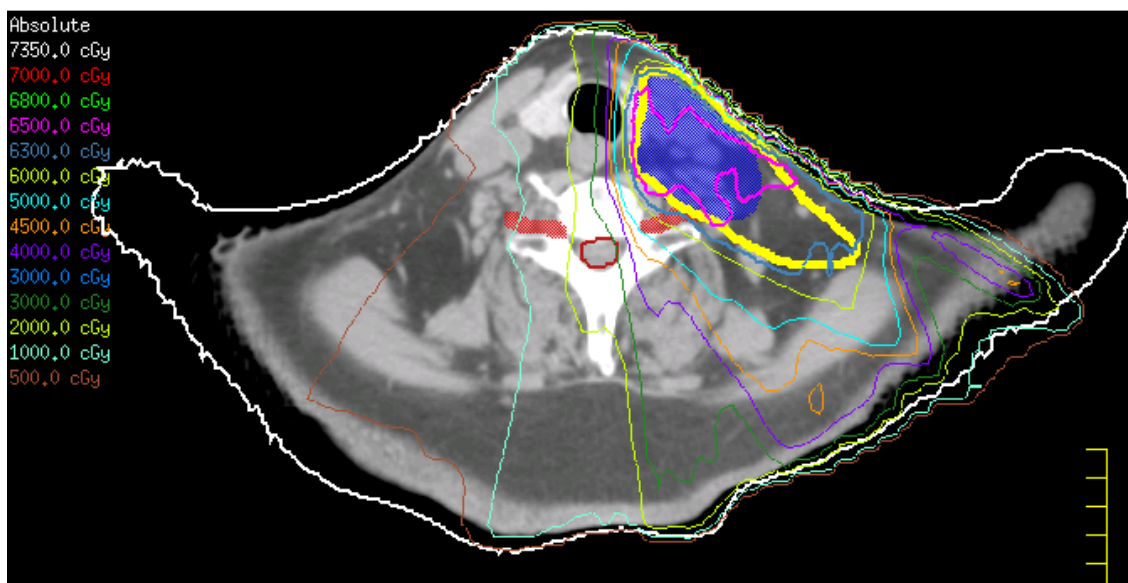


Figure 3.19b: Patient 2 IMRT 5 mm superior shift. 65 Gy and 63 Gy lines no longer cover CTVs.

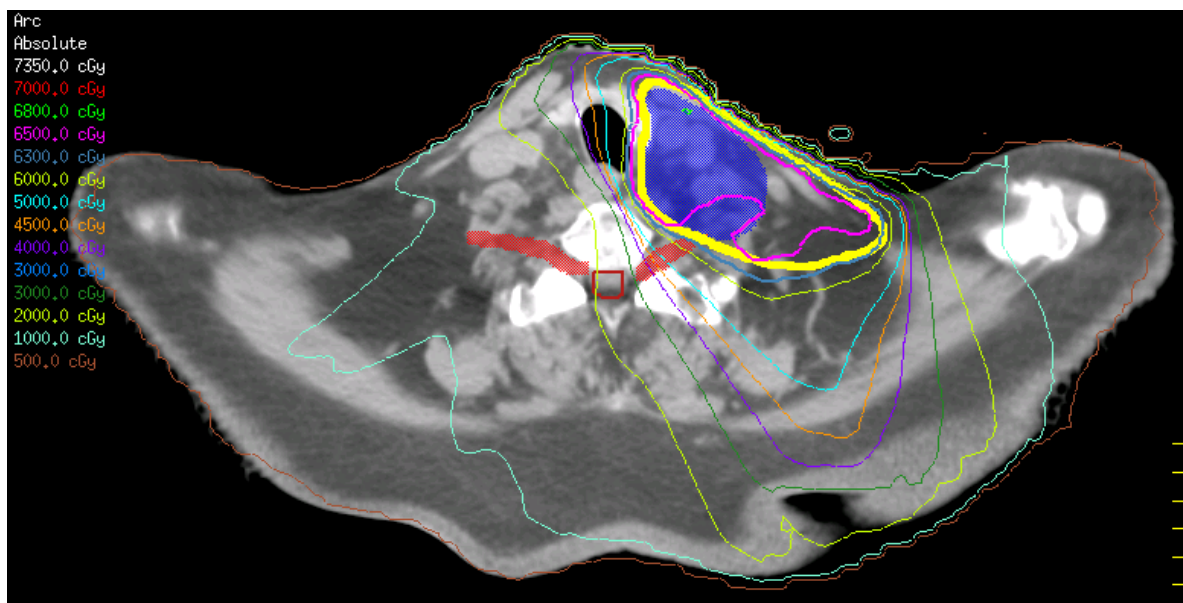


Figure 3.19c: Patient 2 SmartArc no shift. CTV 65 is covered by 65 Gy (spares brachial plexus) and CTV 63 is covered by 63 Gy.

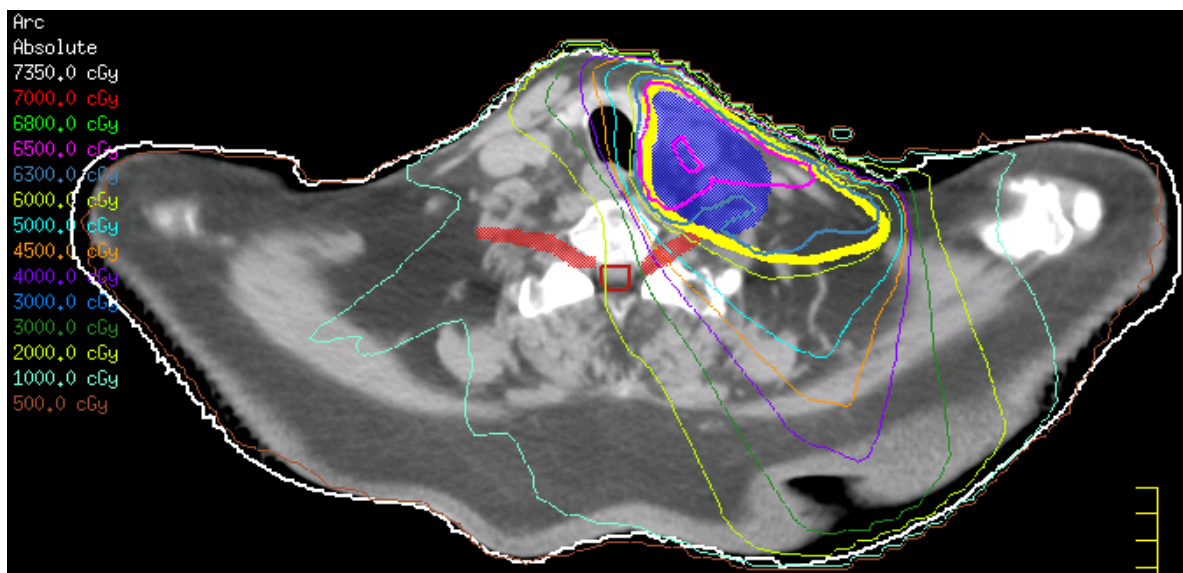


Figure 3.19d: Patient 2 SmartArc 5 mm superior shift. 65 Gy and 63 Gy lines no longer cover CTVs.

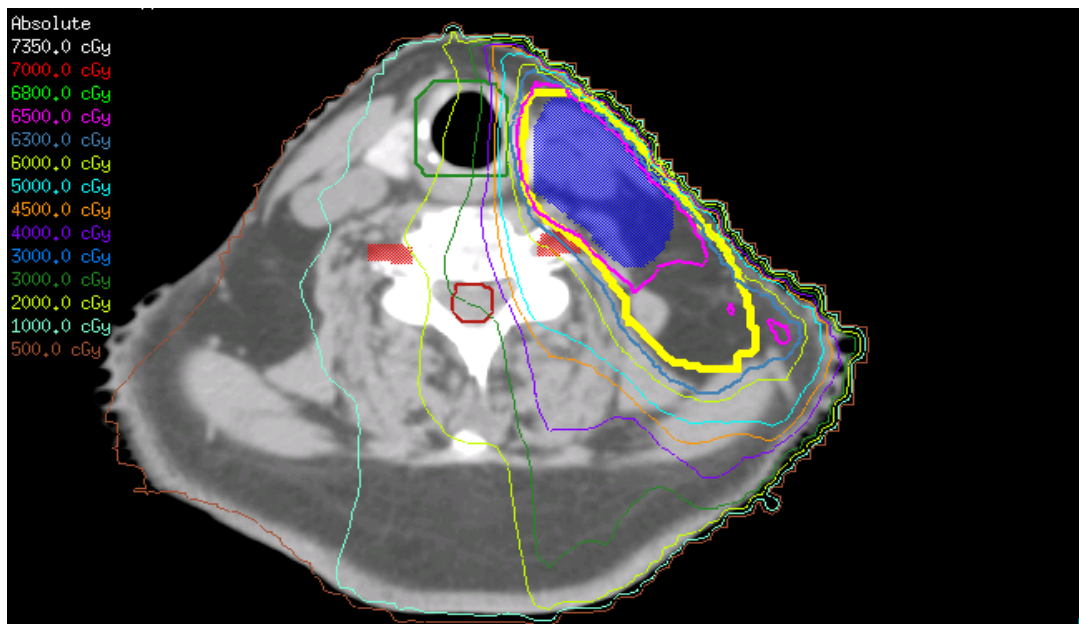


Figure 3.20a: Patient 2 IMRT no shift. CTV 65 (blue) is covered by 65 Gy (pink) and CTV 63 (thick yellow) is covered by 63 Gy (steel blue).

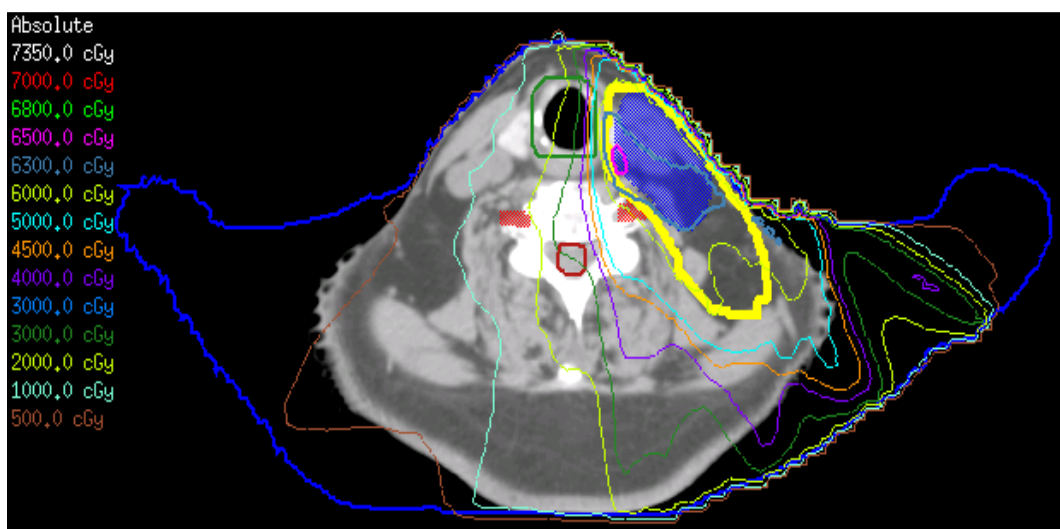


Figure 3.20b: Patient 2 IMRT 15 mm superior shift. 65 Gy and 63 Gy lines no longer cover CTVs.

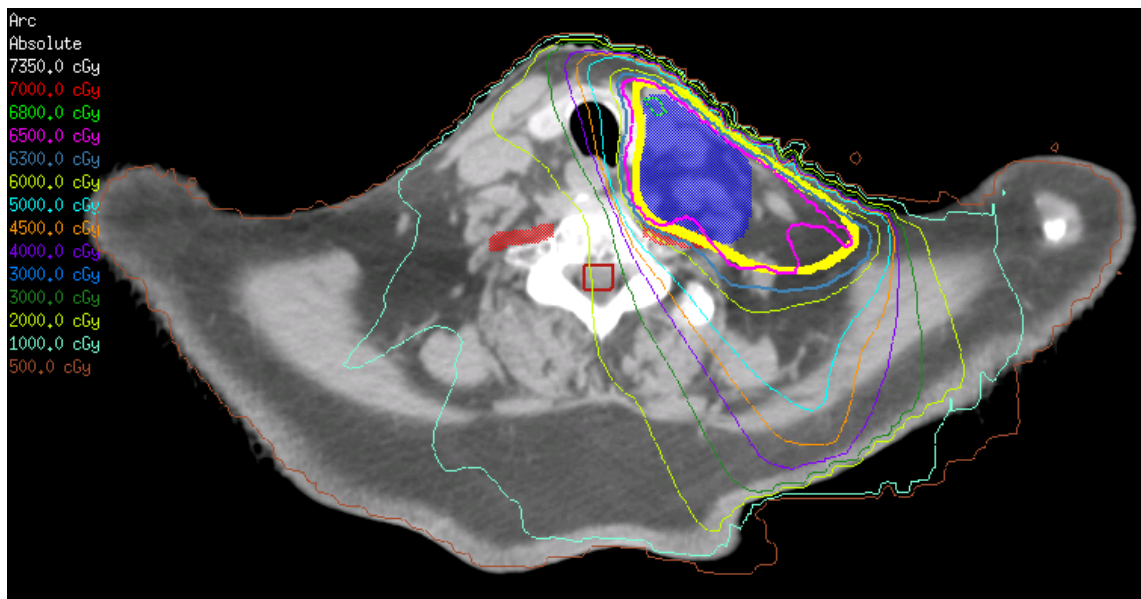


Figure 3.20c: Patient 2 SmartArc no shift. CTV 65 is covered by 65 Gy (spares brachial plexus) and CTV 63 is covered by 63 Gy.

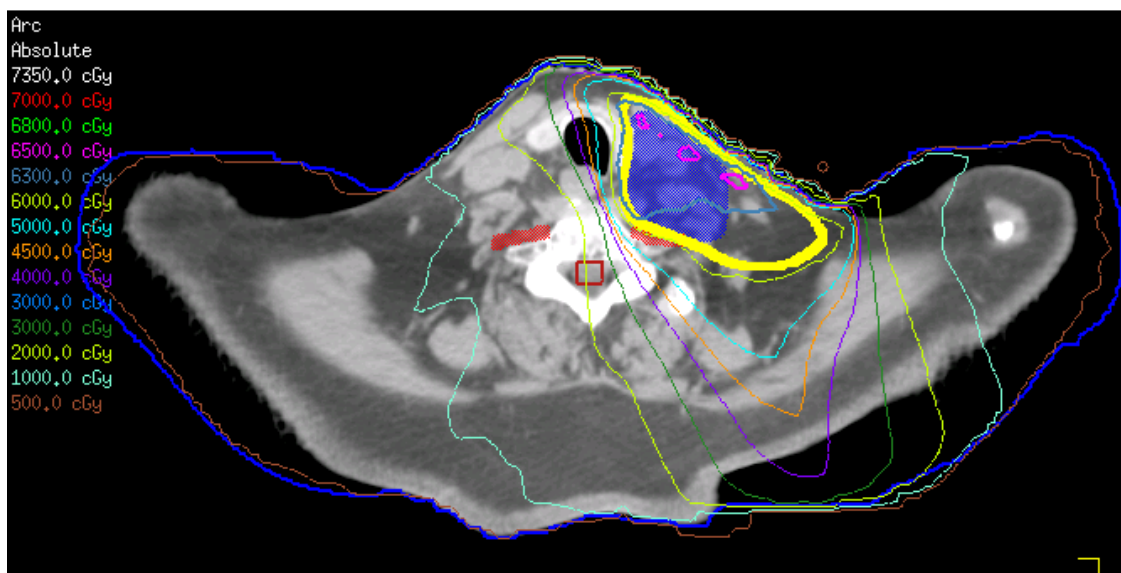


Figure 3.20d: Patient 2 IMRT 15 mm superior shift. 65 Gy and 63 Gy lines no longer cover CTVs.

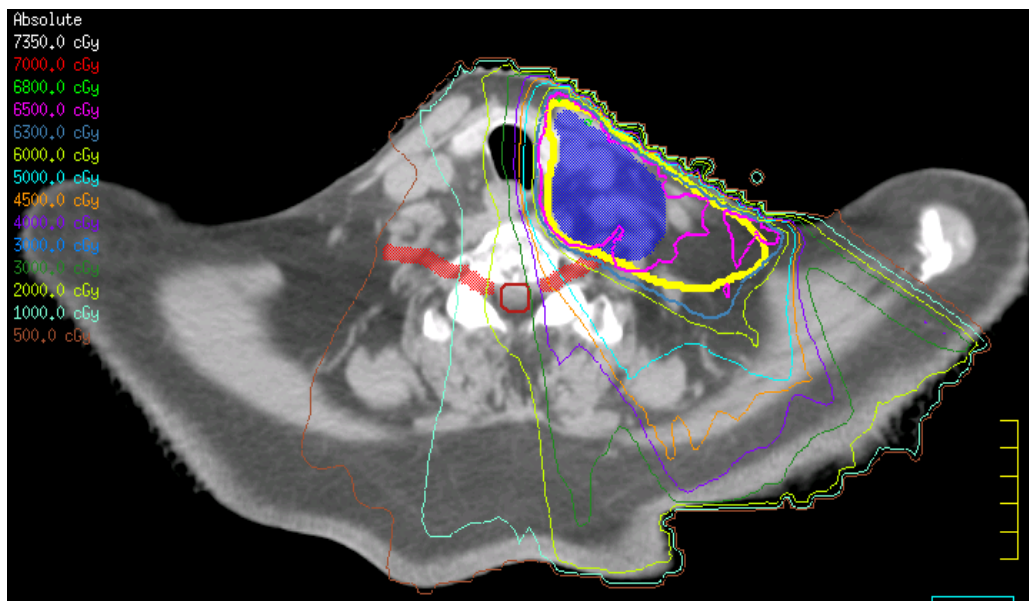


Figure 3.21a: Patient 2 IMRT no shift. CTV 65 (blue) is covered by 65 Gy (pink) and CTV 63 (thick yellow) is covered by 63 Gy (steel blue).

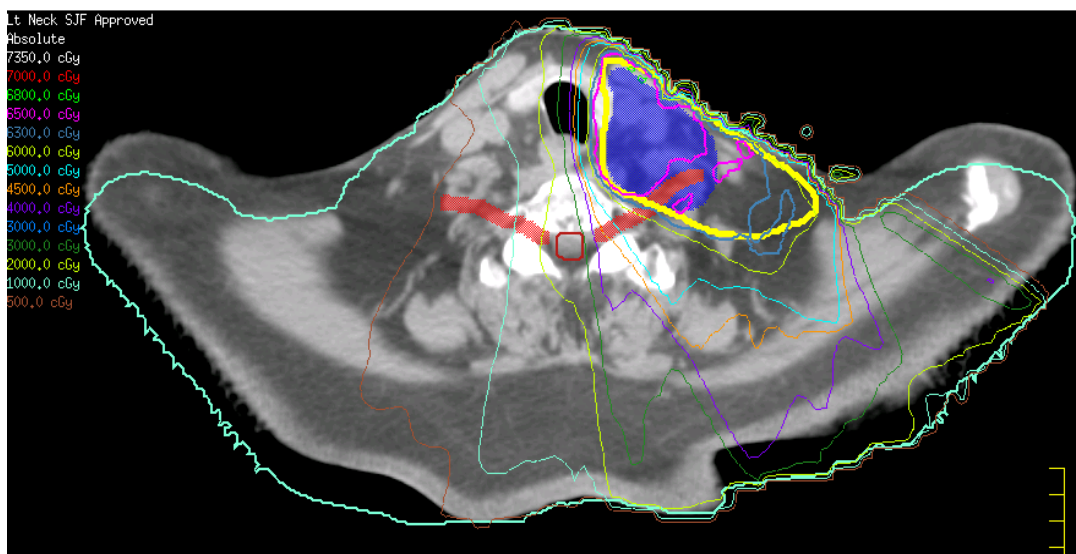


Figure 3.21b: Patient 2 IMRT 15 mm posterior shift. 65 Gy and 63 Gy lines no longer cover CTVs.

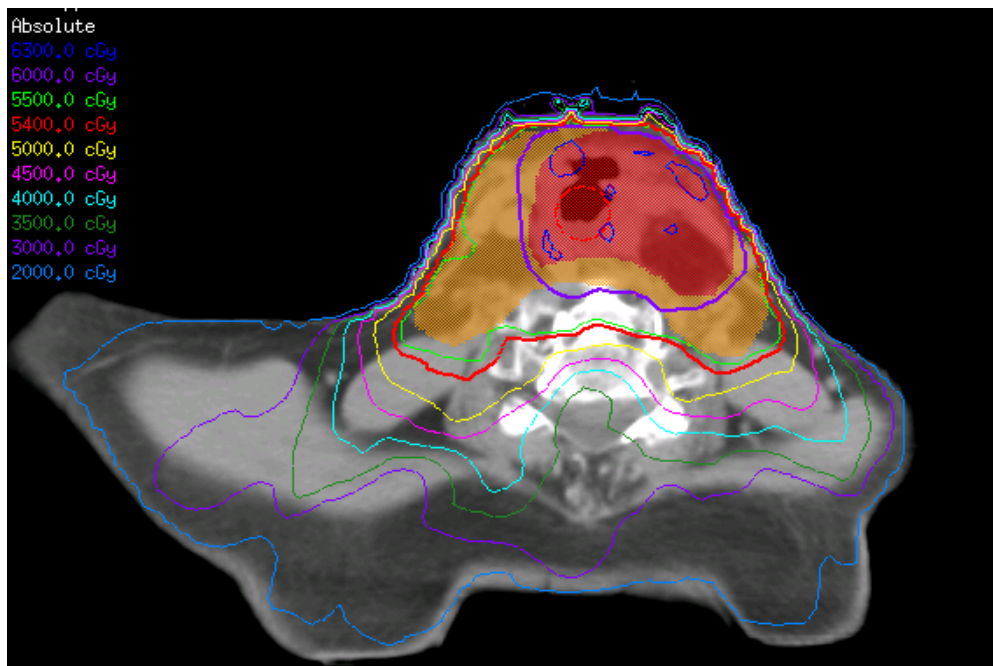


Figure 3.22a: Patient 3 IMRT no shift. CTV 60 (red) is covered by 60 Gy (purple) and CTV 54 (orange) is covered by 54 Gy (red).

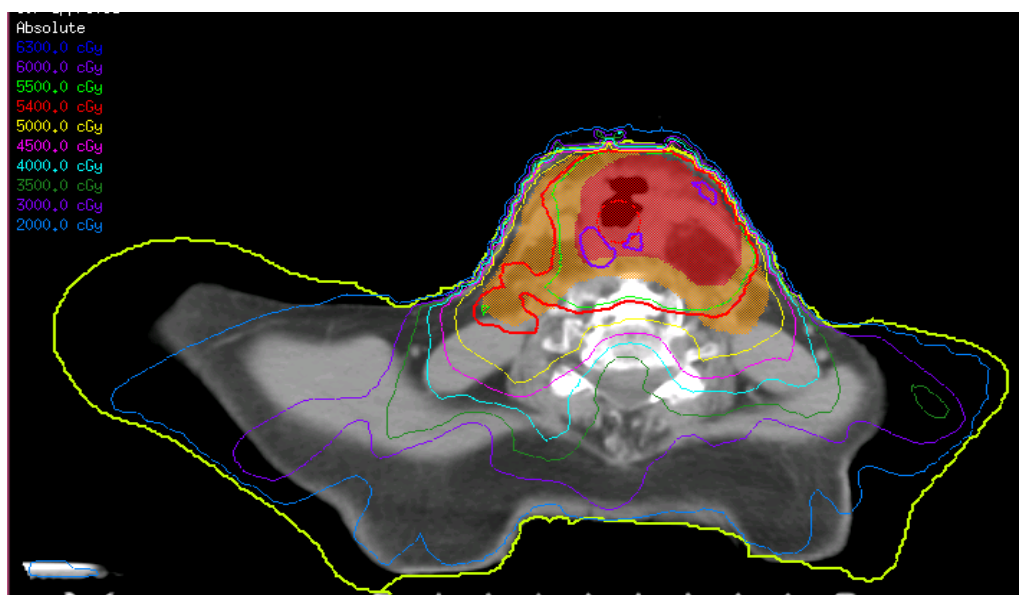


Figure 3.22b: Patient 3 IMRT 15 mm superior shift. 60 Gy and 54 Gy lines no longer cover CTVs.

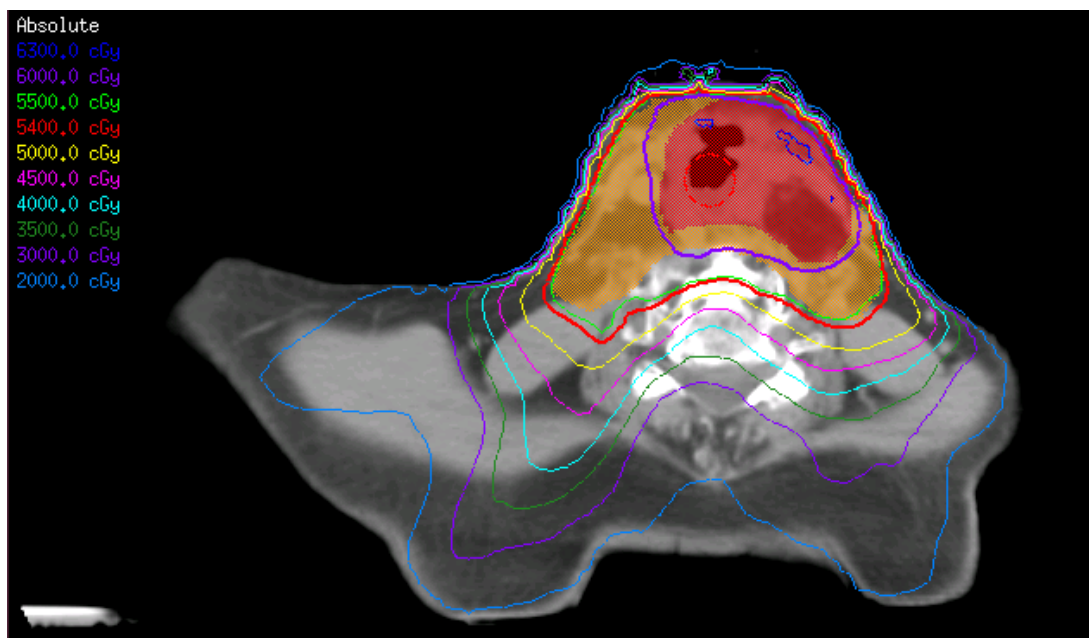


Figure 3.22c: Patient 3 SmartArc no shift. CTV 60 is covered by 60 Gy and CTV 54 is covered by 54 Gy.

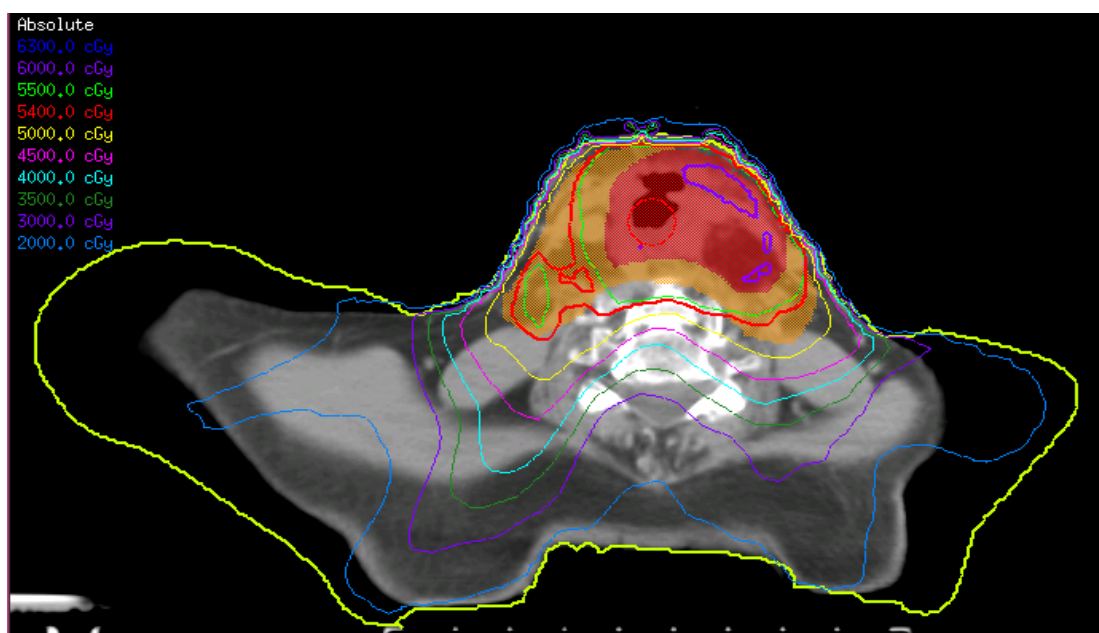


Figure 3.22d: Patient 3 SmartArc 15 mm superior shift. 60 Gy and 54 Gy lines no longer cover CTVs.

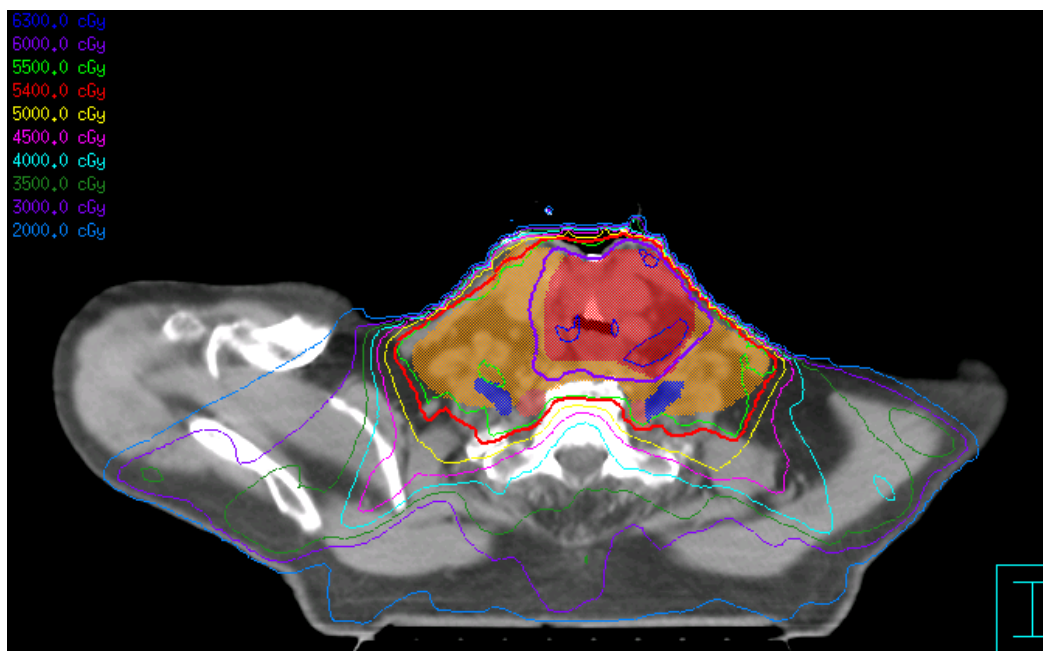


Figure 3.23a: Patient 3 IMRT no shift. CTV 60 (red) is covered by 60 Gy (purple) and CTV 54 (orange) is covered by 54 Gy (red).

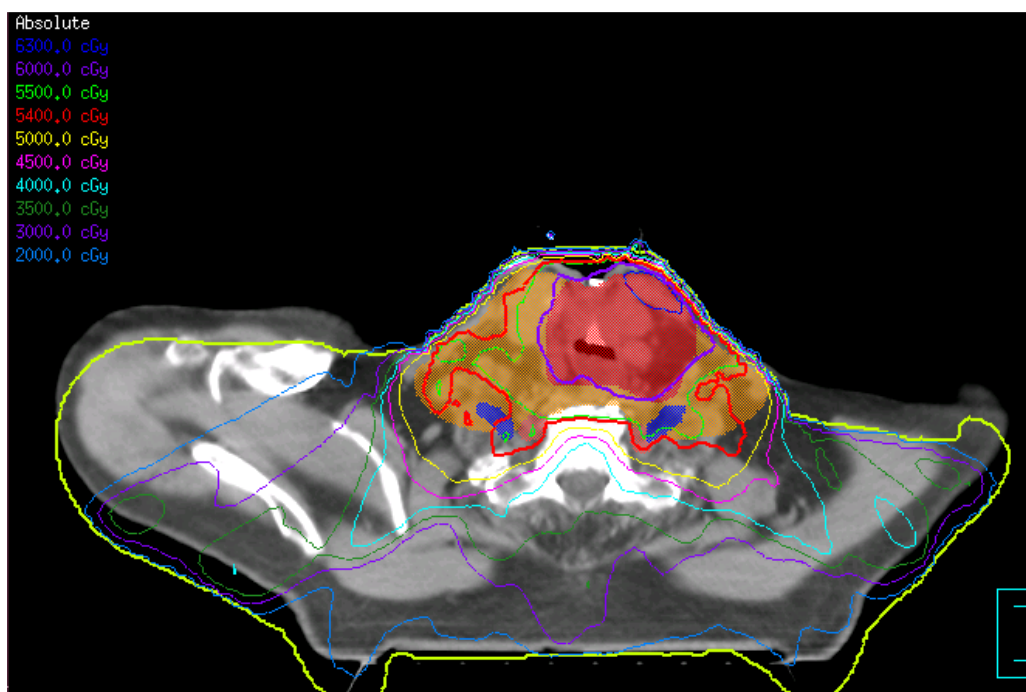


Figure 3.23b: Patient 3 IMRT 15 mm posterior shift. 60 Gy and 54 Gy lines no longer cover CTVs.

While target coverage is lost for superior shifts, it is not re-gained for inferior shifts. For all 3 patients, a plot of the change in coverage to one lower neck target versus direction shows that shifts in opposing superior or inferior directions do not balance out. For IMRT plans the same was true in the AP direction. Coverage was lost with large, posterior shifts that was not made up for with the large, anterior shifts.

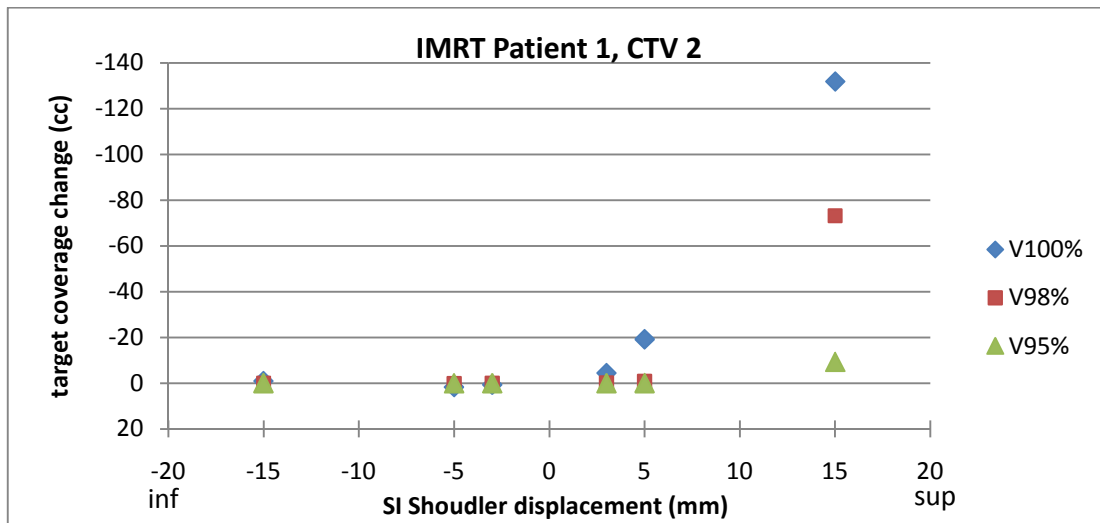


Figure 3.24a: Volume loss Patient 1 IMRT plan. Inferior shifts are to the left and superior to the right. Coverage loss (cc) increases with superior shift but is not gained with inferior shift.

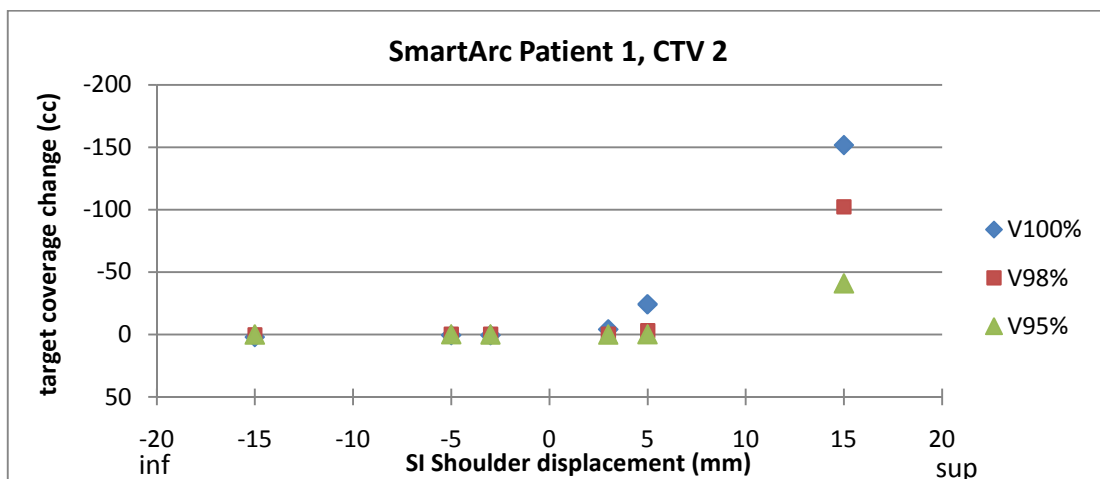


Figure 3.24b: Volume loss Patient 1 SmartArc plan. Inferior shifts are to the left and superior to the right. Coverage loss (cc) increases with superior shift but is not gained

with inferior shift. The same effect on coverage found with IMRT is seen for Smart Arc.

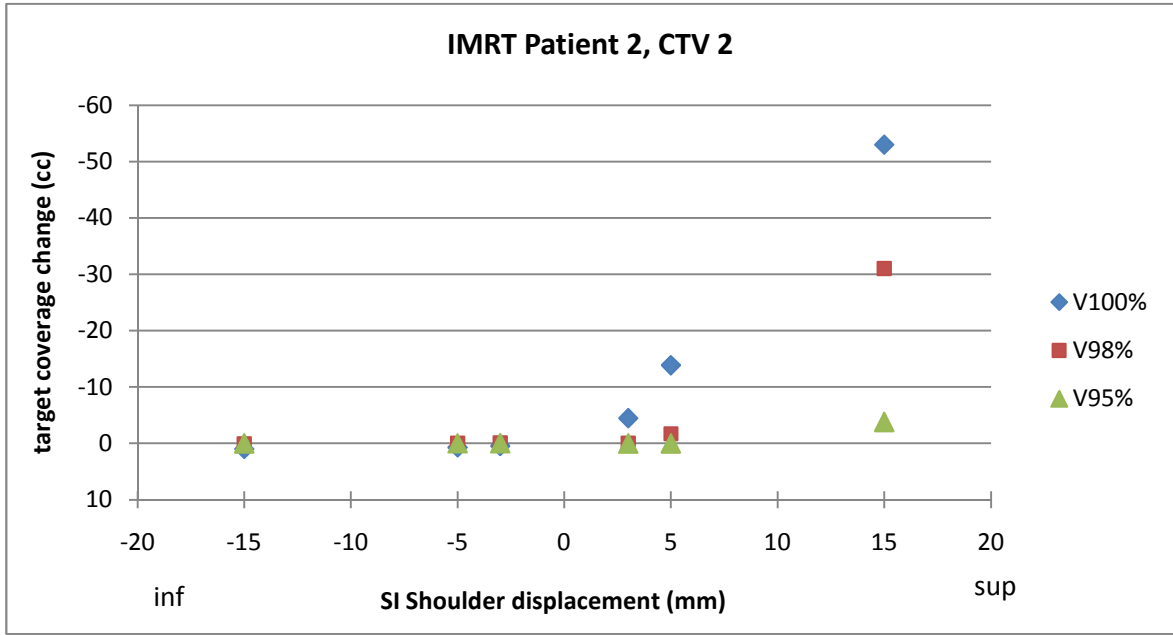


Figure 3.25a: Volume loss Patient 2 IMRT plan. Inferior shifts are to the left and superior to ther right. For Patient 2, Coverage loss (cc) increases with superior shift but is not gained with inferior shift.

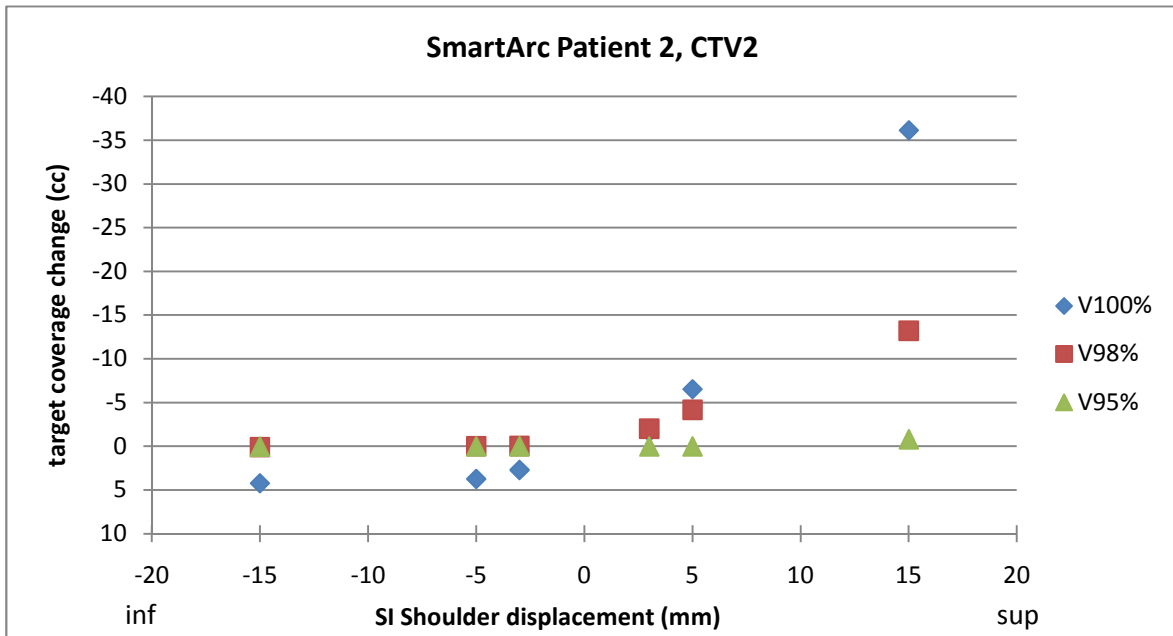


Figure 3.25b: Volume loss Patient 2 SmartArc plan. Inferior shifts are to the left and superior to ther right. Coverage loss (cc) increases with superior shift but is not gained with inferior shift. The same effect on coverage found with IMRT is seen for Smart Arc for Patient 2 as well.

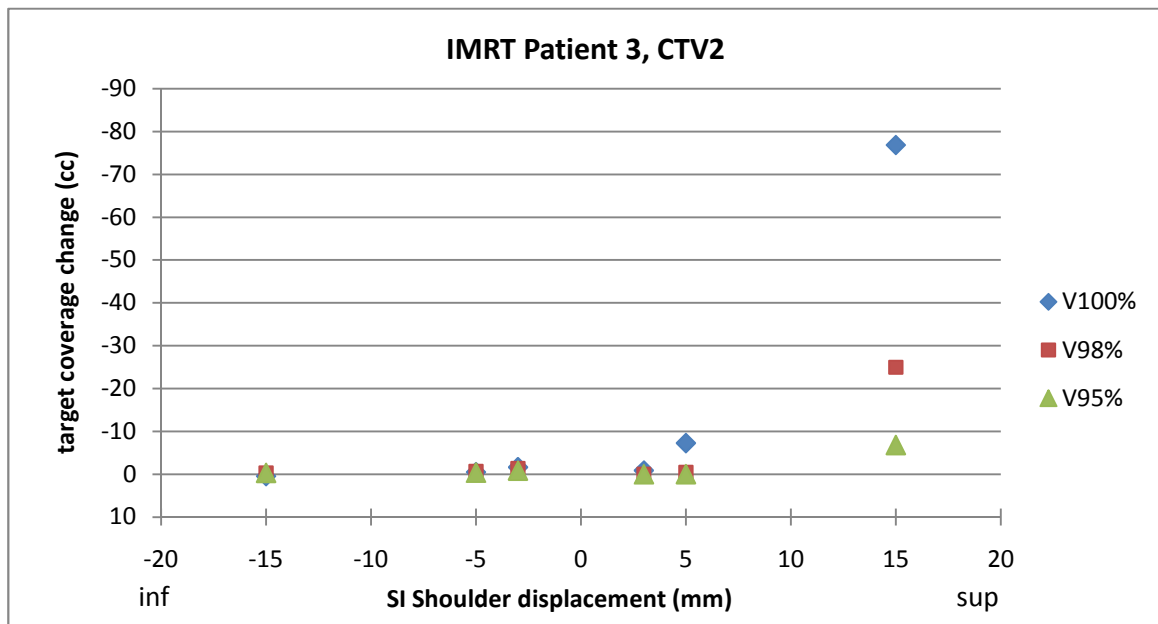


Figure 3.26a: Volume loss Patient 3 IMRT Plan. Inferior shifts are to the left and superior to ther right. For Patient 2, Coverage loss (cc) increases with superior shift but is not gained with inferior shift.

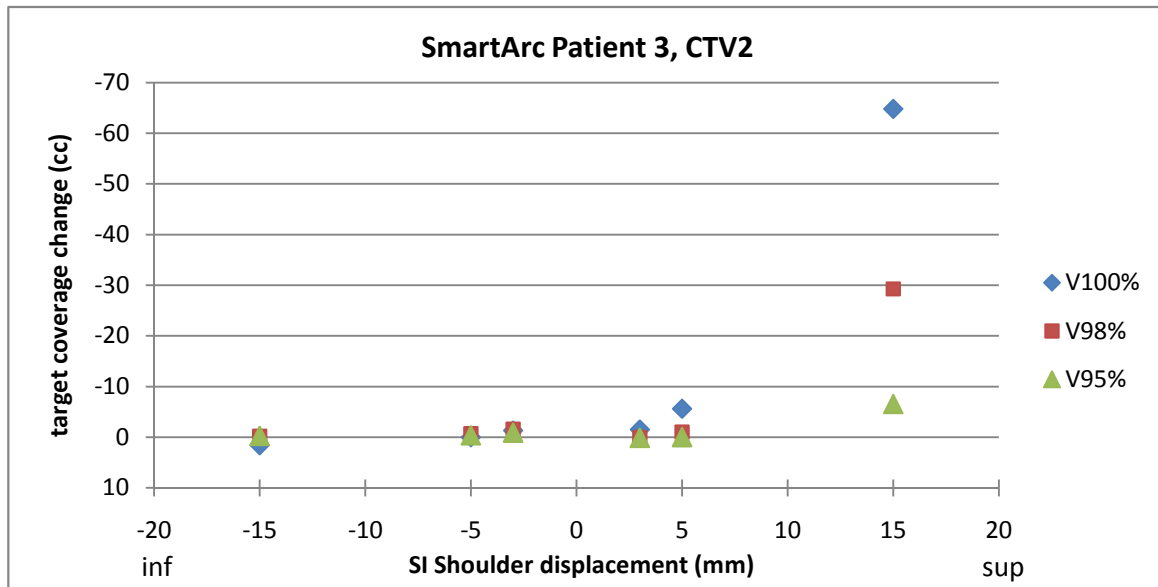


Figure 3.26b: Volume loss Patient 3 SmartArc plan. Inferior shifts are to the left and superior to ther right. Coverage loss (cc) increases with superior shift but is not gained with inferior shift. The same effect on coverage found with IMRT is seen for Smart Arc for Patient 3 as well.

3.2.2 Critical Structure Dose

In addition to decreasing the dose to the target volume, shoulder shifts also have the potential to increase dose to critical structures. The change in dose to the spinal cord and the brachial plexus for each shoulder shift was evaluated in Pinnacle for both IMRT and SmartArc plans. For each shift, the change in dose to 0.1 cc of the spinal cord and the change in the maximum DVH dose (cGy), as well as the change in volume (cc) receiving a typical mean dose of 25 Gy, are shown in Table 3-6. Positive numbers indicate an increase in dose or volume and negative numbers indicate a decrease. An increase in dose of more than 50 cGy, which could be of concern if the cord is near tolerance in the original treatment plan, is highlighted in red. The volume of the spinal cord receiving 45 Gy was also recorded, but it was always 0 cc, so it is not displayed in Table 3-6.

| Table 3-6: Spinal Cord Dose Change | | | | | | | |
|---|--------------------|-----------|-------|-----------|-------|-----------|-------|
| Shift | | Patient 1 | | Patient 2 | | Patient 3 | |
| | | IMRT | Arc | IMRT | Arc | IMRT | Arc |
| 3 mm superior | max DVH dose (cGy) | 0.4 | 0.9 | 0.1 | 0.5 | -8.7 | 2.1 |
| | max 0.1 cc (cGy) | -7 | 0 | 0 | 0 | -9 | -10 |
| | V25 (cc) | -0.01 | -0.01 | -0.06 | -0.02 | -0.04 | -0.01 |
| 5 mm superior | max DVH dose (cGy) | 0.8 | 2.1 | 0.9 | 1.4 | -23.1 | 5.2 |
| | max 0.1 cc (cGy) | -7 | 1 | 0 | 0 | -23 | -10 |
| | V25 (cc) | -0.01 | -0.02 | -0.11 | -0.07 | -0.07 | -0.01 |
| 15 mm superior | max DVH dose (cGy) | -3.5 | 7.4 | 5.2 | 3.6 | -76.7 | 7.8 |
| | max 0.1 cc (cGy) | -10 | 7 | 0 | 0 | -63 | -16 |
| | V25 (cc) | -0.06 | -0.03 | -0.09 | -0.25 | -0.15 | -0.03 |
| 3 mm inferior | max DVH dose (cGy) | -0.4 | -1 | 0.2 | -1.1 | 14.3 | 9.2 |
| | max 0.1 cc (cGy) | 10 | -2 | 0 | 0 | 17 | 8 |
| | V25 (cc) | 0.01 | 0.02 | 0.08 | 0.01 | 0.02 | 0 |
| 5 mm inferior | max DVH dose (cGy) | 0.1 | 0.03 | 0 | -1.3 | 23.9 | 56.2 |
| | max 0.1 cc (cGy) | 15 | -2 | 0 | 0 | 27 | 10 |
| | V25 (cc) | 0.06 | -2.2 | 0.06 | 0.02 | 0.01 | 0 |
| 15 mm inferior | max DVH dose (cGy) | -3.5 | 1.9 | 0.4 | 22.1 | 94.1 | 12.3 |
| | max 0.1 cc (cGy) | 5 | 5 | -5 | 20 | 77 | 24 |
| | V25 (cc) | -0.05 | 0.21 | 0.07 | 0.11 | -0.04 | 0 |
| 3 mm anterior | max DVH dose (cGy) | 0.2 | -0.5 | 0 | 0 | -3 | 0.3 |
| | max 0.1 cc (cGy) | 2 | 0 | 0 | 0 | -3 | -2 |
| | V25 (cc) | 0.01 | 0 | -0.03 | 0.02 | -0.01 | 0 |
| 15 mm anterior | max DVH dose (cGy) | 0.1 | -0.2 | -0.8 | 0 | 25.7 | 1.3 |
| | max 0.1 cc (cGy) | -4 | 0 | 0 | 0 | 25 | -18 |
| | V25 (cc) | 0 | -0.01 | -0.04 | -0.01 | 0 | 0.01 |
| 3 mm posterior | max DVH dose (cGy) | -0.4 | -0.6 | 0 | -0.1 | -5.2 | -0.9 |
| | max 0.1 cc (cGy) | -5 | 0 | 0 | 0 | -3 | 2 |
| | V25 (cc) | -0.02 | 0 | 0.02 | 0 | 0 | 0 |
| 15 mm posterior | max DVH dose (cGy) | -0.8 | -0.03 | 0.6 | -0.4 | -40.6 | -0.6 |
| | max 0.1 cc (cGy) | -2 | 0 | 0 | 0 | -28 | -8 |
| | V25 (cc) | -0.01 | 0 | 0.04 | -0.01 | -0.03 | -0.05 |
| 15 mm Right or Left* *Pt. 1 and 3 Lt, Pt. 2 Rt | max DVH dose (cGy) | 0.4 | -0.4 | -0.1 | 0.1 | -32.2 | 0.1 |
| | max 0.1 cc (cGy) | -2 | 0 | 0 | 0 | -21 | -10 |
| | V25 (cc) | 0 | -0.02 | 0.02 | -0.02 | 0 | 0 |

Table 3-6: Spinal Cord Dose Change. The change in maximum dose reported by the DVH as well as the change in maximum dose to 0.1cc of the spinal cord (cGy), and the change in volume receiving 25 Gy (cc), are shown for specified shifts. Increases in dose greater than 50 cGy are shown in red.

Patient 3's SmartArc plan shows an increase in maximum DVH dose that is greater than 50 cGy for a 5 mm inferior shift. For the IMRT plan, the 15 mm inferior shift shows an increase in maximum DVH dose and dose to 0.1 cc greater than 50 cGy. Patients 1 and 2 do not show changes in cord dose of this magnitude. A plot of change in dose to 0.1 cc of the

cord vs. shoulder shift shows the relationship between displacement and an increase or decrease in dose.

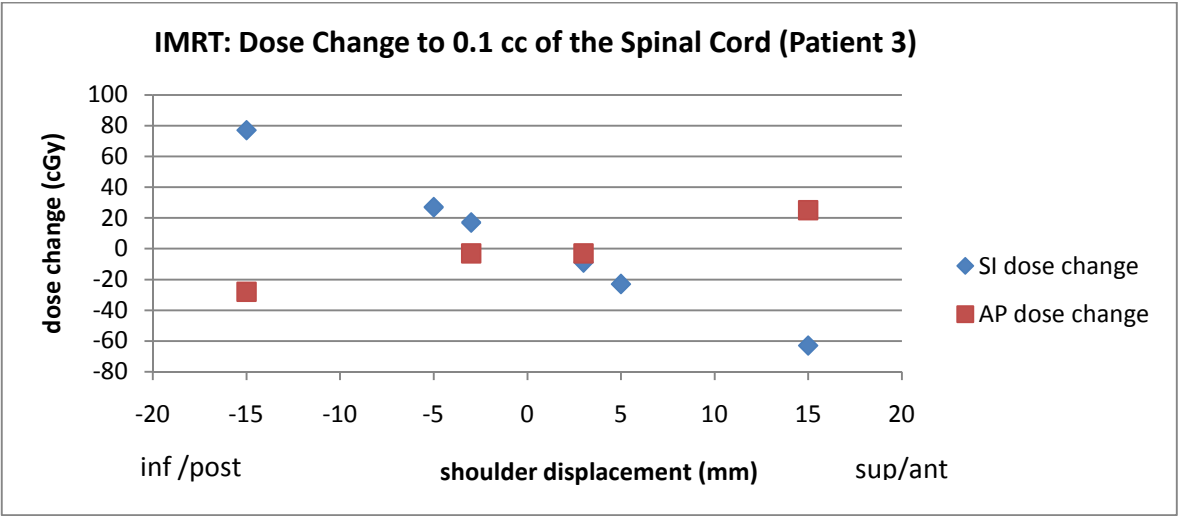


Figure 3.27a: Change in dose to 0.1 cc of the spinal cord plotted vs. shoulder displacement in the superior/inferior and anterior/posterior directions for Patient 3's IMRT plan.

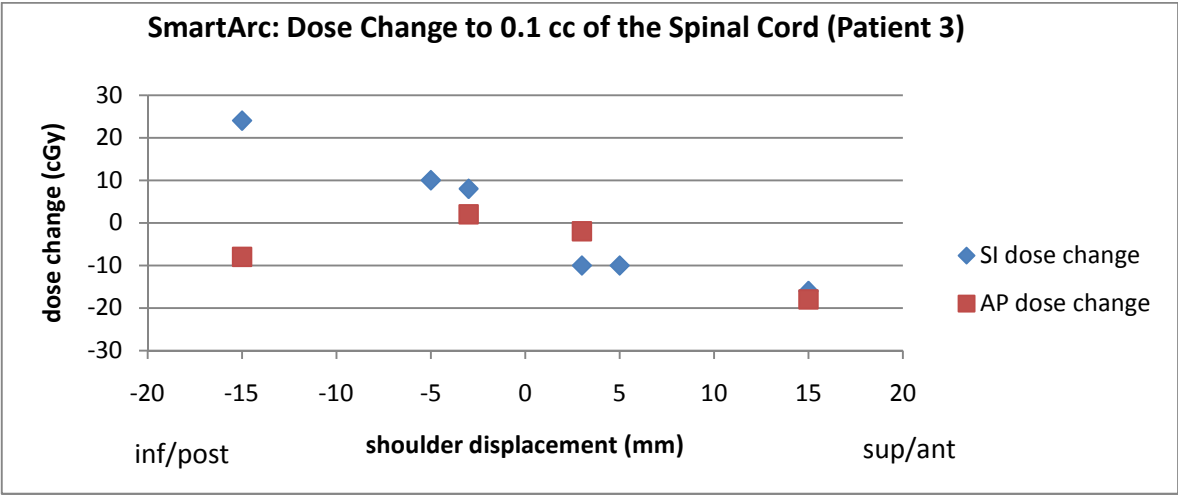


Figure 3.27b: Change in dose to 0.1 cc of the spinal cord plotted vs. shoulder displacement in the superior/inferior and anterior/posterior directions for Patient 3's SmartArc plan.

In the Figure 3.27 above for Patient 3, the dose to 0.1 cc of the spinal cord appears to increase with inferior shifts and decrease with superior shifts. This makes sense based on the

decreased beam attenuation associated with an inferior shift, where the shoulder is pulled out of the beam path. No clear relationship is seen with shifts in the AP direction. In the figures below for Patient1, no clear relationship is seen in either direction.

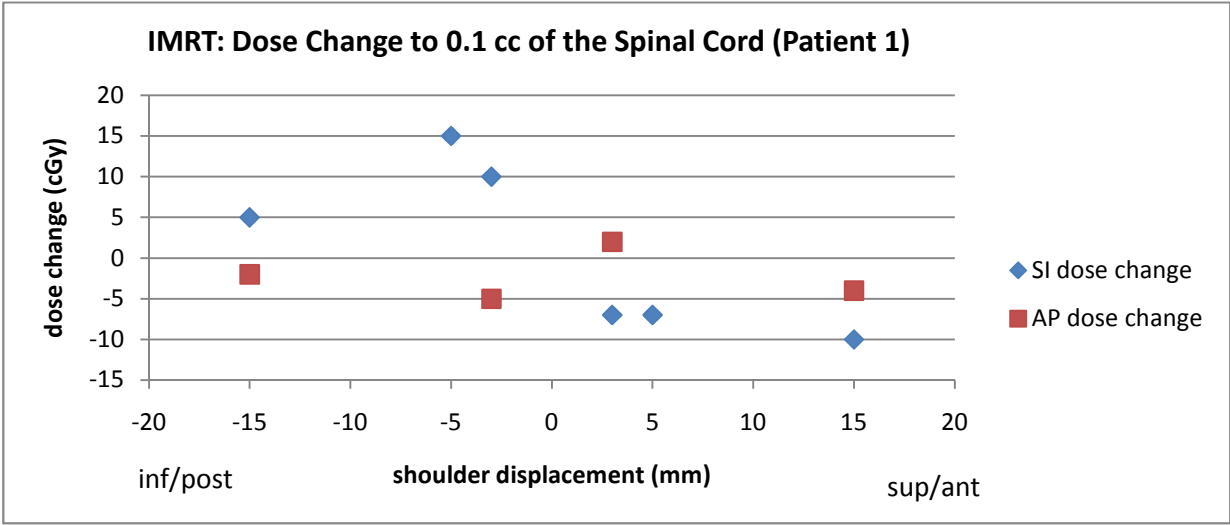


Figure 3.28a: Change in dose to 0.1 cc of the spinal cord plotted vs. shoulder displacement in the superior/inferior and anterior/posterior directions for Patient 1’s IMRT plan.

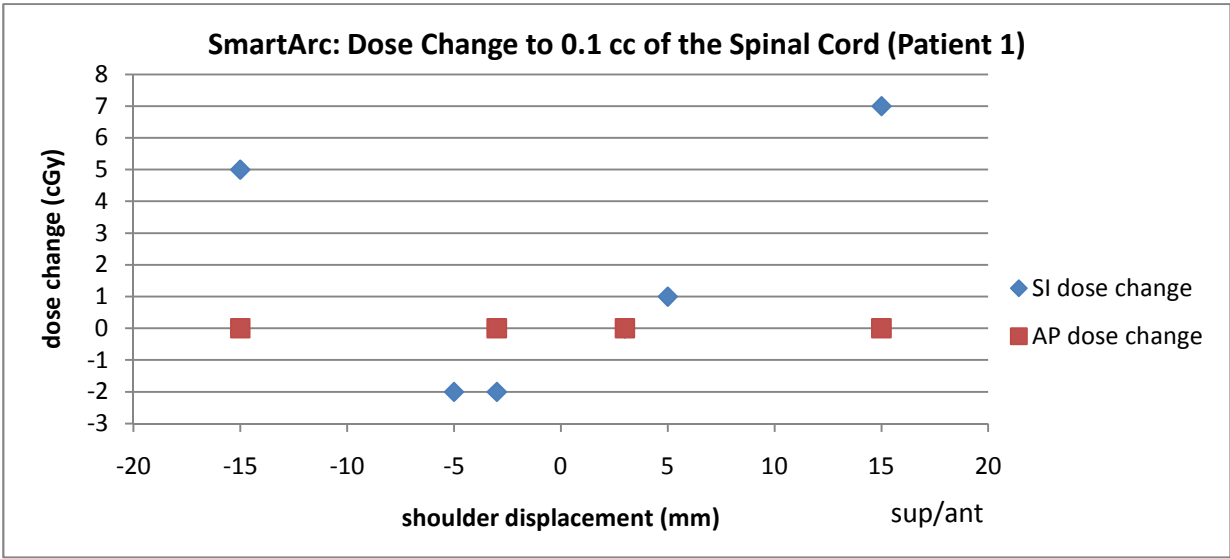


Figure 3.28b: Change in dose to 0.1 cc of the spinal cord plotted vs. shoulder displacement in the superior/inferior and anterior/posterior directions for Patient 1’s SmartArc plan.

In the Figure 3.29 below for Patient 2, there was no change in dose to 0.1 cc of the spinal cord except for the 15 mm superior and inferior directions for the IMRT plan, and the 15 mm inferior direction for the SmartArc plan.

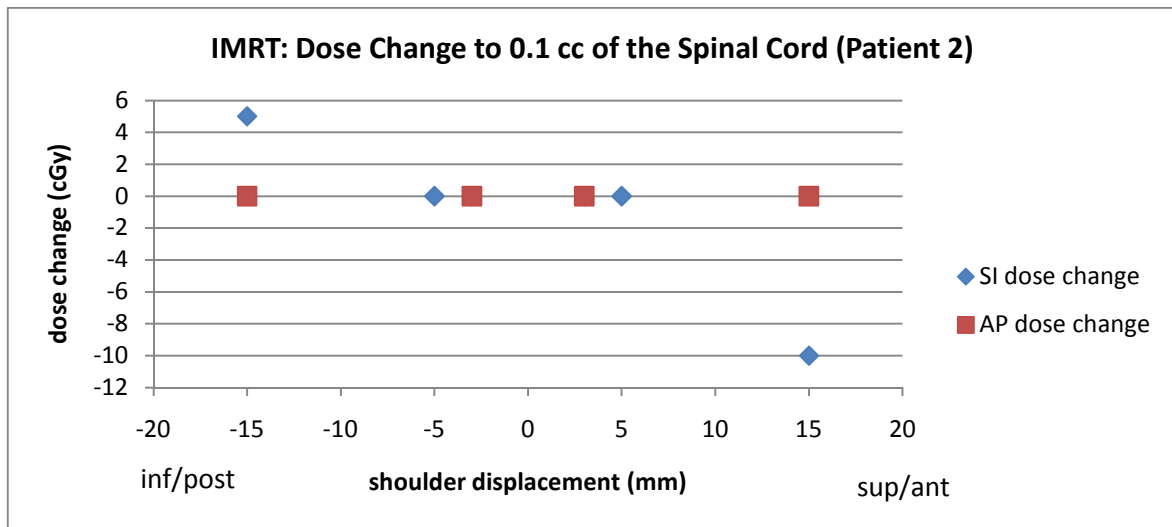


Figure 3.29a: Change in dose to 0.1 cc of the spinal cord plotted vs. shoulder displacement in the superior/inferior and anterior/posterior directions for Patient 2's IMRT plan.

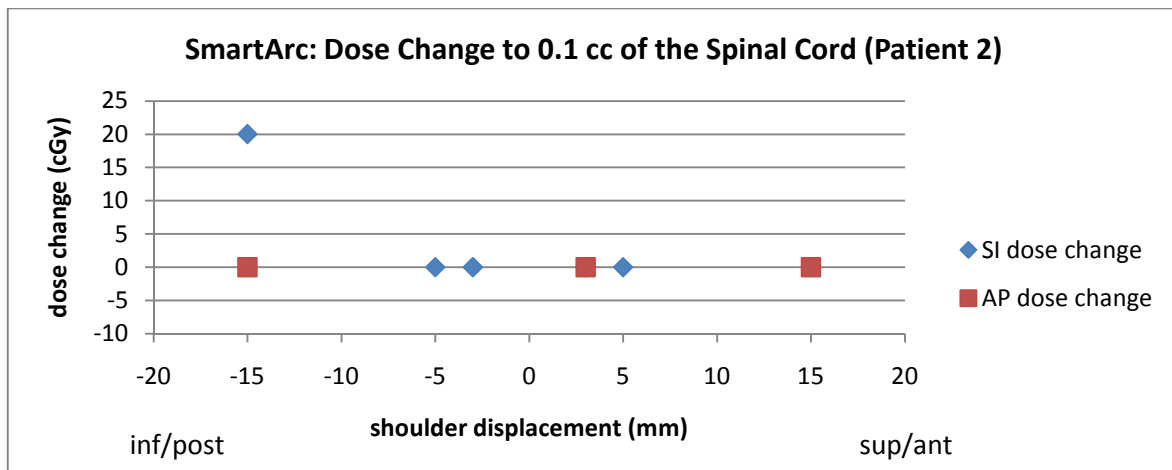


Figure 3.29b: Change in dose to 0.1 cc of the spinal cord plotted vs. shoulder displacement in the superior/inferior and anterior/posterior directions for Patient 2's SmartArc plan.

The change in dose to the brachial plexus was evaluated in the same way as the spinal cord. For each shift, the change in dose to 0.1 cc of the brachial plexus and the change in the maximum DVH dose (cGy), as well as the change in volume (cc) receiving a TD5/5 dose of 60 Gy, are shown in Table 3-7. Positive numbers indicate an increase in dose or volume and negative numbers indicate a decrease. An increase in dose of greater than 50 cGy or an increase in V60 of greater than 1 cc is highlighted in red. The volume of the brachial plexus receiving 75 Gy was also recorded, but it was always 0 cc so it is not shown in Table 3-7.

| Table 3-7: Brachial Plexus Dose Change | | | | | | | | |
|---|--------------------|-----------|-------|-----------|-------|-----------|--------|--|
| Shift | | Patient 1 | | Patient 2 | | Patient 3 | | |
| | | IMRT | Arc | IMRT | Arc | IMRT | Arc | |
| 3 mm superior | max DVH dose (cGy) | 1.1 | 1.9 | -16.2 | -12 | -34.7 | -62.4 | |
| | max 0.1 cc (cGy) | 0 | 0 | -52.5 | -22.5 | -30 | -60 | |
| | V60 (cc) | 0 | -0.04 | -0.08 | -0.09 | -0.01 | -0.01 | |
| 5 mm superior | max DVH dose (cGy) | 2.4 | 4.4 | -47.5 | -22 | -56.6 | -98.8 | |
| | max 0.1 cc (cGy) | 0 | 0 | -80 | -35 | -60 | -90 | |
| | V60 (cc) | 0 | -0.06 | -0.24 | -0.24 | -0.02 | -0.01 | |
| 15 mm superior | max DVH dose (cGy) | 0.6 | 12.4 | -105.6 | -50.6 | -152.8 | -207.8 | |
| | max 0.1 cc (cGy) | -15 | 0 | -110 | -95 | -150 | -213 | |
| | V60 (cc) | 0 | -0.09 | -0.67 | -0.73 | -0.02 | -0.01 | |
| 3 mm inferior | max DVH dose (cGy) | -1.1 | -2.6 | 116.1 | 11.6 | 45.1 | -28.5 | |
| | max 0.1 cc (cGy) | 0 | 40 | 100 | 45 | 40 | 60 | |
| | V60 (cc) | 0 | 0.25 | 0.09 | 0.07 | 0.03 | -0.01 | |
| 5 mm inferior | max DVH dose (cGy) | 5 | -4.4 | 143.3 | 22.5 | 91.3 | 120.8 | |
| | max 0.1 cc (cGy) | 0 | 40 | 130 | 60 | 90 | 97 | |
| | V60 (cc) | 0.01 | 1.03 | 0.09 | 0.09 | 0.08 | 0.2 | |
| 15 mm inferior | max DVH dose (cGy) | 48.9 | 371.8 | 203.4 | 185.5 | 217.7 | 259 | |
| | max 0.1 cc (cGy) | 60 | 410 | 205 | 195 | 210 | 240 | |
| | V60 (cc) | 1.34 | 3.16 | 0.12 | 0.25 | 0.42 | 1.1 | |
| 3 mm anterior | max DVH dose (cGy) | -0.6 | -0.2 | 21.5 | 0.8 | 23.4 | -14.3 | |
| | max 0.1 cc (cGy) | 0 | 0 | 15 | 5 | 20 | -20 | |
| | V60 (cc) | 0 | 0 | 0.02 | 0.01 | 0.01 | -0.01 | |
| 15 mm anterior | max DVH dose (cGy) | -0.9 | 1.4 | 124.8 | 9.6 | 108.9 | -64 | |
| | max 0.1 cc (cGy) | 0 | 0 | 100 | 0 | 100 | -70 | |
| | V60 (cc) | 0 | 0 | 0.11 | 0.03 | 0.09 | -0.01 | |
| 3 mm posterior | max DVH dose (cGy) | -0.6 | -2.2 | -8 | -6.5 | -11.2 | 14.4 | |
| | max 0.1 cc (cGy) | 0 | -5 | -10 | 0 | -10 | 13 | |
| | V60 (cc) | 0 | -0.01 | -0.02 | -0.01 | -0.01 | 0.01 | |
| 15 mm posterior | max DVH dose (cGy) | -0.9 | -1.6 | -11.3 | -6.5 | -95.9 | 79 | |
| | max 0.1 cc (cGy) | 0 | -5 | -45 | -5 | -100 | 70 | |
| | V60 (cc) | 0 | 0.12 | -0.12 | -0.04 | -0.02 | 0.11 | |
| 15 mm Right or Left* *Pt. 1 and 3 Lt, Pt. 2 Rt | max DVH dose (cGy) | 1.1 | 1.6 | 70 | 0.1 | -84 | -59.2 | |
| | max 0.1 cc (cGy) | 0 | 0 | 70 | 25 | -50 | -70 | |
| | V60 (cc) | 0 | 0 | 0.06 | 0.03 | -0.02 | -0.01 | |

Table 3-7: Brachial Plexus Dose Change. The change in maximum dose reported by the DVH as well as the change in maximum dose to 0.1cc of the brachial plexus (cGy), and the change in volume receiving 60 Gy (cc), are shown for specified shifts. Increases in dose greater than 50 cGy are shown in red.

The volume of the brachial plexus getting 60 Gy only increased by more than 1 cc for a 5 and 15 mm inferior shift on Patient 1, however the V60 did not change in any other cases. Inferior shifts of 3 mm and 5 mm can cause increased brachial plexus dose by 1 Gy or more for IMRT and SmartArc plans, as shown for Patient 2. Large, inferior shifts consistently increase the dose by 2 Gy or more in both types of plans. Large, anterior shifts can cause an increase in dose of more than 1 Gy for IMRT plans, as shown for Patients 2 and 3. In addition, superior shifts cause a decrease in dose for both plans, but only the large superior shifts show a decrease in dose of more than 1 Gy for Patients 2 and 3, which does not balance the dose increased caused by large inferior shifts. Large, posterior shifts showed a decrease in dose in the IMRT plan only for Patient 3. The change in dose is less than 1 Gy for right or left shifts for both IMRT and SmartArc plans. A plot of change in dose to 0.1 cc of the brachial plexus vs. shoulder displacement shows the relationship between change in dose and shoulder position in the AP and SI directions.

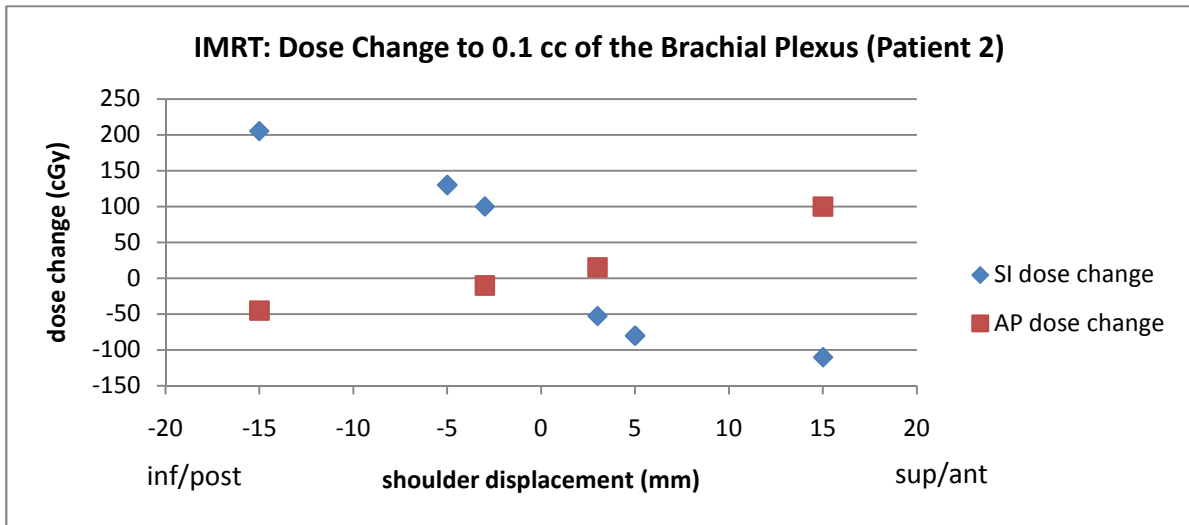


Figure 3.30a: Change in dose to 0.1 cc of the brachial plexus plotted vs. shoulder displacement in the superior/inferior and anterior/posterior directions for Patient 2's IMRT plan.

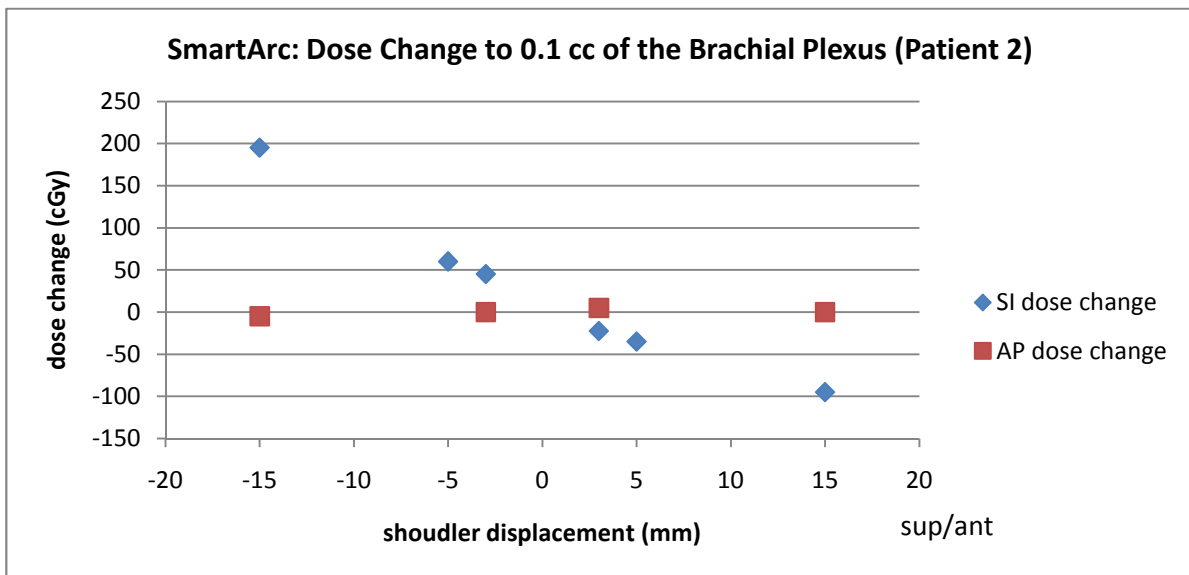


Figure 3.30b: Change in dose to 0.1 cc of the brachial plexus plotted vs. shoulder displacement in the superior/inferior and anterior/posterior directions for Patient 2's SmartArc plan.

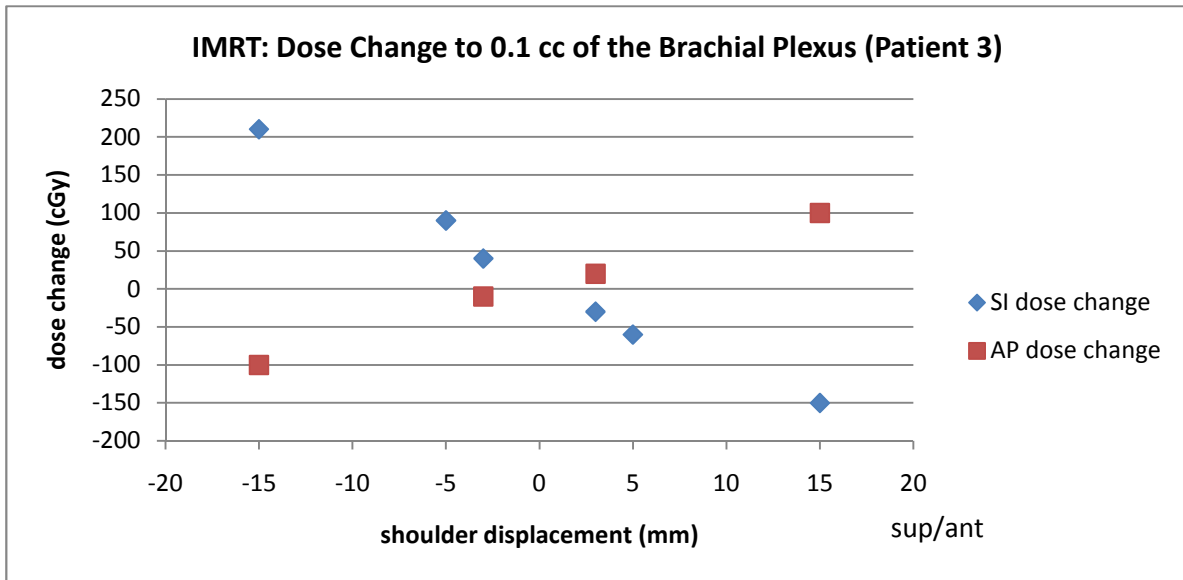


Figure 3.31a: Change in dose to 0.1 cc of the brachial plexus plotted vs. shoulder displacement in the superior/inferior and anterior/posterior directions for Patient 3's IMRT plan.

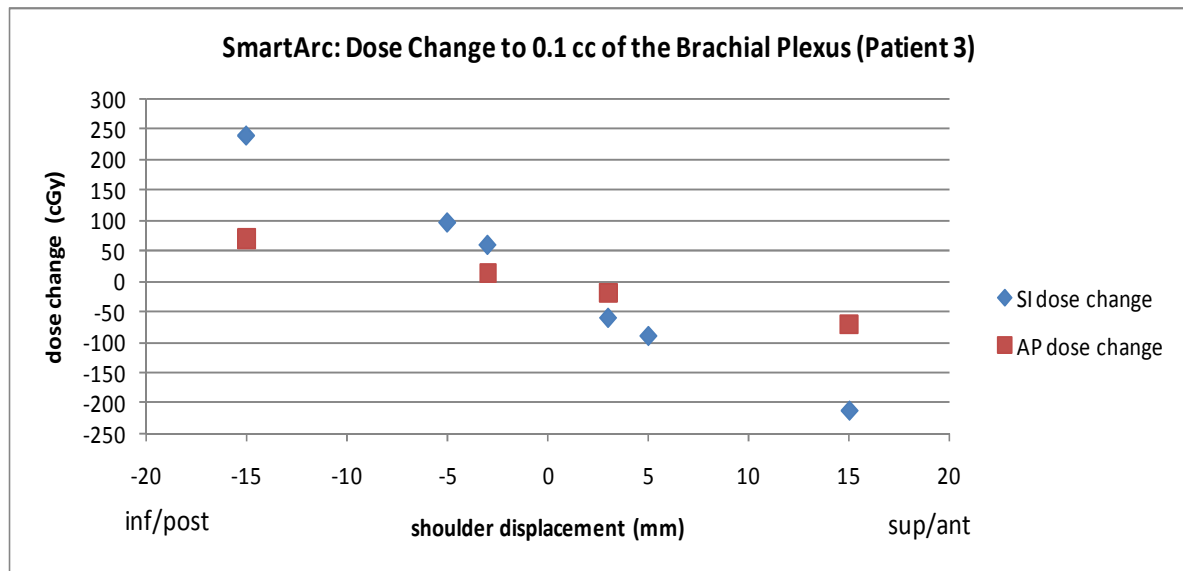


Figure 3.31b: Change in dose to 0.1 cc of the brachial plexus plotted vs. shoulder displacement in the superior/inferior and anterior/posterior directions for Patient 3's SmartArc plan.

In the Figures 3.30-3.31 above for Patient 2 and Patient 3, the dose to 0.1 cc of the brachial plexus appears to increase with inferior shifts and decrease with posterior shifts. In the AP

direction, the dose appears to change consistently for IMRT plans (Fig. 3.30a and 3.31a) where dose increases with large posterior shifts and increases with large anterior shifts. The relationship in the AP direction is not clear for SmartArc plans (Fig. 3.30b and 3.31b). No relationship is found for Patient 1 in either direction (Fig. 3.32a and b).

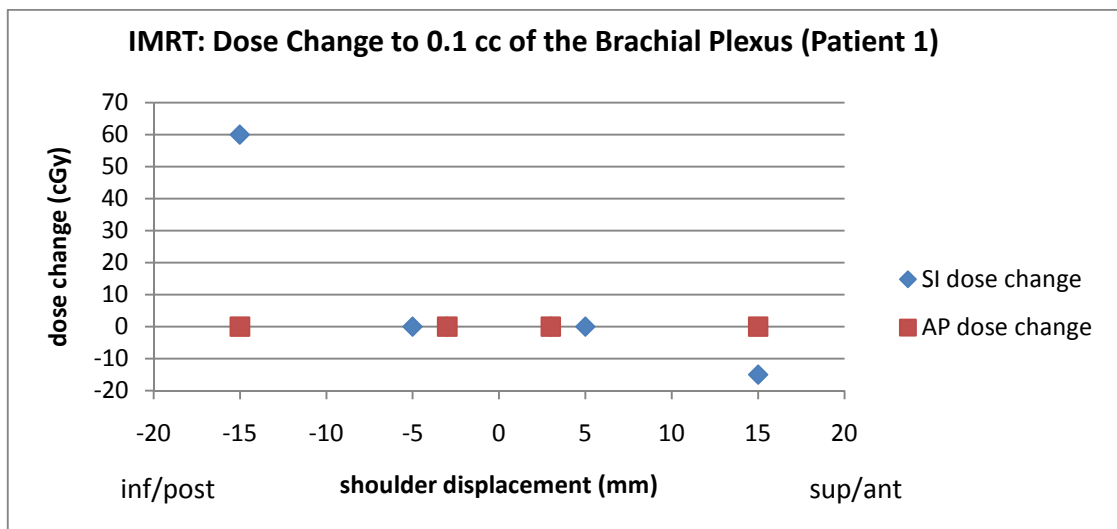


Figure 3.32a: Change in dose to 0.1 cc of the brachial plexus plotted vs. shoulder displacement in the superior/inferior and anterior/posterior directions for Patient 1's IMRT plan.

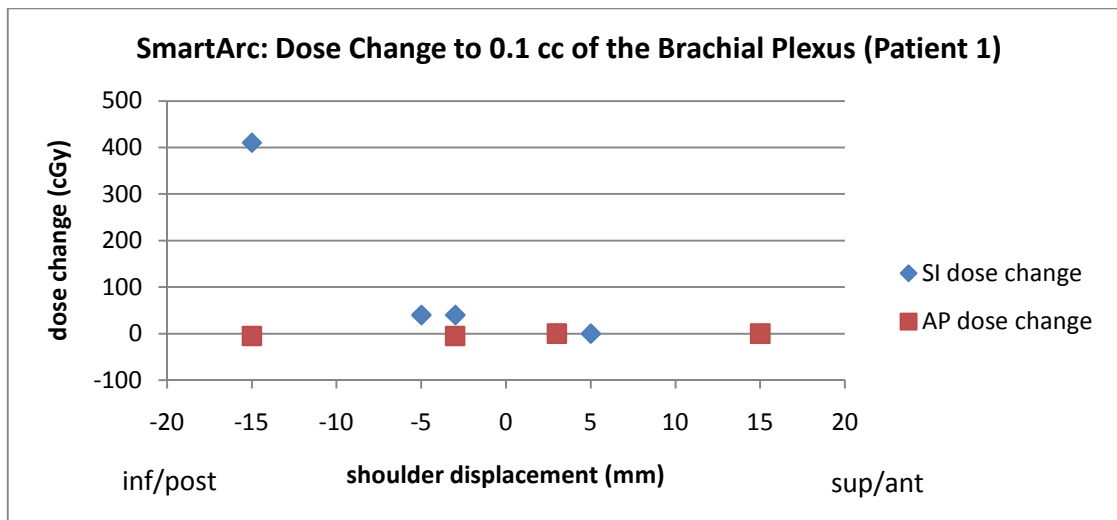


Figure 3.32b: Change in dose to 0.1 cc of the brachial plexus plotted vs. shoulder displacement in the superior/inferior and anterior/posterior directions for Patient 1's SmartArc plan.

3.3 Comparing the Daily CT Shift to the Hand Edited Shift: Confirmation with CAT

The validity of the dosimetric impact of the hand-edited contours was verified by comparing a hand-edited shoulder shift contour calculation against a calculation based on subsequent CT scans that captured the same shifts. A comparison of the target coverage computed after a superior shoulder shift was drawn by hand to the dose distribution on a CT scan that demonstrated the same superior shoulder shift was achieved by the methods described in section 2.4. As discussed, one patient, Case 1, had left shoulder shifts of 1.12 cm left, 0.42 cm anterior, and 1.32 cm superior; and right shoulder shifts of 1.04 cm right, 0.46 cm posterior, and 2.77 cm superior. The other patient, Case 2, had left shoulder shifts of 0.05 cm right, 0.09 cm anterior, and 1.04 cm superior; and right shoulder shifts of 0.06 cm left, 0.36 anterior, and 1.01 cm superior. Both patients showed similar isodose distributions when comparing the hand edited plan to the plan calculated on a daily CT.

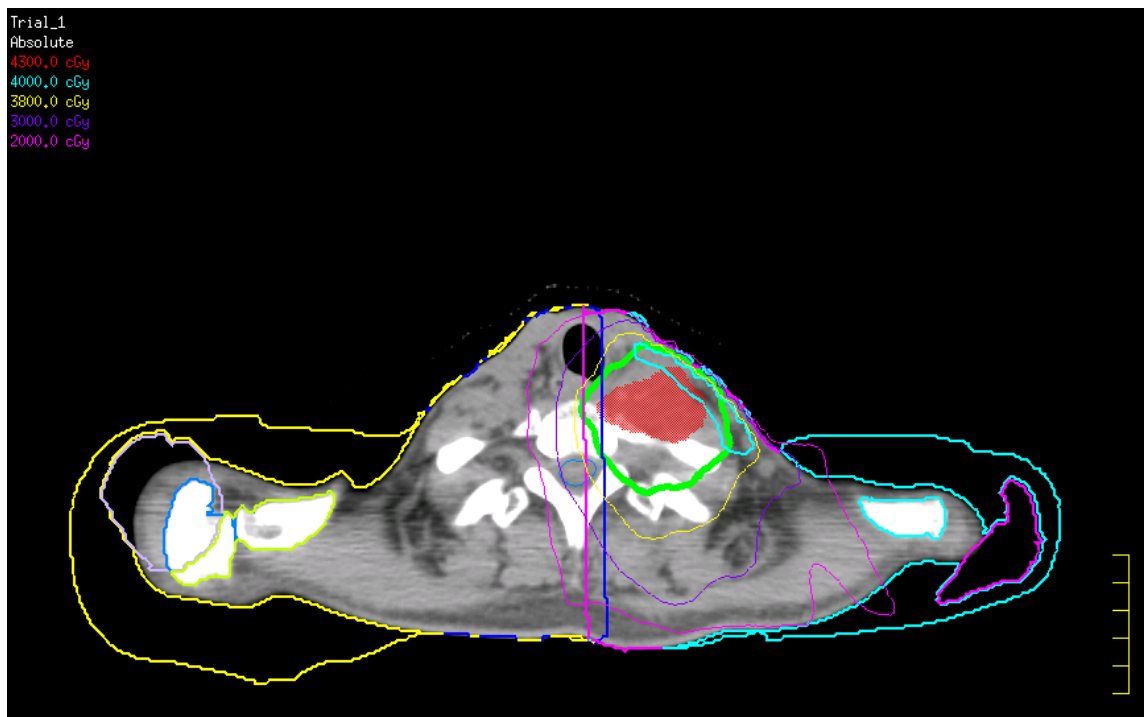


Figure 3.33: Case 1 hand edited shoulder shifts. Edited right shoulder contour is yellow, and edited left shoulder contour is light blue. The 40 Gy line (aqua) only covers a small portion of CTV (red).

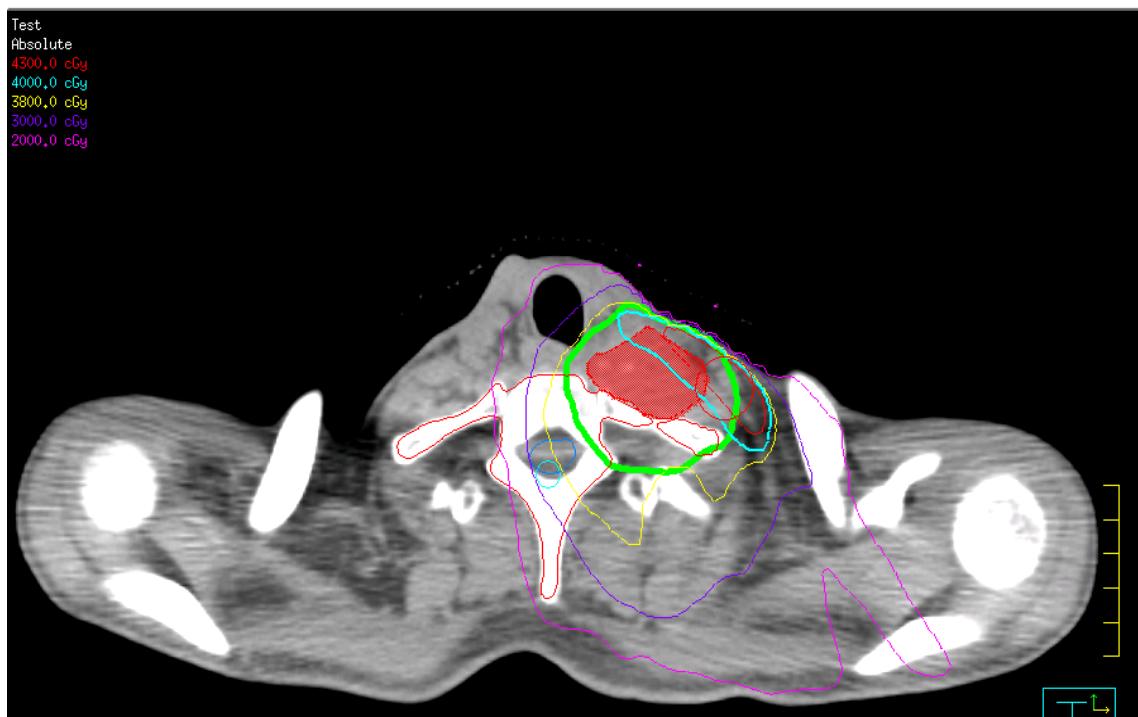


Figure 3.34: Case 1 daily CT with shoulder shifts. 40 Gy line (aqua) covers the same portion of CTV (red).

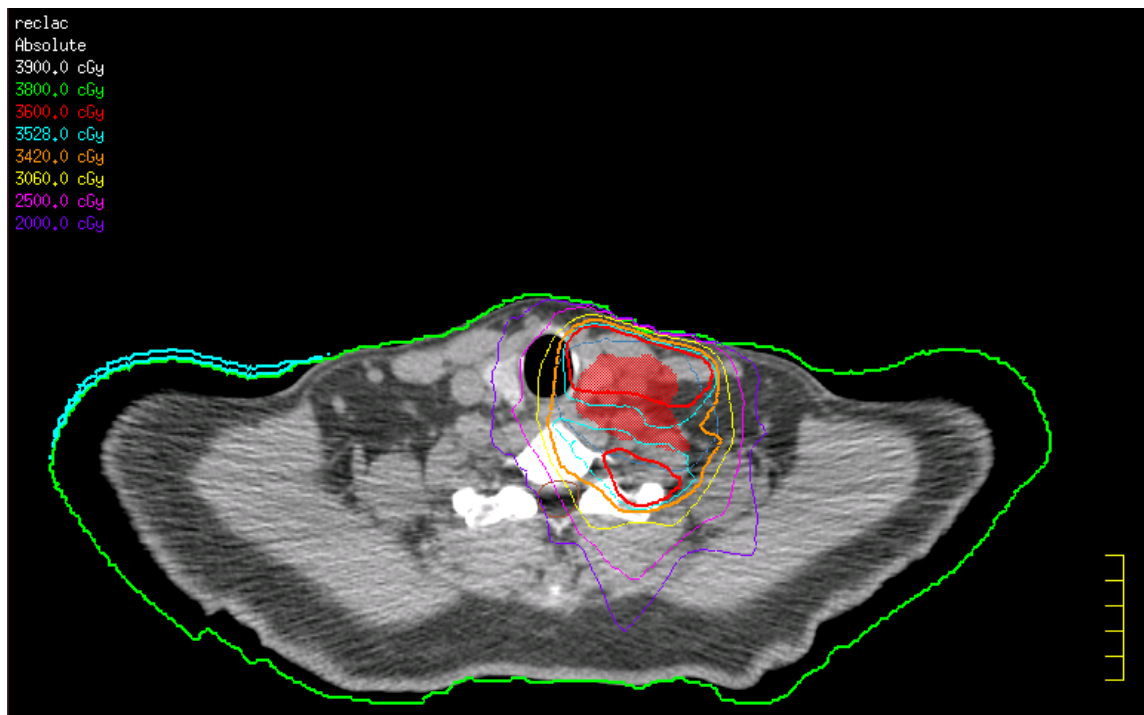


Figure 3.35: Case 2 hand edited shoulder shifts. The edited superior shift is in green and the anterior shift of the right shoulder is in light blue. The isodose lines (red and aqua) no longer cover CTV (red).

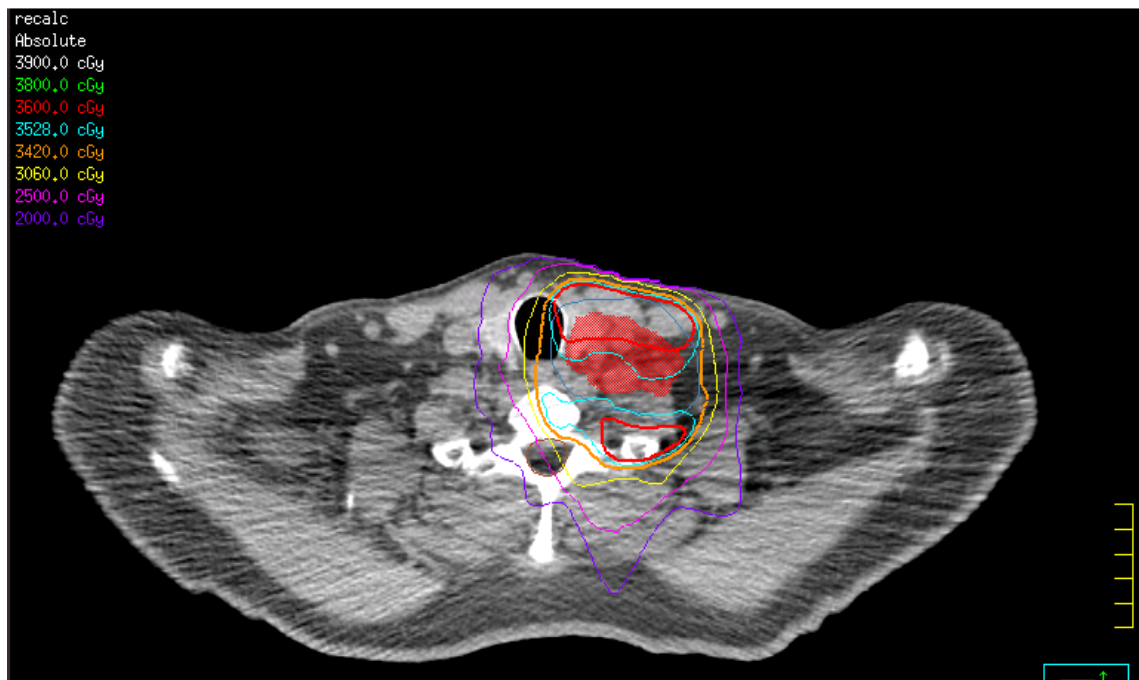


Figure 3.36: Case 2 daily CT with shoulder shifts. Isodose lines have similar distribution around CTV.

For Case 1 (Fig 3.33 and 3.34) the hand editing was similar, but did not create exactly the same external shape as found in the daily CT. For Case 2 (Fig. 3.35 and 3.36) the hand editing approximated the patients shape in the daily CT very well. As mentioned in section 2.4, the image defromation resulted in a change in the volumes of the PTV and CTV from one scan to the other, and the excess volume was subtracted off the larger of the two to obtain comparable changes in target coverage. Table 3-8 shows the calculated change in target coverage for the hand edited and deformed plans.

| Table 3-8: Comparison of Target Coverage lost for hand edited shifts and daily CT (cc) | | | | | | | |
|---|---------------|-------|-----|-------------|---------------|--------|-------|
| | Case 1 | | | | Case 2 | | |
| HAND | V40 | V39.2 | V38 | HAND | V36 | V35.28 | V34.2 |
| GTV40 Gy | -87 | -15 | 0 | PTV 36 Gy | -16 | -12 | 1 |
| CTV40 Gy | -170 | -39 | -2 | CTV 36 Gy | -2 | -6 | 0 |
| CT | V40 | V39.2 | V38 | CT | V36 | V35.28 | V34.2 |
| GTV40 Gy | -56 | -23 | -2 | PTV 36 Gy | -21 | -16 | 4 |
| CTV40 Gy | -114 | -61 | -10 | CTV 36 Gy | -4 | -10 | 0 |

Table 3.8: Comparison of Target Coverage lost of hand edited shifts and daily CT. Both the hand edited shifts and daily CTs calculations showed an increased incovrage loss at higher dose levels.

The data in Table 3-8 above shows that coverage is lost when the shoulders are in a different position on the daily CT as well as when the shift is modeled by hand. All of the losses were captured, and although there were sometimes relatively large differences between specific values when comparing the two techniques, the results are nevertheless convincing that the trends and values determined are reasonable. It is interesting to note that for the majority of cases, the CT calculation resulted in a larger loss of coverage than predicted with the hand-edits.

CHAPTER 4: Discussion

4.1 Interpretation of the Results

4.1.1 Measured shoulder shifts

The shifts we observed were used as a basis to model the shifts in the dosimetric studies. The CT on rails data showed that the largest shifts (over 1 cm) were in the posterior and inferior directions. The inferior shifts occurred later in treatment, but the posterior shifts happened early or late in treatment. The posterior and inferior shifts may have been a result of the patient being more relaxed during treatment than during simulation. The larger inferior shifts may occur later in treatment as a result of weight loss, so the mask no longer fits as well as it did at simulation. In addition, the largest variation of shifts in the SI direction were seen for CT on rails Patient 4, who had a head only mask with a vacuum bag immobilizing the shoulders. This result suggests that the shoulders may be immobilized better in the 5-point head and shoulder mask. The average magnitude of the shift and the average that included direction were both 2-5 mm. As discussed below, a shift of this magnitude in the superior direction could reduce target coverage in the lower neck. However, as seen in Figures 3.24a-3.26b, the effects of shifts in opposite directions do not cancel out. This implies that applying an average shift of humeral head position over the course of treatment that took into account the direction of shoulder displacement relative to C2 (correct isocenter alignment) would not give a useful estimate of dosimetric impact. Instead of an average shoulder position, the frequency of large shifts must be considered.

4.1.2 Dosimetric Impact

For the 3 patients in this study, the superior shifts showed the largest effect on dose. Even with a 3 mm superior shift, up to 4 cc of cold spots were created in the 100% isodose line. For larger superior shifts, the dose distribution was degraded further such that the prescription line no longer covered 95% of the volume, nor did the 95% isodose line cover parts of the target. This dose degradation occurred because a superior shoulder shift brings the shoulder tissue into the lower neck region, thereby increasing the attenuation of the beams. As can be seen in the axial slices shown in Figures 3.17b and d, 3.19b and d, and 3.22b and d, the depth to the target increases with the superior shift, thus reducing the dose to the target. However, an inferior shift of equal magnitude will not cause an increase in coverage, as shown in Figures 3.24a-3.26b. An inferior shift does not cause a large decrease of tissue in the lower neck region; therefore the depth to the target does not change enough to have a large dosimetric impact, although small increases do occur within the volume.

While both IMRT and SmartArc showed target coverage loss for superior shifts, neither consistently showed more loss than the other. This result suggests that the amount of target coverage loss due to superior shifts has more to do with the location of the target and patient anatomy than it does with the type of plan. For example Patient 1's SmartArc plan lost more CTV2 coverage than the IMRT plan with a 15 mm superior shift (Table 3-4 and 3-5). This CTV was a large, anterior, bilateral target (Fig. 3.16a-d) that would have received dose from a large portion of the arc fields as it moved entirely through the shoulders, and as noted earlier, the IMRT plan was heavily weighted towards the posterior beams which would not pass through as much of the shoulder. However, Patient 3 has larger CTV2 coverage loss for the IMRT plan with a 5 mm and 15 mm superior shift (Table 3-4 and 3-5).

This CTV was medial and closer to the primary tumor (Figs. 3.22). In this case, the more uniform distribution of the MU in arc plan seems to be disturbed less than the posteriorly weighted IMRT plan.

In addition to superior shifts, target coverage of the 100% isodose line was lost for a 15 mm posterior shift, but only for IMRT plans. This was most likely due to the fact that most of the MU for the IMRT plans came from the posterior direction. The posterior fields accounted for 67%, 58%, and 55% of the MU for dosimetric Patients 1, 2, and 3, respectively. The posterior shift moved more tissue into the path of these beams and caused the depth of the target to increase. The increased attenuation of the posterior beams resulted in dose lost to the target. This effect was not seen for the SmartArc plans because arc delivery has a more even distribution of the MU. The effect of the 15 mm posterior shift was the only important difference seen between IMRT and SmartArc.

Aside from the 15 mm posterior shift, the coverage loss followed the same trend for IMRT and SmartArc. Anterior, right, left and 3 mm posterior shifts did not show large changes in target coverage. The 3 mm posterior shifts were too small to have an impact on posterior IMRT fields. Anterior shifts did not influence SmartArc for the same reasons that posterior shifts did not, and they did not impact IMRT plans because, as described above, the IMRT fields were strongly weighted towards the posterior. Right or left shifts did not affect either plan type because the targets observed in this study were medially located and would have received most of the MU from posterior and anterior beams from IMRT plans. For right or left shifts in an arc plan, which has a more uniform distribution of MU, the change in dose is more likely to be balanced out by the increase in depth of movement into

an arc segment on one side and the decrease in depth from moving away from a nearly equally weighted arc segment on the opposite side in the same axial position.

In addition to target coverage, the dose to the spinal cord and the brachial plexus was evaluated. As seen in Table 3-5, with the exception of dosimetric Patient 3, no increase in dose over 50 cGy was seen for the spinal cord. Patient 3 demonstrated an increase in dose of >50cGy to 0.1 cc of the cord for a 5 mm and 15 mm inferior shift. For this patient, the small changes in depth with inferior shifts may have caused increase in cord dose. Overall, as seen with Patient's 1 and 2, the cord is usually avoided in the plan and is often far from the target. This avoidance of the cord is still effective even with the shoulder displacement.

As opposed to the spinal cord, the brachial plexus was often not considered in the treatment planning, and was located close to the targets. Therefore changes in depth to the brachial plexus did change the dose received by 0.1 cc. Inferior shifts resulted in the largest increases in brachial plexus dose, as did 15 mm anterior shifts for IMRT plans (Table 3-6). The increase in brachial plexus dose for anterior shifts was likely another result of the heavy weighting of the posterior beams in the IMRT plans. With the shoulders moving forward, the beams were attenuated less. In addition, for Patients 2 and 3, the dose to the brachial plexus decreased with superior shifts due to increased attenuation, and there is an inverse relationship between position in the SI direction and dose to the brachial plexus (Fig. 3.30a-3.31b).

4.1.3 Confirmation with CAT

Using CT on rails data with the CAT software to recompute a treatment plan and compare it to a plan calculated on a CT with shoulder shift contours drawn by hand verified the drawing method by showing the same trend in coverage loss between the two methods.

The isodose lines looked similar between the two methods as seen in Figs. 3.35 and 3.36, which showed that the attenuation effect of the shoulders in the beams is valid for the drawn contours.

Although the dosimetric trends were similar between the two methods, the absolute values for the volume of target coverage lost were sometimes very different (Table 3-8). In most cases the coverage loss calculated on the CTs was greater than on the plans edited by hand. This result is likely due to the fact image deformation algorithm used by CAT did not always transfer the CTVs onto the daily CTs such that they had the same volume and shape as the original CTV (which is visible in Figs. 3.33-3.36), as well as the fact that daily anatomy changes are included in the CT but are not included in the hand edits. Figure 3.34 shows that the change in body position on the table between the first day and the next did not yield the exact translational movement of the shoulders assumed by the shifts drawn in Figure 3.33. Despite these problems with isolating the shoulder and putting the CTVs on the daily CTs, the calculations with CAT did reveal that drawing the shoulders and recalculating the treatment plans on the new contours realistically demonstrated the dosimetric effect of the shoulder shift.

4.2 Clinical Impact

Although large shoulder shifts show a loss in target coverage and increase in brachial plexus dose, the dose changes shown in Tables 3-4 and 3-5 would only occur if there were systematic shifts every day due to patient setup with the shoulders superior or posterior to the simulation CT position. However, for most patients these shifts do not occur for every fraction. In order to understand how shifts change the whole course of treatment, it is

necessary to apply a set of clinical shifts to the treatment plans. An analysis of a patient with a large variation of shifts was chosen to evaluate the clinical impact. CT on rails Patient 1's shoulder shifts were chosen based on the distribution seen in Fig. 3.9, and the shifts were applied fraction by fraction to the 3 patients in the dosimetric study. To match the measured shifts to the modeled shifts in the dosimetric study, shifts of 0.25 cm to 0.39 cm were considered 3 mm shifts; shifts of 0.4 cm to 0.7 cm were considered 5 mm shifts; and shifts of 0.95 and greater were considered 15 mm shifts as a worst-case prediction. The shifts on the right and left shoulder were binned accordingly. Because dosimetric effects on IMRT plans were seen only for superior and 15 mm posterior shifts, these were the shifts of interest when assessing clinical impact. If the right and left shoulder showed different superior or posterior shifts on the same CT, the larger shift was assumed in that direction. If either shoulder showed a posterior and superior shift on the same CT, then it was counted twice, which assumed the dosimetric effects would be additive. CT on rails Patient 1 had 16 fractions of treatment with 1 shift of 3 mm superior, 4 shifts of 5 mm superior, and 7 shifts of 15 mm posterior.

In order to apply the above shifts to the 3 dosimetric patients' treatments, a point dose within the lower neck CTV and the dose to 99% of the CTV were calculated with Pinnacle for each of the superiorly shifted treatment plans and for the 15 mm posterior treatment plan, and these were compared to the original treatment plan. The change in dose was scaled by each patient's number of fractions. Patients 1 and 3 had 30 fractions, and Patient 2 had 33 fractions. Because there were only 16 fractions of shoulder shifts measured, the dose change calculated was considered to be the potential dose lost during the first half of treatment if each dosimetric patient exhibited the same series of shifts as CT on rails

Patient 1. The total dose change was computed by adding the change for one 3 mm superior shift, 4 shifts of 5 mm superior, and 7 shifts of 15 mm posterior. In addition, a hypothetical scenario where the 5 mm superior shifts were changed to 15 mm superior shifts was calculated. From the data shown in Figures 3.9 to 3.12, an assumption was made that shoulder shifts do not improve for the second half of treatment. Doubling the dose lost in the first half of treatment gave an estimate of total dose lost if the shoulder variation remains the same. The change in dose to the CTV can be found in the table below:

| Target Dose change (cGy) in IMRT plan due to selected shifts | | | | | |
|---|---|------------------------|-------------------|--------------------|-------------|
| | | <i>dose per fx</i> | <i>total dose</i> | <i>D99% per fx</i> | <i>D99%</i> |
| Patient 1 | 3 mm sup | -1 | -24 | -1 | -10 |
| | 5 mm sup | -2 | -54 | -2 | -25 |
| | 15 mm post | -3 | -88 | -3 | -15 |
| | 15 mm sup | -4 | -134 | -4 | -414 |
| | Total change* | | -57 | | -14 |
| | Total if 5 mm sup shifts were 15 mm sup | | -79 | | -118 |
| Patient 2 | 3 mm sup | -3 | -89 | -1 | -20 |
| | 5 mm sup | -8 | -248 | -3 | -90 |
| | 15 mm post | 0 | -7 | -2 | -80 |
| | 15 mm sup | -15 | -488 | -11 | -350 |
| | Total change* | | -69 | | -57 |
| | Total if 5 mm sup shifts were 15 mm sup | | -127 | | -120 |
| Patient 3 | 3 mm sup | -1 | -26 | -1 | -30 |
| | 5 mm sup | -2 | -58 | -3 | -90 |
| | 15 mm post | -6 | -167 | -5 | -160 |
| | 15 mm sup | -6 | -175 | -11 | -340 |
| | Total change* | | -95 | | -101 |
| | Total if 5 mm sup shifts were 15 mm sup | | -126 | | -167 |

*Total = 3 mm sup x 1 fx; 5 mm sup x 4 fx; and 15 mm post x 7 fx

Table 4-1: Dose per fraction and total dose lost to a point in the lower neck CTV, to 99% of the CTV, and the total dose lost during treatment for superior and posterior shifts

Table 4-1 shows that if the patients had shown these shifts over their treatment, then 58 cGy to 95 cGy would be lost within the CTV and the dose to 99% of the CTV would decrease as much as 1.0 Gy. Whether or not this is clinically acceptable depends on the severity of disease in this area. For Patient 3, the worst case observed, the CTV evaluated was an area of concern for lymph-node spread, so a loss of 1 Gy may not change clinical outcomes. If the CTV had been a primary disease site, there may be more cause for concern.

In addition to the calculated target dose loss, the hypothetical situation where the 5 mm superior shifts were replaced with 15 mm superior shifts showed higher losses in point dose, and dose to 99% of the CTV. Again, Patient 3 showed the largest dose loss of 1.7 Gy to the CTV. Again, whether this loss is clinically concerning depends on the disease.

Similar to the loss of target coverage, the dose change to the brachial plexus was calculated using the values for dose change to 0.1 cc in Table 3-6. These values were scaled by the number of fractions for each patient. The inferior shifts were counted because the largest increase in brachial plexus dose was seen for these. CT on rails Patient 1 had 6 inferior shifts of 5 mm, 2 inferior shifts of 15 mm. The results are found in the table below:

| Brachial Plexus dose change (cGy) for IMRT plan | | | |
|--|---------------|-----------------------------------|--------------------|
| | | <i>Dose change per fx</i> | <i>Dose change</i> |
| Patient 1 | 5 mm inf | 1 | 40 |
| | 15 mm inf | 14 | 410 |
| | TOTAL* | | 71 |
| Patient 2 | 5 mm inf | 4 | 130 |
| | 15 mm inf | 6 | 205 |
| | TOTAL* | | 72 |
| Patient 3 | 5 mm inf | 3 | 90 |
| | 15 mm inf | 7 | 210 |
| | TOTAL* | | 64 |

***Total = 5 mm inf x 6 fx and 15 mm inf x 2 fx;**

Table 4-2: Dose change per fraction, and total dose change to 0.1 cc of the brachial plexus and total change over treatment for inferior, posterior and superior shifts

The dose change to 0.1 cc of the brachial plexus was not in the range of being dangerous. Patient 1 had the largest increase of 72 cGy for the total treatment. Even if the dose to 0.1 cc of the brachial plexus was close to the TD5/5 dose of 65 Gy, an added 72 cGy may not be harmful, especially because location of maximum dose is not always the same, and the daily increase is only a few cGy so it is unlikely the brachial plexus would receive 65 Gy in any location to see 5% negative effects in 5 years (Chen, et. al 2010)

In conclusion, the dosimetric impact of the most varied shifts observed can cause a loss of 1.0 Gy to the dose covering 99% of the CTV for IMRT plans. This may be important for primary disease sites. However, the dose to the brachial plexus did not increase enough to cause meaningfully increased risk of negative effects.

While regular fractionated IMRT plans show a loss of 1.0 Gy to 99% of the CTV, hypofractionated treatments such as Stereotactic Spine Radiosurgery (SSRS) to the cervical spine may be at greater risk for dose loss to the target. SSRS treatments are usually 1 or 3 fractions, and in the case of cervical spine lesions, the same 5 point mask used for many Head and Neck patients may be used as an immobilization device. SSRS to C6 would place the target in the lower neck-- the area of highest risk of coverage loss due to shoulder variation. As discussed, shifts of 3 mm, 5 mm, and 15 mm in the superior direction, and 15 mm in the posterior direction yield the greatest CTV dose loss in the lower neck. In the first 3 fractions of treatment, there are 3 opportunities for a superior shift and 3 opportunities for a large, posterior shift. For the 4 CT on rails patients in this study, Patient 1 demonstrated 2 large, posterior shifts in the first 3 fractions (Fig. 3.9), Patient 2 demonstrated 0 superior or posterior shifts (Fig. 3.10), Patient 3 demonstrated 2 superior shifts (Fig. 3.11), and Patient 4 demonstrated 1 superior shift (Fig. 3.12-3.13). Of the 12 fractions among these 4 patients, 5 shifts (42%) had the magnitude and direction that result in target coverage loss by the 100% isodose line. Because the SSRS treatments are planned with beams that are entirely posterior and lateral, the dose changes found in this study for regular IMRT plans are likely an underestimate of the dose loss that would be seen in SSRS plans. Furthermore, in the case of SSRS, the spinal cord is near to the target, and dose perturbations may be more important than those seen for the head and neck plans. It may be possible that inferior shoulder shifts could cause notable dose increase to the cord, despite the avoidance created by the plan, which could be dangerous for the patient. In the case of SSRS, shoulder position may be a necessary consideration for patient setup.

4.3 Comparison to the Literature

No prior studies have looked at the dosimetric impact of shoulder variation on treatment plans. Only two prior studies (Court et al. 2008, Gilbeau et al. 2001) have estimated shoulder displacement; they have looked at it as a part of initial isocenter setup, and evaluated whether the shoulder position was incorrect as isocenter was being aligned, but did not evaluate it after isocenter appeared correctly placed on port films. In contrast, our study looked at shoulder displacement independent of correct isocenter setup, and assessed the displacement of the shoulder after isocenter was correctly aligned using 3D CT data.

The shifts observed by Gilbeau et al. were mostly less than 5.5 mm with large shifts of greater than 1 cm seen in the right or left direction. The largest shifts (greater than 1 cm) observed by Court et al. were also in the right or left direction. The results of our study did not match those in the literature, and large shifts over 1 cm were found in the inferior and posterior direction. Our study did not find any large shifts of greater than 1 cm in the right or left direction. The right left shifts observed in the study by Gilbeau et al. were assessed by the position of the clavicle on an AP port film, which has poor image quality. The therapists noted the large, right or left shifts documented by Court if they needed to realign the patient's isocenter after an initial set of port films. Both of these methods are not as accurate as CT imaging. In both cases, the large shifts were seen prior to final isocenter alignment, and because adjusting the setup involves rotating and moving the patient, the shoulders were likely positioned better after the adjustment. Because this study looked at shoulder position after isocenter setup using a more accurate system with CT on rails, the observed shifts can be expected to be different. In addition, the posterior and inferior shifts we observed may be due to patient relaxation after the initial simulation.

While the direction of largest shifts was different between this study and the two above, the general distribution of the magnitude of shifts was similar between studies.

4.4 Future Work

Some of the limitations of this study had to do with good dosimetric isolation of the shoulder variation. The drawing of the shoulder shifts served as a good estimate of translational motion, but the forced density of the tissues resulted in a dose calculation based on a uniform density, which is not an exact representation of the anatomy. In addition, both shoulders do not move together in the same direction, which was assumed for the assessment of dosimetric impact. An approach that was not feasible for this study would be to deform CT images to represent rotational movement of the shoulder and its associated bony anatomy, and then calculate dose to the CTVs on these. However, further issues were found with deformable registration of the structures as described in section 3.3. The volumes of the target were not consistent, so transferring targets from one CT to the next yielded different absolute volumes of coverage loss. A better comparison between CT scans may be to look at the volume of the dose cloud for specific doses rather than absolute volume of the target covered by the dose. This method, or another that circumvented the issue of absolute volume, would be necessary if the original CT scan were to be compared to a deformed CT image.

Because only uniform, translated shifts were analyzed in this study, the dosimetric effects of a shoulder with multi-directional shifts were assumed to be additive when assessing clinical impact, so further investigation with CT data would be necessary to confirm this assumption. In addition, a 5 mm shift was not evaluated in the AP direction. CT

on rails Patient 1 did have shifts 5 mm posterior, and these had to be treated as having no impact on dose when assessing the clinical impact on the dosimetric patients (which was true for the 3 mm shift) because there were no data available. Because large posterior shifts impact IMRT target coverage, the effects of the 5 mm shift may be important.

In addition to looking at the dosimetric effects of more shoulder variation, measurements of more patients' shoulder shifts over the course of treatment would give a better understanding of the frequency of large shifts and of how much shoulder variation is typical. In addition, gathering patient data for different types of masks would serve to assess whether some masks are better than others at immobilizing the shoulders in order to prevent dosimetric effects.

CHAPTER 5: Conclusions

5.1 Summary

When evaluating the shoulder variation for CT on rails patients at MD Anderson, the average magnitude of the measured shoulder shift for each patient was 2-5 mm in each direction, as was the average that accounted for direction (Table 3-1). Maximum shoulder shifts of over 1.5 cm were seen in the posterior and inferior directions (Table 3-2). Taken as an average of all the patients, the magnitude of the shifts each in direction were 2-4 mm and the average net displacement as a 3D vector was 5 mm (Table 3-3).

A displacement of 2-5 mm could have an impact on lower neck target coverage by the 100% isodose line, if the shift is in the superior direction. Displacements of 1.5 cm in the superior direction resulted in coverage loss of the 95% isodose line for IMRT and SmartArc plans, and displacements of 1.5 cm in the posterior direction resulted in coverage loss by the 100% isodose line for IMRT plans. Displacements in the inferior and anterior directions did not show gains in coverage that compensate for these losses, therefore calculating dose based on an average shift over the course of treatment that included direction would not give meaningful results.

In addition to target coverage, dose to the brachial plexus was impacted by large shoulder shifts. Inferior shifts and large anterior shifts caused an increase in the maximum dose to 0.1 cc of the brachial plexus.

When the variety of shoulder shifts over the course of treatment was applied to IMRT plans, up to 1.0 Gy was lost to 99% of the lower neck target, which may be important

depending on the disease in the low neck region. In addition, the brachial plexus dose increased by up to 72 cGy; however this is not likely to be dangerous because this dose was spread out over the volume.

5.2 Conclusions

Our Hypothesis stated that the average shoulder shift over the course of treatment will not have a clinical impact on target coverage or normal tissue doses, however, the dose degradation in absolute volume of target coverage lost will be worse for SmartArc than for IMRT.

The magnitude of the average shift (2-5 mm) could have an impact on lower neck target coverage if this shift is in the superior direction. Because the dosimetric effects of shifts in opposite directions do not balance out, an average shift over the course of treatment that includes the direction would not give a fair estimate of the impact of the patient's shoulder variation. When taking into account a variety of shifts over the course of treatment, 1.0 Gy was lost to 99% of the target and the brachial plexus dose increased by 72cGy. This counters the hypothesis that the shoulder shifts do not have a clinical impact on target coverage, but confirms that they do not impact normal tissue doses.

In addition, IMRT and SmartArc plans were affected similarly by shoulder shifts. For both plans large, superior shifts caused the largest volume of coverage lost to lower neck targets by the 95% isodose line. Large, posterior shifts caused loss of coverage to lower neck targets by the 100% isodose line for IMRT plans only. This result counters the hypothesis that SmartArc would suffer from more coverage loss than IMRT.

Finally, because large shoulder shifts do occur when isocenter is aligned correctly, and even small superior shifts affect target coverage in the lower neck, shoulder position should be taken into consideration for patient setup when there is primary disease in this region.

APPENDIX A: CT on rails patient data extracted from Pinnacle

Table A-1: CT on rails Patient 1 Boney Alignment structure coordinates, humeral head coordinates, and displacement between the two (Left shift, Right shift)

| CT | | Bony Lt | | | | L HH | | | | Lt shift | | |
|----|------|---------|--------|-------|----|-------|--------|------|----|----------|-------|------|
| | RL | AP | SI | | RL | AP | SI | | RL | AP | SI | |
| | Plan | 0 | -36.82 | 93.18 | | 15.02 | -38.01 | 94.7 | | 15.02 | -1.19 | 1.52 |
| | 1 | 0.15 | -51.73 | 3.01 | | 15.34 | -53.02 | 4.46 | | 15.19 | -1.29 | 1.45 |
| | 2 | 0.32 | -51.66 | 2.87 | | 15.48 | -53.44 | 4.44 | | 15.16 | -1.78 | 1.57 |
| | 3 | 0.14 | -51.93 | 3.23 | | 15.45 | -53.48 | 4.75 | | 15.31 | -1.55 | 1.52 |
| | 4 | -0.51 | -51.69 | 2.78 | | 14.88 | -53.47 | 4.48 | | 15.39 | -1.78 | 1.7 |
| | 5 | 0.16 | -51.98 | 3.15 | | 15.5 | -53.64 | 5.36 | | 15.34 | -1.66 | 2.21 |
| | 6 | 0.07 | -51.78 | 3.1 | | 15.27 | -53.23 | 4.55 | | 15.2 | -1.45 | 1.45 |
| | 7 | -0.72 | -51.94 | 2.86 | | 14.59 | -53.07 | 4.36 | | 15.31 | -1.13 | 1.5 |
| | 8 | -0.21 | -52.11 | 3.08 | | 15.07 | -53.44 | 4.87 | | 15.28 | -1.33 | 1.79 |
| | 10 | -0.66 | -52.14 | 2.8 | | 14.9 | -53.39 | 5.13 | | 15.56 | -1.25 | 2.33 |
| | 11 | -0.64 | -52.04 | 2.68 | | 14.93 | -53 | 4.35 | | 15.57 | -0.96 | 1.67 |
| | 12 | -0.29 | -51.99 | 2.42 | | 15.19 | -53.3 | 5.9 | | 15.48 | -1.31 | 3.48 |
| | 13 | -0.92 | -51.92 | 2.69 | | 13.52 | -53.69 | 3.4 | | 14.44 | -1.77 | 0.71 |
| | 14 | -0.45 | -53 | 2.88 | | 14.18 | -53.27 | 3.75 | | 14.63 | -0.27 | 0.87 |
| | 15 | -1.18 | -52.56 | 2.65 | | 14.3 | -53.42 | 3.63 | | 15.48 | -0.86 | 0.98 |
| | 16 | -1 | -52.3 | 2.63 | | 14.38 | -53.04 | 4.54 | | 15.38 | -0.74 | 1.91 |
| | | | | | | | | | | | | |
| | | | | | | | | | | | | |
| | | | | | | | | | | | | |
| | | | | | | | | | | | | |
| | | | | | | | | | | | | |
| | | | | | | | | | | | | |
| | | | | | | | | | | | | |
| | | | | | | | | | | | | |
| | | | | | | | | | | | | |
| | | | | | | | | | | | | |
| | | | | | | | | | | | | |
| | | | | | | | | | | | | |
| | | | | | | | | | | | | |
| | | | | | | | | | | | | |
| | | | | | | | | | | | | |
| | | | | | | | | | | | | |
| | | | | | | | | | | | | |
| | | | | | | | | | | | | |
| | | | | | | | | | | | | |
| | | | | | | | | | | | | |
| | | | | | | | | | | | | |
| | | | | | | | | | | | | |
| | | | | | | | | | | | | |
| | | | | | | | | | | | | |
| | | | | | | | | | | | | |
| | | | | | | | | | | | | |
| | | | | | | | | | | | | |
| | | | | | | | | | | | | |
| | | | | | | | | | | | | |
| | | | | | | | | | | | | |
| | | | | | | | | | | | | |
| | | | | | | | | | | | | |
| | | | | | | | | | | | | |
| | | | | | | | | | | | | |
| | | | | | | | | | | | | |
| | | | | | | | | | | | | |
| | | | | | | | | | | | | |
| | | | | | | | | | | | | |
| | | | | | | | | | | | | |
| | | | | | | | | | | | | |
| | | | | | | | | | | | | |
| | | | | | | | | | | | | |
| | | | | | | | | | | | | |
| | | | | | | | | | | | | |
| | | | | | | | | | | | | |
| | | | | | | | | | | | | |
| | | | | | | | | | | | | |
| | | | | | | | | | | | | |
| | | | | | | | | | | | | |
| | | | | | | | | | | | | |
| | | | | | | | | | | | | |
| | | | | | | | | | | | | |
| | | | | | | | | | | | | |
| | | | | | | | | | | | | |
| | | | | | | | | | | | | |
| | | | | | | | | | | | | |
| | | | | | | | | | | | | |
| | | | | | | | | | | | | |
| | | | | | | | | | | | | |
| | | | | | | | | | | | | |
| | | | | | | | | | | | | |
| | | | | | | | | | | | | |
| | | | | | | | | | | | | |
| | | | | | | | | | | | | |
| | | | | | | | | | | | | |
| | | | | | | | | | | | | |
| | | | | | | | | | | | | |
| | | | | | | | | | | | | |
| | | | | | | | | | | | | |
| | | | | | | | | | | | | |
| | | | | | | | | | | | | |
| | | | | | | | | | | | | |
| | | | | | | | | | | | | |
| | | | | | | | | | | | | |

Table A-2: CT on rails Patient 2 C2 coordinates, humeral head coordinates, and displacement between the two

| CT | C2 | | | | L HH | | | | Lt shift | | |
|------|-------|--------|--------|--|-------|--------|--------|--|----------|-------|-------|
| | RL | AP | SI | | RL | AP | SI | | RL | AP | SI |
| Plan | -0.15 | -35.68 | -42.88 | | 17.52 | -38.24 | -30.31 | | 17.67 | -2.56 | 12.57 |
| 1 | 0.85 | -50.15 | -5.18 | | 18.08 | -52.79 | 7.35 | | 17.23 | -2.64 | 12.53 |
| 2 | -0.01 | -49.54 | -5.34 | | 17.54 | -52.23 | 7.23 | | 17.55 | -2.69 | 12.57 |
| 3 | 0 | -45.03 | -5.42 | | 17.46 | -47.74 | 7.17 | | 17.46 | -2.71 | 12.59 |
| 4 | -0.02 | -50.75 | -5.4 | | 17.31 | -53.32 | 7.37 | | 17.33 | -2.57 | 12.77 |
| 5 | -0.11 | -49.71 | -5.37 | | 17.57 | -52.25 | 7.3 | | 17.68 | -2.54 | 12.67 |
| 6 | -0.08 | -49.54 | -5.25 | | 17.37 | -52.35 | 7.23 | | 17.45 | -2.81 | 12.48 |
| 7 | -0.11 | -49.92 | -5.02 | | 17.39 | -52.52 | 7.34 | | 17.5 | -2.6 | 12.36 |
| 8 | -0.08 | -50.37 | -5.29 | | 17.53 | -52.89 | 7.46 | | 17.61 | -2.52 | 12.75 |
| 9 | -0.07 | -50.31 | -5.43 | | 17.47 | -52.73 | 7.4 | | 17.54 | -2.42 | 12.83 |
| 10 | -0.05 | -48.69 | -5.41 | | 17.51 | -51.41 | 6.92 | | 17.56 | -2.72 | 12.33 |
| 11 | 0.1 | -49.92 | -5.51 | | 17.59 | -52.46 | 7.5 | | 17.49 | -2.54 | 13.01 |
| 12 | 0 | -50.45 | -5.44 | | 17.49 | -53.29 | 7.07 | | 17.49 | -2.84 | 12.51 |
| 13 | -0.06 | -49.32 | -5.38 | | 17.46 | -51.84 | 7.2 | | 17.52 | -2.52 | 12.58 |
| 14 | 0.02 | -49.85 | -5.38 | | 17.7 | -52.51 | 7.43 | | 17.68 | -2.66 | 12.81 |
| 15 | 0.18 | -51.13 | -5.36 | | 17.53 | -53.54 | 7.45 | | 17.35 | -2.41 | 12.81 |
| 17 | 0.5 | -49.08 | -5.44 | | 17.91 | -52 | 7.39 | | 17.41 | -2.92 | 12.83 |
| 18 | 0.39 | -51.15 | -5.4 | | 17.76 | -53.75 | 7.07 | | 17.37 | -2.6 | 12.47 |
| 19 | 0.04 | -50.4 | -5.4 | | 17.69 | -53.39 | 7.3 | | 17.65 | -2.99 | 12.7 |
| 20 | 0.06 | -50.31 | -5.34 | | 17.78 | -52.49 | 7.48 | | 17.72 | -2.18 | 12.82 |
| 21 | 0.13 | -50.71 | -5.41 | | 17.68 | -53.15 | 7.16 | | 17.55 | -2.44 | 12.57 |
| 22 | -0.18 | -50.41 | -5.32 | | 17.37 | -52.81 | 7.41 | | 17.55 | -2.4 | 12.73 |
| 23 | -0.14 | -49.62 | -5.27 | | 17.19 | -52 | 7.24 | | 17.33 | -2.38 | 12.51 |
| 24 | 0.09 | -50.04 | -5.39 | | 17.5 | -52.62 | 7.25 | | 17.41 | -2.58 | 12.64 |
| 25 | 0.86 | -49.78 | -5.4 | | 18.37 | -52.39 | 7.1 | | 17.51 | -2.61 | 12.5 |
| 26 | -0.01 | -49.99 | -5.52 | | 17.61 | -52.45 | 7.36 | | 17.62 | -2.46 | 12.88 |
| 28 | -0.17 | -51.66 | -5.56 | | 17.11 | -54.41 | 7 | | 17.28 | -2.75 | 12.56 |
| 29 | -0.25 | -51.83 | -5.41 | | 17.18 | -54.18 | 7.46 | | 17.43 | -2.35 | 12.87 |
| 30 | -0.04 | -51.68 | -5.33 | | 17.31 | -54.07 | 7.56 | | 17.35 | -2.39 | 12.89 |
| 31 | -0.31 | -51.56 | -5.52 | | 17.3 | -54.3 | 7.24 | | 17.61 | -2.74 | 12.76 |

| CT | C2 | | | | R HH | | | | Rt shift | | |
|------|-------|--------|--------|--|--------|--------|--------|--|----------|-------|-------|
| | RL | AP | SI | | RL | AP | SI | | RL | AP | SI |
| Plan | -0.15 | -35.68 | -42.88 | | -19.78 | -38.07 | -30.34 | | -19.63 | -2.39 | 12.54 |
| 1 | 0.85 | -50.15 | -5.18 | | -19.02 | -52.1 | 7.38 | | -19.87 | -1.95 | 12.56 |
| 2 | -0.01 | -49.54 | -5.34 | | -19.77 | -51.85 | 7.46 | | -19.76 | -2.31 | 12.8 |
| 3 | 0 | -45.03 | -5.42 | | -19.64 | -47.29 | 7.27 | | -19.64 | -2.26 | 12.69 |
| 4 | -0.02 | -50.75 | -5.4 | | -19.75 | -52.95 | 7.29 | | -19.73 | -2.2 | 12.69 |
| 5 | -0.11 | -49.71 | -5.37 | | -19.62 | -52.05 | 7.27 | | -19.51 | -2.34 | 12.64 |
| 6 | -0.08 | -49.54 | -5.25 | | -19.52 | -52.11 | 7.52 | | -19.44 | -2.57 | 12.77 |
| 7 | -0.11 | -49.92 | -5.02 | | -19.37 | -52.14 | 7.14 | | -19.26 | -2.22 | 12.16 |
| 8 | -0.08 | -50.37 | -5.29 | | -19.61 | -52.57 | 7.55 | | -19.53 | -2.2 | 12.84 |
| 9 | -0.07 | -50.31 | -5.43 | | -19.9 | -52.72 | 7.33 | | -19.83 | -2.41 | 12.76 |
| 10 | -0.05 | -48.69 | -5.41 | | -19.56 | -51 | 7.37 | | -19.51 | -2.31 | 12.78 |
| 11 | 0.1 | -49.92 | -5.51 | | -19.33 | -52.45 | 6.8 | | -19.43 | -2.53 | 12.31 |
| 12 | 0 | -50.45 | -5.44 | | -19.29 | -52.92 | 7.14 | | -19.29 | -2.47 | 12.58 |
| 13 | -0.06 | -49.32 | -5.38 | | -19.46 | -51.43 | 7.08 | | -19.4 | -2.11 | 12.46 |
| 14 | 0.02 | -49.85 | -5.38 | | -19.22 | -52.69 | 7.41 | | -19.24 | -2.84 | 12.79 |
| 15 | 0.18 | -51.13 | -5.36 | | -19.34 | -53.44 | 7.01 | | -19.52 | -2.31 | 12.37 |
| 17 | 0.5 | -49.08 | -5.44 | | -19.11 | -51.67 | 7.34 | | -19.61 | -2.59 | 12.78 |
| 18 | 0.39 | -51.15 | -5.4 | | -18.89 | -53.75 | 7.2 | | -19.28 | -2.6 | 12.6 |
| 19 | 0.04 | -50.4 | -5.4 | | -19.19 | -53.08 | 7.12 | | -19.23 | -2.68 | 12.52 |
| 20 | 0.06 | -50.31 | -5.34 | | -18.97 | -52.46 | 7.28 | | -19.03 | -2.15 | 12.62 |
| 21 | 0.13 | -50.71 | -5.41 | | -19.27 | -52.86 | 7.35 | | -19.4 | -2.15 | 12.76 |
| 22 | -0.18 | -50.41 | -5.32 | | -19.21 | -52.73 | 7.18 | | -19.03 | -2.32 | 12.5 |
| 23 | -0.14 | -49.62 | -5.27 | | -19.3 | -51.69 | 7.42 | | -19.16 | -2.07 | 12.69 |
| 24 | 0.09 | -50.04 | -5.39 | | -19.07 | -52.13 | 7.36 | | -19.16 | -2.09 | 12.75 |
| 25 | 0.86 | -49.78 | -5.4 | | -18.38 | -51.99 | 7.26 | | -19.24 | -2.21 | 12.66 |
| 26 | -0.01 | -49.99 | -5.52 | | -18.88 | -52.09 | 7.57 | | -18.87 | -2.1 | 13.09 |
| 28 | -0.17 | -51.66 | -5.56 | | -19.47 | -54.22 | 6.95 | | -19.3 | -2.56 | 12.51 |
| 29 | -0.25 | -51.83 | -5.41 | | -19.36 | -53.97 | 7.05 | | -19.11 | -2.14 | 12.46 |
| 30 | -0.04 | -51.68 | -5.33 | | -19.46 | -54.13 | 7.12 | | -19.42 | -2.45 | 12.45 |
| 31 | -0.31 | -51.56 | -5.52 | | -19.67 | -54.11 | 6.91 | | -19.36 | -2.55 | 12.43 |

Table A-3: CT on rails Patient 3 C2 coordinates, humeral head coordinates, and displacement between the two

| CT | C2 | | | L HH | | | Lt shift | | |
|------|-------|--------|-------|--------|--------|-------|----------|-------|-------|
| | RL | AP | SI | RL | AP | SI | RL | AP | SI |
| plan | -0.41 | -36.37 | 10.67 | 17.05 | -40.61 | 24.21 | 17.46 | -4.24 | 13.54 |
| 1 | 0.44 | -49.74 | -5.58 | 17.66 | -53.39 | 8.17 | 17.22 | -3.65 | 13.75 |
| 2 | 0.16 | -49.69 | -6.03 | 17.81 | -53.01 | 8.12 | 17.65 | -3.32 | 14.15 |
| 3 | -0.23 | -49.84 | -6.06 | 17.08 | -53.51 | 7.53 | 17.31 | -3.67 | 13.59 |
| 4 | -0.22 | -49.71 | -5.96 | 17.12 | -53.39 | 7.58 | 17.34 | -3.68 | 13.54 |
| 5 | 0.08 | -49.88 | -6.06 | 17.25 | -53.49 | 7.41 | 17.17 | -3.61 | 13.47 |
| 6 | 0.37 | -49.64 | -6.28 | 17.59 | -53.57 | 7.39 | 17.22 | -3.93 | 13.67 |
| 7 | 0.88 | -49.62 | -6.08 | 17.99 | -53.46 | 7.46 | 17.11 | -3.84 | 13.54 |
| 8 | 0.36 | -49.61 | -6.05 | 17.44 | -53.47 | 7.51 | 17.08 | -3.86 | 13.56 |
| 9 | 0.34 | -49.66 | -6.29 | 17.3 | -53.47 | 7.3 | 16.96 | -3.81 | 13.59 |
| 10 | 0.75 | -49.63 | -6.07 | 17.72 | -53.67 | 7.28 | 16.97 | -4.04 | 13.35 |
| | | | | | | | | | |
| | | | | | | | | | |
| | | | | | | | | | |
| | | | | | | | | | |
| | | | | | | | | | |
| | | | | | | | | | |
| | | | | | | | | | |
| | | | | | | | | | |
| | | | | | | | | | |
| | | | | | | | | | |
| CT | C2 | | | R HH | | | Rt shift | | |
| | RL | AP | SI | RL | AP | SI | RL | AP | SI |
| plan | -0.41 | -36.37 | 10.67 | -18.17 | -40.16 | 25.09 | -17.76 | -3.79 | 14.42 |
| 1 | 0.44 | -49.74 | -5.58 | -17.46 | -53.1 | 8.5 | -17.9 | -3.36 | 14.08 |
| 2 | 0.16 | -49.69 | -6.03 | -17.52 | -53.31 | 7.68 | -17.68 | -3.62 | 13.71 |
| 3 | -0.23 | -49.84 | -6.06 | -18.17 | -53.04 | 8 | -17.94 | -3.2 | 14.06 |
| 4 | -0.22 | -49.71 | -5.96 | -18.18 | -52.96 | 8.1 | -17.96 | -3.25 | 14.06 |
| 5 | 0.08 | -49.88 | -6.06 | -18.02 | -52.93 | 7.85 | -18.1 | -3.05 | 13.91 |
| 6 | 0.37 | -49.64 | -6.28 | -17.49 | -53.02 | 7.93 | -17.86 | -3.38 | 14.21 |
| 7 | 0.88 | -49.62 | -6.08 | -16.64 | -52.92 | 8.02 | -17.52 | -3.3 | 14.1 |
| 8 | 0.36 | -49.61 | -6.05 | -17.39 | -53.09 | 8.01 | -17.75 | -3.48 | 14.06 |
| 9 | 0.34 | -49.66 | -6.29 | -17.33 | -52.95 | 7.3 | -17.67 | -3.29 | 13.59 |
| 10 | 0.75 | -49.63 | -6.07 | -16.8 | -53.41 | 7.72 | -17.55 | -3.78 | 13.79 |

Table A-4a: CT on rails Patient 4, First plan, boney alignment structure coordinates, humeral head coordinates, and displacement between the two

| CT | Vertebrae | | | L HH | | | Lt shift | | |
|------|-----------|-------|-------|--------|------|-------|----------|------|-------|
| | RL | AP | SI | RL | AP | SI | RL | AP | SI |
| plan | -0.23 | 0.7 | -7.26 | 18.46 | 5.85 | -7.49 | 18.69 | 5.15 | -0.23 |
| 1 | -1.61 | -4.17 | -0.13 | 17.38 | 0.87 | 0.23 | 18.99 | 5.04 | 0.36 |
| 2 | -0.91 | -3.98 | -7.34 | 17.77 | 1.41 | -7.31 | 18.68 | 5.39 | 0.03 |
| 3 | -1.02 | -2.43 | -6.74 | 17.6 | 3.01 | -7.05 | 18.62 | 5.44 | -0.31 |
| 4 | -2.01 | -4.21 | -6.68 | 16.77 | 0.73 | -6.75 | 18.78 | 4.94 | -0.07 |
| 5 | -0.65 | -3.58 | -7.9 | 17.93 | 1.81 | -7.69 | 18.58 | 5.39 | 0.21 |
| 6 | -0.25 | -3.19 | -8.01 | 18.58 | 1.92 | -7.24 | 18.83 | 5.11 | 0.77 |
| 7 | -1.29 | -4.2 | -7.85 | 17.55 | 1.1 | -7.59 | 18.84 | 5.3 | 0.26 |
| 8 | -0.97 | -4.48 | -7.9 | 17.79 | 0.6 | -6.36 | 18.76 | 5.08 | 1.54 |
| 9 | -1.74 | -3.89 | -8.14 | 16.97 | 1.28 | -7.64 | 18.71 | 5.17 | 0.5 |
| | | | | | | | | | |
| | | | | | | | | | |
| | | | | | | | | | |
| | | | | | | | | | |
| | | | | | | | | | |
| | | | | | | | | | |
| | | | | | | | | | |
| | | | | | | | | | |
| CT | Vertebrae | | | R HH | | | Rt shift | | |
| | RL | AP | SI | RL | AP | SI | RL | AP | SI |
| plan | -0.23 | 0.7 | -7.26 | -18.97 | 4.97 | -6.83 | -18.74 | 4.27 | 0.43 |
| 1 | -1.61 | -4.17 | -0.13 | -20.01 | 0.35 | -0.02 | -18.4 | 4.52 | 0.11 |
| 2 | -0.91 | -3.98 | -7.34 | -19.62 | 0.19 | -6.83 | -18.71 | 4.17 | 0.51 |
| 3 | -1.02 | -2.43 | -6.74 | -19.6 | 1.62 | -6.04 | -18.58 | 4.05 | 0.7 |
| 4 | -2.01 | -4.21 | -6.68 | -20.59 | 0.49 | -5.97 | -18.58 | 4.7 | 0.71 |
| 5 | -0.65 | -3.58 | -7.9 | -19.46 | 0.64 | -7.6 | -18.81 | 4.22 | 0.3 |
| 6 | -0.25 | -3.19 | -8.01 | -18.93 | 0.97 | -6.25 | -18.68 | 4.16 | 1.76 |
| 7 | -1.29 | -4.2 | -7.85 | -19.86 | 0.31 | -6.38 | -18.57 | 4.51 | 1.47 |
| 8 | -0.97 | -4.48 | -7.9 | -19.73 | -0.3 | -6.43 | -18.76 | 4.18 | 1.47 |
| 9 | -1.74 | -3.89 | -8.14 | -20.44 | 0.65 | -7.41 | -18.7 | 4.54 | 0.73 |

Table A-4b: CT on rails Patient 4, Replan, boney alignment structure coordinates, humeral head coordinates, and displacement between the two

| CT | Vertebrae | | | L HH | | | Lt shift | | |
|------|-----------|-------|-------|--------|-------|-------|----------|------|-------|
| | RL | AP | SI | RL | AP | SI | RL | AP | SI |
| plan | 0.08 | -0.19 | -6.25 | 18.78 | 4.24 | -9.82 | 18.7 | 4.43 | -3.57 |
| 1 | -1.64 | -4.22 | 0.8 | 16.79 | 0.29 | -2.53 | 18.43 | 4.51 | -3.33 |
| 2 | -0.8 | -4.23 | 0.58 | 17.4 | 0.59 | -2.68 | 18.2 | 4.82 | -3.26 |
| 3 | -1.02 | -3.23 | 0.3 | 17.39 | 1.33 | -2.64 | 18.41 | 4.56 | -2.94 |
| 5 | -1.28 | -3.8 | 0.82 | 16.84 | 0.94 | -3.25 | 18.12 | 4.74 | -4.07 |
| 6 | 0.37 | -3.14 | 0.56 | 18.76 | 0.85 | -2.85 | 18.39 | 3.99 | -3.41 |
| 7 | -0.48 | -4.86 | 1.37 | 17.83 | -0.14 | -2.08 | 18.31 | 4.72 | -3.45 |
| 8 | -1.94 | -3.63 | 0.82 | 16.25 | 0.9 | -2.45 | 18.19 | 4.53 | -3.27 |
| 9 | -0.45 | -4.14 | -0.71 | 18.09 | -0.43 | -2.91 | 18.54 | 3.71 | -2.2 |
| 10 | -0.51 | -4.65 | -0.05 | 18.09 | -0.41 | -2.9 | 18.6 | 4.24 | -2.85 |
| 11 | -1.41 | -3.61 | 0.51 | 16.91 | 0.74 | -2.31 | 18.32 | 4.35 | -2.82 |
| 12 | -1.56 | -4.32 | 0.84 | 16.71 | 0.31 | -2.32 | 18.27 | 4.63 | -3.16 |
| 13 | -1.03 | -4.26 | 0.08 | 17.23 | 0.41 | -3.06 | 18.26 | 4.67 | -3.14 |
| 14 | -0.94 | -4.53 | 0.45 | 17.38 | 0.39 | -2.17 | 18.32 | 4.92 | -2.62 |
| 15 | -1.48 | -4.13 | -0.23 | 16.7 | 1.02 | -3.04 | 18.18 | 5.15 | -2.81 |
| 16 | -1.45 | -3.95 | -0.08 | 17.06 | 0.68 | -2.69 | 18.51 | 4.63 | -2.61 |
| 18 | -0.65 | -4.96 | 0.12 | 17.69 | -0.56 | -2.5 | 18.34 | 4.4 | -2.62 |
| | | | | | | | | | |
| | | | | | | | | | |
| | | | | | | | | | |
| | | | | | | | | | |
| | | | | | | | | | |
| CT | Vertebrae | | | R HH | | | Rt shift | | |
| | RL | AP | SI | RL | AP | SI | RL | AP | SI |
| plan | 0.08 | -0.19 | -6.25 | -17.47 | 5.02 | -8.06 | -17.55 | 5.21 | -1.81 |
| 1 | -1.64 | -4.22 | 0.8 | -19.06 | 0.67 | -1.31 | -17.42 | 4.89 | -2.11 |
| 2 | -0.8 | -4.23 | 0.58 | -18.14 | 0.7 | -1.09 | -17.34 | 4.93 | -1.67 |
| 3 | -1.02 | -3.23 | 0.3 | -18.35 | 1.74 | -1.7 | -17.33 | 4.97 | -2 |
| 5 | -1.28 | -3.8 | 0.82 | -18.51 | 1.08 | -1.35 | -17.23 | 4.88 | -2.17 |
| 6 | 0.37 | -3.14 | 0.56 | -17.02 | 1.77 | -1.43 | -17.39 | 4.91 | -1.99 |
| 7 | -0.48 | -4.86 | 1.37 | -17.67 | 0.25 | -1.35 | -17.19 | 5.11 | -2.72 |
| 8 | -1.94 | -3.63 | 0.82 | -19.14 | 1.14 | -1.84 | -17.2 | 4.77 | -2.66 |
| 9 | -0.45 | -4.14 | -0.71 | -17.88 | 0.49 | -2.01 | -17.43 | 4.63 | -1.3 |
| 10 | -0.51 | -4.65 | -0.05 | -17.88 | 0.5 | -2 | -17.37 | 5.15 | -1.95 |
| 11 | -1.41 | -3.61 | 0.51 | -18.77 | 0.88 | -1.3 | -17.36 | 4.49 | -1.81 |
| 12 | -1.56 | -4.32 | 0.84 | -18.99 | 0.71 | -1.33 | -17.43 | 5.03 | -2.17 |
| 13 | -1.03 | -4.26 | 0.08 | -18.43 | 0.54 | -1.87 | -17.4 | 4.8 | -1.95 |
| 14 | -0.94 | -4.53 | 0.45 | -18.37 | 0.72 | -1.55 | -17.43 | 5.25 | -2 |
| 15 | -1.48 | -4.13 | -0.23 | -19.03 | 1.13 | -1.57 | -17.55 | 5.26 | -1.34 |
| 16 | -1.45 | -3.95 | -0.08 | -18.98 | 0.27 | -1.81 | -17.53 | 4.22 | -1.73 |
| 18 | -0.65 | -4.96 | 0.12 | -18.02 | -0.49 | -1.63 | -17.37 | 4.47 | -1.75 |

APPENDIX B: Dosimetric data extracted from Pinnacle

Table B-1: Dosimetric Patient 1 target volumes and structure doses

| Structure analysis | | | | Volume = cc | | Dose = cGy | | | | |
|--------------------|--------|--------|--------|-------------|------|--------------|---------------|--------------|-------------|------------|
| IMRT Plan | V100% | V98% | V95% | V45 | V25 | max dose 1cc | DVH max point | V75 (TD50/5) | V60 (TD5/5) | max 0.1 cc |
| CTV 6000 | 214.72 | 216.06 | 216.49 | | | | | | | |
| CTV 5700 | 379.35 | 387.86 | 390.3 | | | | | | | |
| CTV 5400 | 77.82 | 78.81 | 79.08 | | | | | | | |
| Cord | | | | 0 | 3.58 | 2775 | 2977.8 | | | 2900 |
| Brachial plexus | | | | | | | 6181.3 | 0 | 0.15 | 6100 |
| Arc plan | | | | | | | | | | |
| CTV 6000 | 210.42 | 214.48 | 216.05 | | | | | | | |
| CTV 5700 | 369.26 | 381.52 | 387.75 | | | | | | | |
| CTV 5400 | 77.14 | 78.25 | 78.86 | | | | | | | |
| Cord | | | | 0 | 6.44 | 3905 | 4222.3 | | | 4078 |
| Brachial plexus | | | | | | | 6171.2 | 0 | 0.33 | 6100 |
| 3mm sup | | | | | | | | | | |
| IMRT Plan | V100% | V98% | V95% | V45 | V25 | max dose 1cc | DVH max point | V75 (TD50/5) | V60 (TD5/5) | max 0.1 cc |
| CTV 6000 | 214.74 | 216.06 | 216.49 | | | | | | | |
| CTV 5700 | 375 | 387.71 | 390.28 | | | | | | | |
| CTV 5400 | 76.78 | 78.68 | 79.07 | | | | | | | |
| Cord | | | | 0 | 3.57 | 2770 | 2978.2 | | | 2893 |
| Brachial plexus | | | | | | | 6182.4 | 0 | 0.15 | 6100 |
| Arc plan | | | | | | | | | | |
| CTV 6000 | 210.48 | 214.5 | 216.06 | | | | | | | |
| CTV 5700 | 365.04 | 381.26 | 387.71 | | | | | | | |
| CTV 5400 | 75.64 | 77.95 | 78.78 | | | | | | | |
| Cord | | | | 0 | 6.43 | 3905 | 4223.2 | | | 4078 |
| Brachial plexus | | | | | | | 6173.1 | 0 | 0.29 | 6100 |
| 3mm inf | | | | | | | | | | |
| IMRT Plan | V100% | V98% | V95% | V45 | V25 | max dose 1cc | DVH max point | V75 (TD50/5) | V60 (TD5/5) | max 0.1 cc |
| CTV 6000 | 214.68 | 216.05 | 216.48 | | | | | | | |
| CTV 5700 | 380.08 | 387.82 | 390.27 | | | | | | | |
| CTV 5400 | 77.8 | 78.77 | 79.06 | | | | | | | |
| Cord | | | | 0 | 3.59 | 2785 | 2977.4 | | | 2910 |
| Brachial plexus | | | | | | | 6180.2 | 0 | 0.15 | 6100 |
| Arc plan | | | | | | | | | | |
| CTV 6000 | 210.32 | 214.45 | 216.04 | | | | | | | |
| CTV 5700 | 369.73 | 381.36 | 387.64 | | | | | | | |
| CTV 5400 | 77.68 | 78.41 | 78.86 | | | | | | | |
| Cord | | | | 0 | 6.46 | 3903 | 4221.3 | | | 4076 |
| Brachial plexus | | | | | | | 6168.6 | 0 | 0.58 | 6160 |
| 5mm sup | | | | | | | | | | |
| IMRT Plan | V100% | V98% | V95% | V45 | V25 | max dose 1cc | DVH max point | V75 (TD50/5) | V60 (TD5/5) | max 0.1 cc |
| CTV 6000 | 214.77 | 216.08 | 216.49 | | | | | | | |
| CTV 5700 | 360.23 | 386.97 | 390.26 | | | | | | | |
| CTV 5400 | 74.58 | 78.37 | 79.02 | | | | | | | |
| Cord | | | | 0 | 3.57 | 2769 | 2978.6 | | | 2893 |
| Brachial plexus | | | | | | | 6183.7 | 0 | 0.15 | 6100 |
| Arc plan | | | | | | | | | | |
| CTV 6000 | 210.6 | 214.55 | 216.07 | | | | | | | |
| CTV 5700 | 344.96 | 378.46 | 387.52 | | | | | | | |
| CTV 5400 | 67.35 | 76.85 | 78.64 | | | | | | | |
| Cord | | | | 0 | 6.42 | 3905 | 4224.4 | | | 4079 |
| Brachial plexus | | | | | | | 6175.6 | 0 | 0.27 | 6100 |

Table B-1 cont'd

| | | | | | | | | | | |
|------------------|--------|--------|--------|-----|------|--------------|---------------|--------------|-------------|------------|
| 5mm inf | | | | | | | | | | |
| IMRT Plan | V100% | V98% | V95% | V45 | V25 | max dose 1cc | DVH max point | V75 (TD50/5) | V60 (TD5/5) | max 0.1 cc |
| CTV 6000 | 214.88 | 216.09 | 216.49 | | | | | | | |
| CTV 5700 | 381.11 | 388.01 | 390.29 | | | | | | | |
| CTV 5400 | 77.8 | 78.72 | 79.04 | | | | | | | |
| Cord | | | | 0 | 3.64 | 2790 | 2977.9 | | | 2915 |
| Brachial plexus | | | | | | | 6186.3 | 0 | 0.16 | 6100 |
| Arc plan | | | | | | | | | | |
| CTV 6000 | 210.2 | 214.41 | 216.02 | | | | | | | |
| CTV 5700 | 369.75 | 381.19 | 387.53 | | | | | | | |
| CTV 5400 | 77.95 | 78.49 | 78.85 | | | | | | | |
| Cord | | | | 0 | 6.47 | 3905 | 4220.1 | | | 4076 |
| Brachial plexus | | | | | | | 6166.8 | 0 | 1.36 | 6140 |
| 15mm sup | | | | | | | | | | |
| IMRT Plan | V100% | V98% | V95% | V45 | V25 | max dose 1cc | DVH max point | V75 (TD50/5) | V60 (TD5/5) | max 0.1 cc |
| CTV 6000 | 214.81 | 216.13 | 216.5 | | | | | | | |
| CTV 5700 | 247.56 | 314.7 | 380.95 | | | | | | | |
| CTV 5400 | 48.41 | 74.01 | 78.58 | | | | | | | |
| Cord | | | | 0 | 3.52 | 2768 | 2974.3 | | | 2890 |
| Brachial plexus | | | | | | | 6181.9 | 0 | 0.15 | 6085 |
| Arc plan | | | | | | | | | | |
| CTV 6000 | 211.23 | 214.75 | 216.13 | | | | | | | |
| CTV 5700 | 217.49 | 279.23 | 346.73 | | | | | | | |
| CTV 5400 | 34.4 | 55.97 | 69.31 | | | | | | | |
| Cord | | | | 0 | 6.41 | 3910 | 4229.7 | | | 4085 |
| Brachial plexus | | | | | | | 6183.6 | 0 | 0.24 | 6100 |
| 15mm inf | | | | | | | | | | |
| IMRT Plan | V100% | V98% | V95% | V45 | V25 | max dose 1cc | DVH max point | V75 (TD50/5) | V60 (TD5/5) | max 0.1 cc |
| CTV 6000 | 214.77 | 216.08 | 216.49 | | | | | | | |
| CTV 5700 | 381.07 | 387.91 | 390.25 | | | | | | | |
| CTV 5400 | 76.43 | 78.11 | 78.51 | | | | | | | |
| Cord | | | | 0 | 3.63 | 2782 | 2974.3 | | | 2905 |
| Brachial plexus | | | | | | | 6230.2 | 0 | 1.49 | 6160 |
| Arc plan | | | | | | | | | | |
| CTV 6000 | 210.62 | 214.47 | 216.03 | | | | | | | |
| CTV 5700 | 371.19 | 381.85 | 387.71 | | | | | | | |
| CTV 5400 | 78.13 | 78.44 | 78.7 | | | | | | | |
| Cord | | | | 0 | 6.65 | 3910 | 4224.2 | | | 4083 |
| Brachial plexus | | | | | | | 6543 | 0 | 3.49 | 6510 |
| 3mm post | | | | | | | | | | |
| IMRT Plan | V100% | V98% | V95% | V45 | V25 | max dose 1cc | DVH max point | V75 (TD50/5) | V60 (TD5/5) | max 0.1 cc |
| CTV 6000 | 214.69 | 216.06 | 216.48 | | | | | | | |
| CTV 5700 | 377.44 | 386.99 | 389.96 | | | | | | | |
| CTV 5400 | 76.02 | 78.14 | 78.83 | | | | | | | |
| Cord | | | | 0 | 3.56 | 2772 | 2977.4 | | | 2895 |
| Brachial plexus | | | | | | | 6180.7 | 0 | 0.15 | 6100 |
| Arc plan | | | | | | | | | | |
| CTV 6000 | 210.36 | 214.46 | 216.05 | | | | | | | |
| CTV 5700 | 367.9 | 380.64 | 387.3 | | | | | | | |
| CTV 5400 | 76.24 | 77.62 | 78.47 | | | | | | | |
| Cord | | | | 0 | 6.44 | 3905 | 4221.7 | | | 4078 |
| Brachial plexus | | | | | | | 6169 | 0 | 0.32 | 6095 |

Table B-1 cont'd

| | | | | | | | | | | |
|------------------|--------|--------|--------|-----|------|--------------|---------------|--------------|-------------|------------|
| 3mm ant | | | | | | | | | | |
| IMRT Plan | V100% | V98% | V95% | V45 | V25 | max dose 1cc | DVH max point | V75 (TD50/5) | V60 (TD5/5) | max 0.1 cc |
| CTV 6000 | 214.72 | 216.06 | 216.49 | | | | | | | |
| CTV 5700 | 379.22 | 387.73 | 390.23 | | | | | | | |
| CTV 5400 | 77.65 | 78.83 | 79.07 | | | | | | | |
| Cord | | | | 0 | 3.59 | 2775 | 2978 | | | 2902 |
| Brachial plexus | | | | | | | 6180.7 | 0 | 0.15 | 6100 |
| Arc plan | | | | | | | | | | |
| CTV 6000 | 210.41 | 214.48 | 216.05 | | | | | | | |
| CTV 5700 | 368.87 | 381.4 | 387.57 | | | | | | | |
| CTV 5400 | 76.5 | 78.08 | 78.82 | | | | | | | |
| Cord | | | | 0 | 6.44 | 3905 | 4221.8 | | | 4078 |
| Brachial plexus | | | | | | | 6171 | 0 | 0.33 | 6100 |
| | | | | | | | | | | |
| 15mm post | | | | | | | | | | |
| IMRT Plan | V100% | V98% | V95% | V45 | V25 | max dose 1cc | DVH max point | V75 (TD50/5) | V60 (TD5/5) | max 0.1 cc |
| CTV 6000 | 214.7 | 216.07 | 216.49 | | | | | | | |
| CTV 5700 | 367.82 | 387.57 | 390.25 | | | | | | | |
| CTV 5400 | 72.39 | 77.82 | 78.89 | | | | | | | |
| Cord | | | | 0 | 3.57 | 2774 | 2977 | | | 2898 |
| Brachial plexus | | | | | | | 6182.4 | 0 | 0.15 | 6100 |
| Arc plan | | | | | | | | | | |
| CTV 6000 | 210.35 | 214.46 | 216.04 | | | | | | | |
| CTV 5700 | 368.07 | 381.13 | 387.61 | | | | | | | |
| CTV 5400 | 77.35 | 78.28 | 78.84 | | | | | | | |
| Cord | | | | 0 | 6.44 | 3905 | 4222 | | | 4078 |
| Brachial plexus | | | | | | | 6169.6 | 0 | 0.45 | 6095 |
| | | | | | | | | | | |
| 15mm ant | | | | | | | | | | |
| IMRT Plan | V100% | V98% | V95% | V45 | V25 | max dose 1cc | DVH max point | V75 (TD50/5) | V60 (TD5/5) | max 0.1 cc |
| CTV 6000 | 214.73 | 216.05 | 216.49 | | | | | | | |
| CTV 5700 | 378.45 | 387.68 | 390.31 | | | | | | | |
| CTV 5400 | 73.49 | 78.16 | 79.07 | | | | | | | |
| Cord | | | | 0 | 3.58 | 2772 | 2977.9 | | | 2896 |
| Brachial plexus | | | | | | | 6180.4 | 0 | 0.15 | 6100 |
| Arc plan | | | | | | | | | | |
| CTV 6000 | 210.46 | 214.5 | 216.06 | | | | | | | |
| CTV 5700 | 366.95 | 381.49 | 387.84 | | | | | | | |
| CTV 5400 | 76.63 | 78.19 | 78.84 | | | | | | | |
| Cord | | | | 0 | 6.43 | 3905 | 4222.1 | | | 4078 |
| Brachial plexus | | | | | | | 6172.6 | 0 | 0.33 | 6100 |
| | | | | | | | | | | |
| 15mm Left | | | | | | | | | | |
| IMRT Plan | V100% | V98% | V95% | V45 | V25 | max dose 1cc | DVH max point | V75 (TD50/5) | V60 (TD5/5) | max 0.1 cc |
| CTV 6000 | 214.73 | 216.07 | 216.49 | | | | | | | |
| CTV 5700 | 378.24 | 387.92 | 390.29 | | | | | | | |
| CTV 5400 | 77.74 | 78.87 | 79.09 | | | | | | | |
| Cord | | | | 0 | 3.58 | 2773 | 2978.2 | | | 2898 |
| Brachial plexus | | | | | | | 6182.4 | 0 | 0.15 | 6100 |
| Arc plan | | | | | | | | | | |
| CTV 6000 | 210.5 | 214.51 | 216.06 | | | | | | | |
| CTV 5700 | 366.48 | 381.56 | 387.77 | | | | | | | |
| CTV 5400 | 77.19 | 78.27 | 78.83 | | | | | | | |
| Cord | | | | 0 | 6.42 | 3905 | 4221.9 | | | 4078 |
| Brachial plexus | | | | | | | 6172.8 | 0 | 0.33 | 6100 |

Table B-2: Dosimetric Patient 2 target volumes and structure doses

| Structure analysis | | | | Volume = cc | | Dose = cGy | | | | |
|----------------------|--------|--------|--------|-------------|-------|--------------|---------------|--------------|-------------|------------|
| IMRT Plan | V100% | V98% | V95% | V45 | V25 | max dose 1cc | DVH max point | V75 (TD50/5) | V60 (TD5/5) | max 0.1 cc |
| CTV 7000 | 213.72 | 216.52 | 218.1 | | | | | | | |
| CTV 6500 | 95.25 | 97.03 | 97.49 | | | | | | | |
| CTV 6300 | 501.75 | 504.42 | 506.43 | | | | | | | |
| Cord | | | | 0 | 12.6 | 3690 | 4217 | | | 3920 |
| Brachial plexus | | | | | | | 6587.4 | 0 | 6.42 | 6555 |
| Arc plan | | | | | | | | | | |
| CTV 7000 | 209.33 | 212.93 | 216.05 | | | | | | | |
| CTV 6500 | 91.23 | 96.75 | 97.28 | | | | | | | |
| CTV 6300 | 499.37 | 502.27 | 504.79 | | | | | | | |
| Cord | | | | 0 | 8.68 | 3620 | 4373.4 | | | 4000 |
| Brachial plexus | | | | | | | 6585.9 | 0 | 6.62 | 6505 |
| 3mm sup shift | | | | | | | | | | |
| IMRT Plan | V100% | V98% | V95% | V45 | V25 | max dose 1cc | DVH max point | V75 (TD50/5) | V60 (TD5/5) | max 0.1 cc |
| CTV 7000 | 213.83 | 216.55 | 218.1 | | | | | | | |
| CTV 6500 | 90.79 | 97.02 | 97.5 | | | | | | | |
| CTV 6300 | 500.6 | 504.57 | 506.5 | | | | | | | |
| Cord | | | | 0 | 12.54 | 3690 | 4217.1 | | | 3920 |
| Brachial plexus | | | | | | | 6571.2 | 0 | 6.34 | 6502.5 |
| Arc plan | | | | | | | | | | |
| CTV 7000 | 209.4 | 212.99 | 216.08 | | | | | | | |
| CTV 6500 | 89.62 | 94.74 | 97.3 | | | | | | | |
| CTV 6300 | 499.4 | 502.51 | 504.93 | | | | | | | |
| Cord | | | | 0 | 8.66 | 3620 | 4373.9 | | | 4000 |
| Brachial plexus | | | | | | | 6573.9 | 0 | 6.53 | 6482.5 |
| 3mm inf shift | | | | | | | | | | |
| IMRT Plan | V100% | V98% | V95% | V45 | V25 | max dose 1cc | DVH max point | V75 (TD50/5) | V60 (TD5/5) | max 0.1 cc |
| CTV 7000 | 213.63 | 216.49 | 218.09 | | | | | | | |
| CTV 6500 | 95.71 | 96.92 | 97.46 | | | | | | | |
| CTV 6300 | 498.09 | 501.96 | 505.09 | | | | | | | |
| Cord | | | | 0 | 12.68 | 3690 | 4217.2 | | | 3920 |
| Brachial plexus | | | | | | | 6703.5 | 0 | 6.51 | 6655 |
| Arc plan | | | | | | | | | | |
| CTV 7000 | 209.27 | 212.88 | 216.01 | | | | | | | |
| CTV 6500 | 93.96 | 96.72 | 97.27 | | | | | | | |
| CTV 6300 | 496.58 | 500.39 | 503.82 | | | | | | | |
| Cord | | | | 0 | 8.69 | 3617.5 | 4372.3 | | | 4000 |
| Brachial plexus | | | | | | | 6597.5 | 0 | 6.69 | 6550 |
| 5mm sup shift | | | | | | | | | | |
| IMRT Plan | V100% | V98% | V95% | V45 | V25 | max dose 1cc | DVH max point | V75 (TD50/5) | V60 (TD5/5) | max 0.1 cc |
| CTV 7000 | 213.89 | 216.62 | 218.12 | | | | | | | |
| CTV 6500 | 81.4 | 95.33 | 97.49 | | | | | | | |
| CTV 6300 | 492.47 | 503.49 | 506.6 | | | | | | | |
| Cord | | | | 0 | 12.49 | 3690 | 4217.9 | | | 3920 |
| Brachial plexus | | | | | | | 6539.9 | 0 | 6.18 | 6475 |
| Arc plan | | | | | | | | | | |
| CTV 7000 | 209.44 | 213.02 | 216.1 | | | | | | | |
| CTV 6500 | 84.72 | 92.58 | 97.3 | | | | | | | |
| CTV 6300 | 494.63 | 502.6 | 505.06 | | | | | | | |
| Cord | | | | 0 | 8.61 | 3620 | 4374.8 | | | 4000 |
| Brachial plexus | | | | | | | 6563.9 | 0 | 6.38 | 6470 |

Table B-2 cont'd

| | | | | | | | | | | |
|-----------------------|--------|--------|--------|-----|-------|--------------|---------------|--------------|-------------|------------|
| 5mm inf shift | | | | | | | | | | |
| IMRT Plan | V100% | V98% | V95% | V45 | V25 | max dose 1cc | DVH max point | V75 (TD50/5) | V60 (TD5/5) | max 0.1 cc |
| CTV 7000 | 213.65 | 216.48 | 218.08 | | | | | | | |
| CTV 6500 | 95.97 | 96.99 | 97.47 | | | | | | | |
| CTV 6300 | 501.09 | 503.82 | 506.04 | | | | | | | |
| Cord | | | | 0 | 12.66 | 3790 | 4217 | | | 3920 |
| Brachial plexus | | | | | | | 6730.7 | 0 | 6.51 | 6685 |
| Arc plan | | | | | | | | | | |
| CTV 7000 | 209.24 | 212.88 | 216.01 | | | | | | | |
| CTV 6500 | 94.98 | 96.74 | 97.28 | | | | | | | |
| CTV 6300 | 498.87 | 501.82 | 504.48 | | | | | | | |
| Cord | | | | 0 | 8.7 | 3620 | 4372.1 | | | 4000 |
| Brachial plexus | | | | | | | 6608.4 | 0 | 6.71 | 6565 |
| 15mm sup shift | | | | | | | | | | |
| IMRT Plan | V100% | V98% | V95% | V45 | V25 | max dose 1cc | DVH max point | V75 (TD50/5) | V60 (TD5/5) | max 0.1 cc |
| CTV 7000 | 214.23 | 216.73 | 218.17 | | | | | | | |
| CTV 6500 | 42.29 | 66.02 | 93.69 | | | | | | | |
| CTV 6300 | 437.82 | 469.71 | 494.03 | | | | | | | |
| Cord | | | | 0 | 12.51 | 3696 | 4222.2 | | | 3920 |
| Brachial plexus | | | | | | | 6481.8 | 0 | 5.75 | 6445 |
| Arc plan | | | | | | | | | | |
| CTV 7000 | 209.67 | 213.19 | 216.22 | | | | | | | |
| CTV 6500 | 55.1 | 83.55 | 96.48 | | | | | | | |
| CTV 6300 | 462.92 | 491.12 | 505.03 | | | | | | | |
| Cord | | | | 0 | 8.43 | 3612.5 | 4377 | | | 4000 |
| Brachial plexus | | | | | | | 6535.3 | 0 | 5.89 | 6410 |
| 15mm inf shift | | | | | | | | | | |
| IMRT Plan | V100% | V98% | V95% | V45 | V25 | max dose 1cc | DVH max point | V75 (TD50/5) | V60 (TD5/5) | max 0.1 cc |
| CTV 7000 | 213.52 | 216.44 | 218.07 | | | | | | | |
| CTV 6500 | 96.24 | 97.14 | 97.49 | | | | | | | |
| CTV 6300 | 502.3 | 504.58 | 506.45 | | | | | | | |
| Cord | | | | 0 | 12.67 | 3915 | 4217.4 | | | 3915 |
| Brachial plexus | | | | | | | 6790.8 | 0 | 6.54 | 6760 |
| Arc plan | | | | | | | | | | |
| CTV 7000 | 210.44 | 213.57 | 216.35 | | | | | | | |
| CTV 6500 | 95.47 | 96.85 | 97.32 | | | | | | | |
| CTV 6300 | 500.4 | 502.77 | 505.05 | 0 | 8.79 | 3627.5 | 4395.5 | | | 4020 |
| Cord | | | | | | | 6771.4 | 0 | 6.87 | 6700 |
| Brachial plexus | | | | | | | | | | |
| 3mm ant shift | | | | | | | | | | |
| IMRT Plan | V100% | V98% | V95% | V45 | V25 | max dose 1cc | DVH max point | V75 (TD50/5) | V60 (TD5/5) | max 0.1 cc |
| CTV 7000 | 213.77 | 216.52 | 218.1 | | | | | | | |
| CTV 6500 | 95.96 | 97.15 | 97.5 | | | | | | | |
| CTV 6300 | 502.45 | 504.83 | 506.6 | | | | | | | |
| Cord | | | | 0 | 12.57 | 3690 | 4217 | | | 3920 |
| Brachial plexus | | | | | | | 6608.9 | 0 | 6.44 | 6570 |
| Arc plan | | | | | | | | | | |
| CTV 7000 | 209.34 | 212.94 | 216.05 | | | | | | | |
| CTV 6500 | 91.54 | 96.76 | 97.29 | | | | | | | |
| CTV 6300 | 499.78 | 502.52 | 504.91 | | | | | | | |
| Cord | | | | 0 | 8.68 | 3618 | 4373.4 | | | 4000 |
| Brachial plexus | | | | | | | 6586.7 | 0 | 6.63 | 6510 |

Table B-2 Cont'd

| | | | | | | | | | | |
|------------------------|--------|--------|--------|-----|-------|--------------|---------------|--------------|-------------|------------|
| 3mm post shift | | | | | | | | | | |
| IMRT Plan | V100% | V98% | V95% | V45 | V25 | max dose 1cc | DVH max point | V75 (TD50/5) | V60 (TD5/5) | max 0.1 cc |
| CTV 7000 | 213.71 | 216.51 | 218.1 | | | | | | | |
| CTV 6500 | 94.43 | 97.02 | 97.48 | | | | | | | |
| CTV 6300 | 501.25 | 504.33 | 506.44 | | | | | | | |
| Cord | | | | 0 | 12.62 | 3690 | 4217 | | | 3920 |
| Brachial plexus | | | | | | | 6579.4 | 0 | 6.4 | 6545 |
| Arc plan | | | | | | | | | | |
| CTV 7000 | 209.32 | 212.91 | 216.04 | | | | | | | |
| CTV 6500 | 91.13 | 96.74 | 97.28 | | | | | | | |
| CTV 6300 | 499.16 | 502.2 | 504.8 | | | | | | | |
| Cord | | | | 0 | 8.68 | 3620 | 4373.3 | | | 4000 |
| Brachial plexus | | | | | | | 6579.4 | 0 | 6.61 | 6505 |
| 15mm ant shift | | | | | | | | | | |
| IMRT Plan | V100% | V98% | V95% | V45 | V25 | max dose 1cc | DVH max point | V75 (TD50/5) | V60 (TD5/5) | max 0.1 cc |
| CTV 7000 | 213.77 | 216.52 | 218.1 | | | | | | | |
| CTV 6500 | 96.63 | 97.22 | 97.51 | | | | | | | |
| CTV 6300 | 503.1 | 505.13 | 506.71 | | | | | | | |
| Cord | | | | 0 | 12.56 | 3690 | 4216.2 | | | 3920 |
| Brachial plexus | | | | | | | 6712.2 | 0 | 6.53 | 6655 |
| Arc plan | | | | | | | | | | |
| CTV 7000 | 209.39 | 212.98 | 216.08 | | | | | | | |
| CTV 6500 | 92.75 | 96.76 | 97.29 | | | | | | | |
| CTV 6300 | 500.1 | 502.67 | 504.99 | | | | | | | |
| Cord | | | | 0 | 8.67 | 3620 | 4373.4 | | | 4000 |
| Brachial plexus | | | | | | | 6595.5 | 0 | 6.65 | 6505 |
| 15mm post shift | | | | | | | | | | |
| IMRT Plan | V100% | V98% | V95% | V45 | V25 | max dose 1cc | DVH max point | V75 (TD50/5) | V60 (TD5/5) | max 0.1 cc |
| CTV 7000 | 213.73 | 216.54 | 218.1 | | | | | | | |
| CTV 6500 | 87.68 | 96.61 | 97.37 | | | | | | | |
| CTV 6300 | 494.3 | 502.62 | 505.69 | | | | | | | |
| Cord | | | | 0 | 12.64 | 3690 | 4217.6 | | | 3920 |
| Brachial plexus | | | | | | | 6576.1 | 0 | 6.3 | 6510 |
| Arc plan | | | | | | | | | | |
| CTV 7000 | 209.28 | 212.88 | 216.02 | | | | | | | |
| CTV 6500 | 89.94 | 95.32 | 97.24 | | | | | | | |
| CTV 6300 | 498.02 | 501.34 | 504.25 | | | | | | | |
| Cord | | | | 0 | 8.67 | 3620 | 4373 | | | 4000 |
| Brachial plexus | | | | | | | 6579.4 | 0 | 6.58 | 6500 |
| 15mm RT shift | | | | | | | | | | |
| IMRT Plan | V100% | V98% | V95% | V45 | V25 | max dose 1cc | DVH max point | V75 (TD50/5) | V60 (TD5/5) | max 0.1 cc |
| CTV 7000 | 213.72 | 216.51 | 218.1 | | | | | | | |
| CTV 6500 | 96.3 | 97.14 | 97.5 | | | | | | | |
| CTV 6300 | 502.06 | 504.54 | 506.46 | | | | | | | |
| Cord | | | | 0 | 12.62 | 3690 | 4216.9 | | | 3920 |
| Brachial plexus | | | | | | | 6657.4 | 0 | 6.48 | 6625 |
| Arc plan | | | | | | | | | | |
| CTV 7000 | 209.31 | 212.91 | 216.03 | | | | | | | |
| CTV 6500 | 92.27 | 96.76 | 97.28 | | | | | | | |
| CTV 6300 | 499.43 | 502.25 | 504.77 | | | | | | | |
| Cord | | | | 0 | 8.66 | 3620 | 4373.5 | | | 4000 |
| Brachial plexus | | | | | | | 6586 | 0 | 6.65 | 6530 |

Table B-3: Dosimetric Patient 3 target volumes and structure doses

| Structure analysis | | | | Volume = cc | | Dose = cGy | | | | |
|--------------------|--------|--------|--------|-------------|-------|--------------|---------------|--------------|-------------|------------|
| IMRT Plan | V100% | V98% | V95% | V45 | V25 | max dose 1cc | DVH max point | V75 (TD50/5) | V60 (TD5/5) | max 0.1 cc |
| CTV 6000 | 167.92 | 168.79 | 169.3 | | | | | | | |
| CTV 5400 | 409.83 | 411.3 | 411.6 | | | | | | | |
| Cord | | | | 0 | 13.58 | 3808 | 4015.2 | | | 3905 |
| Brachial plexus | | | | | | | 6071.9 | 0 | 0.02 | 5910 |
| Arc plan | | | | | | | | | | |
| CTV 6000 | 167.37 | 168.49 | 169.27 | | | | | | | |
| CTV 5400 | 404.52 | 409.32 | 411.2 | | | | | | | |
| Cord | | | | 0 | 19.63 | 3801 | 3982.9 | | | 3910 |
| Brachial plexus | | | | | | | 6043.8 | 0 | 0.01 | 5940 |
| | | | | | | | | | | |
| 3mm sup | | | | | | | | | | |
| IMRT Plan | V100% | V98% | V95% | V45 | V25 | max dose 1cc | DVH max point | V75 (TD50/5) | V60 (TD5/5) | max 0.1 cc |
| CTV 6000 | 167.68 | 168.99 | 169.52 | | | | | | | |
| CTV 5400 | 408.97 | 411.33 | 411.61 | | | | | | | |
| Cord | | | | 0 | 13.54 | 3794 | 4006.5 | | | 3896 |
| Brachial plexus | | | | | | | 6037.2 | 0 | 0.01 | 5880 |
| Arc plan | | | | | | | | | | |
| CTV 6000 | 167.14 | 168.5 | 169.35 | | | | | | | |
| CTV 5400 | 403.04 | 409.36 | 411.28 | | | | | | | |
| Cord | | | | 0 | 19.62 | 3796 | 3985 | | | 3900 |
| Brachial plexus | | | | | | | 5981.4 | 0 | 0 | 5880 |
| | | | | | | | | | | |
| 3mm inf | | | | | | | | | | |
| IMRT Plan | V100% | V98% | V95% | V45 | V25 | max dose 1cc | DVH max point | V75 (TD50/5) | V60 (TD5/5) | max 0.1 cc |
| CTV 6000 | 167.94 | 168.6 | 169.12 | | | | | | | |
| CTV 5400 | 408.21 | 409.96 | 410.77 | | | | | | | |
| Cord | | | | 0 | 13.6 | 3819 | 4029.5 | | | 3922 |
| Brachial plexus | | | | | | | 6117 | 0 | 0.05 | 5950 |
| Arc plan | | | | | | | | | | |
| CTV 6000 | 167.44 | 168.41 | 169.13 | | | | | | | |
| CTV 5400 | 403.23 | 407.71 | 410.24 | | | | | | | |
| Cord | | | | 0 | 19.63 | 3810 | 3981.6 | | | 3918 |
| Brachial plexus | | | | | | | 6115.4 | 0 | 0.09 | 6000 |
| | | | | | | | | | | |
| 5mm sup | | | | | | | | | | |
| IMRT Plan | V100% | V98% | V95% | V45 | V25 | max dose 1cc | DVH max point | V75 (TD50/5) | V60 (TD5/5) | max 0.1 cc |
| CTV 6000 | 165.68 | 168.93 | 169.55 | | | | | | | |
| CTV 5400 | 402.58 | 410.87 | 411.59 | | | | | | | |
| Cord | | | | 0 | 13.51 | 3788 | 3992.1 | | | 3882 |
| Brachial plexus | | | | | | | 6015.3 | 0 | 0 | 5850 |
| Arc plan | | | | | | | | | | |
| CTV 6000 | 166.91 | 168.52 | 169.38 | | | | | | | |
| CTV 5400 | 398.92 | 408.3 | 411.14 | | | | | | | |
| Cord | | | | 0 | 19.62 | 3796 | 3988.1 | | | 3900 |
| Brachial plexus | | | | | | | 5945 | 0 | 0 | 5850 |

Table B-3 cont'd

| | | | | | | | | | | |
|------------------|--------|--------|--------|-----|-------|--------------|---------------|--------------|-------------|------------|
| 5mm inf | | | | | | | | | | |
| IMRT Plan | V100% | V98% | V95% | V45 | V25 | max dose 1cc | DVH max point | V75 (TD50/5) | V60 (TD5/5) | max 0.1 cc |
| CTV 6000 | 168.15 | 168.69 | 169.16 | | | | | | | |
| CTV 5400 | 409.36 | 410.66 | 411.24 | | | | | | | |
| Cord | | | | 0 | 13.59 | 3828 | 4039.1 | | | 3932 |
| Brachial plexus | | | | | | | 6163.2 | 0 | 0.1 | 6000 |
| Arc plan | | | | | | | | | | |
| CTV 6000 | 167.65 | 168.5 | 169.15 | | | | | | | |
| CTV 5400 | 404.55 | 408.63 | 410.8 | | | | | | | |
| Cord | | | | 0 | 19.63 | 3811 | 4039.1 | | | 3920 |
| Brachial plexus | | | | | | | 6164.6 | 0 | 0.21 | 6037 |
| 15mm sup | | | | | | | | | | |
| IMRT Plan | V100% | V98% | V95% | V45 | V25 | max dose 1cc | DVH max point | V75 (TD50/5) | V60 (TD5/5) | max 0.1 cc |
| CTV 6000 | 109.9 | 148.42 | 167.74 | | | | | | | |
| CTV 5400 | 332.99 | 386.34 | 404.8 | | | | | | | |
| Cord | | | | 0 | 13.43 | 3756 | 3938.5 | | | 3842 |
| Brachial plexus | | | | | | | 5919.1 | 0 | 0 | 5760 |
| Arc plan | | | | | | | | | | |
| CTV 6000 | 118.3 | 161.03 | 168.94 | | | | | | | |
| CTV 5400 | 339.73 | 380.04 | 404.62 | | | | | | | |
| Cord | | | | 0 | 19.6 | 3788 | 3990.7 | | | 3894 |
| Brachial plexus | | | | | | | 5836 | 0 | 0 | 5727 |
| 15mm inf | | | | | | | | | | |
| IMRT Plan | V100% | V98% | V95% | V45 | V25 | max dose 1cc | DVH max point | V75 (TD50/5) | V60 (TD5/5) | max 0.1 cc |
| CTV 6000 | 168.45 | 168.98 | 169.35 | | | | | | | |
| CTV 5400 | 410.31 | 411 | 411.28 | | | | | | | |
| Cord | | | | 0 | 13.54 | 3865 | 4109.3 | | | 3982 |
| Brachial plexus | | | | | | | 6289.6 | 0 | 0.44 | 6120 |
| Arc plan | | | | | | | | | | |
| CTV 6000 | 168.18 | 168.89 | 169.42 | | | | | | | |
| CTV 5400 | 406.11 | 409.14 | 410.9 | | | | | | | |
| Cord | | | | 0 | 19.63 | 3824 | 3995.2 | | | 3934 |
| Brachial plexus | | | | | | | 6302.8 | 0 | 1.11 | 6180 |
| 3mm ant | | | | | | | | | | |
| IMRT Plan | V100% | V98% | V95% | V45 | V25 | max dose 1cc | DVH max point | V75 (TD50/5) | V60 (TD5/5) | max 0.1 cc |
| CTV 6000 | 168.71 | 169.33 | 169.67 | | | | | | | |
| CTV 5400 | 410.1 | 411.2 | 411.52 | | | | | | | |
| Cord | | | | 0 | 13.57 | 3806 | 4012.2 | | | 3902 |
| Brachial plexus | | | | | | | 6095.3 | 0 | 0.03 | 5930 |
| Arc plan | | | | | | | | | | |
| CTV 6000 | 168.33 | 169.14 | 169.61 | | | | | | | |
| CTV 5400 | 404.41 | 409.25 | 411.13 | | | | | | | |
| Cord | | | | 0 | 19.63 | 3801 | 3983.2 | | | 3908 |
| Brachial plexus | | | | | | | 6029.5 | 0 | 0 | 5920 |

Table B-3 cont'd

| | | | | | | | | | | |
|------------------|--------|--------|--------|-----|-------|--------------|---------------|--------------|-------------|------------|
| 3mm post | | | | | | | | | | |
| IMRT Plan | V100% | V98% | V95% | V45 | V25 | max dose 1cc | DVH max point | V75 (TD50/5) | V60 (TD5/5) | max 0.1 cc |
| CTV 6000 | 167.25 | 168.6 | 169.27 | | | | | | | |
| CTV 5400 | 406.49 | 409.79 | 411.03 | | | | | | | |
| Cord | | | | 0 | 13.57 | 3802 | 4010 | | | 3902 |
| Brachial plexus | | | | | | | 6060.7 | 0 | 0.01 | 5900 |
| Arc plan | | | | | | | | | | |
| CTV 6000 | 166.94 | 168.28 | 169.24 | | | | | | | |
| CTV 5400 | 402.05 | 407.69 | 410.55 | | | | | | | |
| Cord | | | | 0 | 19.63 | 3803 | 3982 | | | 3912 |
| Brachial plexus | | | | | | | 6058.2 | 0 | 0.02 | 5953 |
| 15mm ant | | | | | | | | | | |
| IMRT Plan | V100% | V98% | V95% | V45 | V25 | max dose 1cc | DVH max point | V75 (TD50/5) | V60 (TD5/5) | max 0.1 cc |
| CTV 6000 | 167.64 | 169.25 | 169.69 | | | | | | | |
| CTV 5400 | 410.81 | 411.41 | 411.57 | | | | | | | |
| Cord | | | | 0 | 13.58 | 3831 | 4040.9 | | | 3930 |
| Brachial plexus | | | | | | | 6180.8 | 0 | 0.11 | 6010 |
| Arc plan | | | | | | | | | | |
| CTV 6000 | 167.74 | 168.94 | 169.54 | | | | | | | |
| CTV 5400 | 406.89 | 409.47 | 411.47 | | | | | | | |
| Cord | | | | 0 | 19.64 | 3790 | 3984.2 | | | 3892 |
| Brachial plexus | | | | | | | 5979.8 | 0 | 0 | 5870 |
| 15mm post | | | | | | | | | | |
| IMRT Plan | V100% | V98% | V95% | V45 | V25 | max dose 1cc | DVH max point | V75 (TD50/5) | V60 (TD5/5) | max 0.1 cc |
| CTV 6000 | 164.23 | 167.76 | 168.89 | | | | | | | |
| CTV 5400 | 385.01 | 407.24 | 410.88 | | | | | | | |
| Cord | | | | 0 | 13.55 | 3872 | 3974.6 | | | 3877 |
| Brachial plexus | | | | | | | 5976 | 0 | 0 | 5810 |
| Arc plan | | | | | | | | | | |
| CTV 6000 | 166.96 | 168.21 | 169.17 | | | | | | | |
| CTV 5400 | 401.37 | 407.23 | 410.35 | | | | | | | |
| Cord | | | | 0 | 19.58 | 3796 | 3982.3 | | | 3902 |
| Brachial plexus | | | | | | | 6122.8 | 0 | 0.12 | 6010 |
| 15mm Left | | | | | | | | | | |
| IMRT Plan | V100% | V98% | V95% | V45 | V25 | max dose 1cc | DVH max point | V75 (TD50/5) | V60 (TD5/5) | max 0.1 cc |
| CTV 6000 | 165.69 | 168.53 | 169.43 | | | | | | | |
| CTV 5400 | 408.05 | 410.67 | 411.44 | | | | | | | |
| Cord | | | | | 13.58 | 3783 | 3983 | | | 3884 |
| Brachial plexus | | | | | | | 5987.9 | 0 | 0 | 5860 |
| Arc plan | | | | | | | | | | |
| CTV 6000 | 167.16 | 168.49 | 169.41 | | | | | | | |
| CTV 5400 | 402.17 | 408.94 | 411.15 | | | | | | | |
| Cord | | | | 0 | 19.63 | 3801 | 3983 | | | 3900 |
| Brachial plexus | | | | | | | 5984.6 | 0 | 0 | 5870 |

BIBLIOGRAPHY

1. ACS. (2010, 2010). "American Cancer Society." Learn About Cancer Retrieved January 18, 2011.
2. Bentel, G. (1996). Radiation Therapy Planning. New York, McGraw Hill.
3. Bzdusek, K., H. Friberger, B. Hardemark, D. Robinson, M. Kraus. (2009). "Development and evaluation of an efficient approach to volumetric arc therapy planning." Med Phys **36**(6): 2328-39.
4. Chen, A. M., W. H. Hall, BQ Li, M. Guiou, C. Wrgiht, M. Mathai, A. Dublin, J.A. Purdy . (2010). "Intensity-modulated radiotherapy increases dose to the brachial plexus compared with conventional radiotherapy for head and neck cancer." Br J Radiol.
5. Clemente, S., B. Wu, G. Sanguineti, V. Fusco, F. Ricchetti, J. Wong, T. McNutt.
"SmartArc-Based Volumetric Modulated Arc Therapy for Oropharyngeal Cancer: A Dosimetric Comparison with Both Intensity-Modulated Radiation Therapy and Helical Tomotherapy." Int J Radiat Oncol Biol Phys.
6. Court, L. E., L. Wolfsberger, A.M. Allen, S. James, R.B. Tishler. (2008). "Clinical experience of the importance of daily portal imaging for head and neck IMRT treatments." J Appl Clin Med Phys **9**(3): 2756.
7. Gilbeau, L., M. Octave-Prignot, T Loncol, L. Renard, P. Scalliet, V. Gregoire. (2001).
"Comparison of setup accuracy of three different thermoplastic masks for the treatment of brain and head and neck tumors." Radiother Oncol **58**(2): 155-62.
8. Joiner, M., Albert van der Kogel (2009). Basic Clinical Radiobiology. London, Hodder Arnold.

9. Kahn, F. M. (2003). The Physics of Radiation Therapy. Philadelphia, PA, Lippincott, Williams, & Wilkins.
10. Lee, N., D. R. Puri, A. Blanco, K.S. C. Chao. (2007). "Intensity-modulated radiation therapy in head and neck cancers: an update." Head Neck **29**(4): 387-400.
11. Ozyigit, G., T. Yang, K.S. C. Chao. (2004). "Intensity-modulated radiation therapy for head and neck cancer." Curr Treat Options Oncol **5**(1): 3-9.
12. Zhang, L., A. S. Garden, J. Lo, K.K. Ang, A. Ahamad, W.H. Morrison, D.I. Rosenthal. M.S. Chambers, X.R. Zhu, R. Mohan, L. Dong. (2006). "Multiple regions-of-interest analysis of setup uncertainties for head-and-neck cancer radiotherapy." Int J Radiat Oncol Biol Phys **64**(5): 1559-69.

VITA

Emily Neubauer was born in Albany, NY and grew up in Schodack, NY. She attended Emma Willard School in Troy, NY, and graduated Cum Laude in 2000. In 2010 she was awarded the “Outstanding Young Alumna Award” by the Emma Willard Alumnae Council. Following secondary school, she attended Yale University in New Haven, CT and earned an Intensive Bachelor of Science in Physics in 2004. After 2 years of wandering around Upstate NY, California and Washington, DC, Emily moved to Boston, MA to become a dosimetrist at Massachusetts General Hospital. She became a Certified Medical Dosimetrist in 2009. She came to The Graduate School of Biomedical Science in Houston, TX in the fall of 2009.

Permanent Address:

1984 Brookview Rd.

Castleton, NY 12033